



**HAL**  
open science

## Chiroptical and Potential In Vitro Anti-Inflammatory Properties of Viniferin Stereoisomers from Grapevine (*Vitis vinifera* L)

Guillaume Buffeteau, Ruth Hornedo-Ortega, Julien Gabaston, Nicolas Daugey, Antonio Palos-Pinto, Anne Thienpont, Thierry Brotin, Jean-Michel Mérillon, Thierry Buffeteau, Pierre Waffo-Teguo

### ► To cite this version:

Guillaume Buffeteau, Ruth Hornedo-Ortega, Julien Gabaston, Nicolas Daugey, Antonio Palos-Pinto, et al.. Chiroptical and Potential In Vitro Anti-Inflammatory Properties of Viniferin Stereoisomers from Grapevine (*Vitis vinifera* L). *Food Chemistry*, 2022, 393, pp.133359. 10.1016/j.foodchem.2022.133359 . hal-03839816

**HAL Id: hal-03839816**

**<https://hal.science/hal-03839816v1>**

Submitted on 4 Nov 2022

**HAL** is a multi-disciplinary open access archive for the deposit and dissemination of scientific research documents, whether they are published or not. The documents may come from teaching and research institutions in France or abroad, or from public or private research centers.

L'archive ouverte pluridisciplinaire **HAL**, est destinée au dépôt et à la diffusion de documents scientifiques de niveau recherche, publiés ou non, émanant des établissements d'enseignement et de recherche français ou étrangers, des laboratoires publics ou privés.

# Food Chemistry

## Chiroptical and Potential In Vitro Anti-Inflammatory Properties of Viniferin Stereoisomers from Grapevine (*Vitis vinifera* L.) --Manuscript Draft--

<b>Manuscript Number:</b>	FOODCHEM-D-22-01901R1
<b>Article Type:</b>	Research Article (max 7,500 words)
<b>Keywords:</b>	stilbene, viniferins, stereoisomers, chirality, vine, anti-inflammatory
<b>Corresponding Author:</b>	Pierre Waffo-Teguo, Ph. D, Pharm. D Université de Bordeaux Villenave d'ornon, FRANCE
<b>First Author:</b>	Guillaume Buffeteau
<b>Order of Authors:</b>	Guillaume Buffeteau Ruth Hornedo-Ortega, PhD Julien Gabaston, PhD Nicolas Daugey, PhD Antonio Palos-Pinto Anne Thienpont, PhD Thierry Brotin, PhD Jean-Michel Mérillon, PhD Thierry Buffeteau, PhD Pierre Waffo-Teguo, Ph. D, Pharm. D
<b>Abstract:</b>	Determination of stereochemistry and enantiomeric excess in chiral natural molecules is a research of great interest because enantiomers can exhibit different biological activities. Viniferin stilbene dimers are natural molecules present in grape berries and wine but also, in larger amount, in stalks of grapevine. Four stereoisomers of viniferin stilbene dimers (7aS,8aS)-E-ε-viniferin (1a), (7aR,8aR)-E-ε-viniferin (1b), (7aS,8aR)-E-ε-viniferin (2a), and (7aR,8aS)-E-ω-viniferin (2b) were isolated from grapevine stalks of Cabernet Sauvignon, Merlot and Sauvignon Blanc, using a combination of centrifugal partition chromatography (CPC), preparative and chiral HPLC. The structure elucidation of these molecules was achieved by NMR whereas the absolute configurations of the four stereoisomers were investigated by vibrational circular dichroism spectroscopy in combination with density functional theory (DFT) calculations. This study unambiguously established the (+)-(7aS,8aS) and (+)-(7aR,8aS) configurations for E-ε-viniferin and E-ω-viniferin, respectively. Finally, we show that Cabernet Sauvignon provided the quasi enantiopure (+)-(7aS,8aS)-E-ε-viniferin compound which presents the best anti-inflammatory and anti-oxidant activities.

February 17, 2022

Dr. Paul Finglas  
Editor-in-Chief, Food Chemistry  
Quadram Institute Bioscience, NR4 7UA, Norwich,  
United Kingdom

Dear Dr. Paul Finglas,

We would like to submit for publication as a Full paper in *Food Chemistry* a manuscript entitled **“Chiroptical and Potential *In Vitro* Anti-Inflammatory Properties of Viniferin Stereoisomers from Grapevine (*Vitis vinifera* L.)”** by Guillaume Buffeteau *et al.* No related work has been submitted in others Journals and this manuscript has been submitted exclusively to *Food Chemistry*. All authors have seen and approved the submission of the manuscript.

In this manuscript, we report the absolute configuration of two enantiomers of *E-ε*-viniferins and *E-ω*-viniferins extracted from branches of grapevine using vibrational circular dichroism, electronic circular dichroism, and NMR experiments. This study shows that the proportion of the two enantiomers of *E-ε*-viniferin and the enantiomeric excess are cultivar-dependent. For example, Cabernet Sauvignon variety gives the dextrorotatory form of *E-ε*-viniferin and the Merlot variety gives preferentially the levorotatory form, whereas Sauvignon Blanc exhibits a lower value of specific rotation that probably means the presence of rather racemic mixture. Moreover, we demonstrate for the first time that viniferin stereoisomers possess anti-inflammatory and anti-oxidant activities. Even though their structures are quite similar, this paper shows that the bioactivities of the four viniferin stereoisomers are different according to their configuration.

We think that this manuscript will be of wide interest to the readership of the *Food Chemistry*.

Thank you very much for your consideration of our manuscript.

Yours sincerely,

Professor P. Waffo-Téguo  
Université Bordeaux  
ISVV - GESVAB  
210, Chemin de Leysotte  
33882 Villenave d'Ornon  
FRANCE  
E-mail: [pierre.waffo-teguo@u-bordeaux.fr](mailto:pierre.waffo-teguo@u-bordeaux.fr)  
Tel: (33) 5 57 57 59 55

# Chiroptical and Potential *In Vitro* Anti-Inflammatory Properties of Viniferin Stereoisomers from Grapevine (*Vitis vinifera* L.)

Guillaume Buffeteau,<sup>a</sup> Ruth Hornedo-Ortega,<sup>a</sup> Julien Gabaston,<sup>a</sup> Nicolas Daugey,<sup>b</sup> Antonio Palos-Pinto,<sup>a</sup> Anne Thienpont,<sup>b</sup> Thierry Brotin,<sup>c</sup> Jean-Michel Mérillon,<sup>a</sup> Thierry Buffeteau<sup>b,\*</sup> and Pierre Waffo-Teguo<sup>a,\*</sup>

<sup>a</sup>Univ. Bordeaux, UFR des Sciences Pharmaceutiques, Unité OENO UMR 1366 INRAE, Bordeaux INP - Institut des Sciences de la Vigne et du Vin, CS 50008 - 210, chemin de Leysotte, 33882 Villenave d'Ornon, France..

<sup>b</sup>Univ. Bordeaux, Institut des Sciences Moléculaires, UMR 5255 - CNRS, 351 Cours de la Libération, F-33405 Talence, France.

<sup>c</sup>Université Lyon 1, Ecole Normale Supérieure de Lyon, CNRS UMR 5182, Laboratoire de Chimie, 69364 Lyon, France.

## Highlights

- Viniferins were isolated from vine stalks using a combination of CPC and Prep. HPLC
- The enantiomers of *E-ε*-viniferins and *E-ω*-viniferins were purified by chiral HPLC
- The stereochemistry was investigated by NMR and VCD associated to DFT calculations
- The enantiomeric excess of *E-ε*-viniferin were grape variety-dependent
- Stereoisomers of viniferins showed anti-inflammatory and antioxidant activities

**Declaration of interests**

The authors declare that they have no known competing financial interests or personal relationships that could have appeared to influence the work reported in this paper.

The authors declare the following financial interests/personal relationships which may be considered as potential competing interests:

1           **Chiroptical and Potential *In Vitro* Anti-Inflammatory Properties of**  
2           **Viniferin Stereoisomers from Grapevine (*Vitis vinifera* L.)**

3  
4 Guillaume Buffeteau,<sup>a</sup> Ruth Hornedo-Ortega,<sup>a</sup> Julien Gabaston,<sup>a</sup> Nicolas Daugey,<sup>b</sup> Antonio  
5 Palos-Pinto,<sup>a</sup> Anne Thienpont,<sup>b</sup> Thierry Brotin,<sup>c</sup> Jean-Michel Mérillon,<sup>a</sup> Thierry Buffeteau<sup>b,\*</sup>  
6 and Pierre Waffo-Teguo<sup>a,\*</sup>

7  
8 <sup>a</sup>Univ. Bordeaux, UFR des Sciences Pharmaceutiques, Unité OENO UMR 1366 INRAE,  
9 Bordeaux INP - Institut des Sciences de la Vigne et du Vin, CS 50008 - 210, chemin de  
10 Leysotte, 33882 Villenave d'Ornon, France.

11 <sup>b</sup>Université de Bordeaux, Institut des Sciences Moléculaires, UMR 5255 - CNRS, 351 Cours  
12 de la Libération, F-33405 Talence, France.

13 <sup>c</sup>Université Lyon 1, Ecole Normale Supérieure de Lyon, CNRS UMR 5182, Laboratoire de  
14 Chimie, 69364 Lyon, France.

15  
16 **Corresponding Author:**

17 \*Tel.: +33-55-757-5955. Fax: +33-55-757-5952. E-mail: [pierre.waffo-teguo@u-bordeaux.fr](mailto:pierre.waffo-teguo@u-bordeaux.fr)

18 Univ. Bordeaux, UFR des Sciences Pharmaceutiques, Unité OENO UMR 1366 INRAE,  
19 Bordeaux INP - Institut des Sciences de la Vigne et du Vin, CS 50008 - 210, chemin de  
20 Leysotte, 33882 Villenave d'Ornon, France..

21 **Abstract**

22 Four stereoisomers of viniferin stilbene dimers (*7aS,8aS*)-*E-ε*-viniferin (**1a**), (*7aR,8aR*)-*E-ε*-  
23 viniferin (**1b**), (*7aS,8aR*)-*E-ω*-viniferin (**2a**), and (*7aR,8aS*)-*E-ω*-viniferin (**2b**) were isolated  
24 from grapevine stalks of various varieties (Cabernet Sauvignon, Merlot, Sauvignon Blanc)  
25 using a combination of centrifugal partition chromatography (CPC), preparative HPLC and  
26 chiral HPLC. The structure elucidation of these molecules was achieved by NMR whereas the  
27 absolute configurations of the four stereoisomers were investigated by vibrational circular  
28 dichroism (VCD) spectroscopy in combination with density functional theory (DFT)  
29 calculations. This VCD study, associated with NMR results, unambiguously established the  
30 (+)-(*7aS,8aS*) configuration for *E-ε*-viniferin and the (+)-(*7aR,8aS*) configuration for *E-ω*-  
31 viniferin. The anti-inflammatory and anti-oxidant activities of the four viniferin stereoisomers  
32 were also evaluated and we demonstrated for the first time that viniferin stereoisomers possess  
33 different bioactivities according to their configuration. Finally, this study reveals that Cabernet  
34 Sauvignon grape variety allows to extract a quasi enantiopure (+)-(*7aS,8aS*)-*E-ε*-viniferin  
35 compound which present the best anti-inflammatory and anti-oxidant activities.

36 **Keywords:** stilbene, viniferins, stereoisomers, chirality, vine, anti-inflammatory

37

## 38 **1. Introduction**

39 Chirality plays a major role for the synthesis and development of drugs, since most of  
40 the drugs discovered are chiral. The pharmacological activity of drugs depends mainly on its  
41 interaction with biological targets such as proteins, nucleic acids and bio membranes. One  
42 enantiomer of a chiral drug may be a medicine for particular disease, whereas another  
43 enantiomer of the molecule may be inactive or in some cases can be toxic. Hence, the  
44 determination of the absolute configuration of the enantiomers plays an essential role in drugs  
45 (Alkadi & Jbeily, 2018).

46 The hydroxylated derivatives of stilbene, especially resveratrol and its congeners have  
47 attracted much attention owing to their various benefits in human health. It is now accepted that  
48 resveratrol possesses a large number of pharmacological properties including cardioprotective  
49 (Saiko et al., 2008), neuroprotective (Richard et al., 2011), and chemopreventive effects (Ko et  
50 al., 2017). More than one thousand stilbenoids have been identified until now, and several  
51 articles tried to make a catalog (Shen et al., 2009; Rivière et al., 2012; Keylor et al., 2015).  
52 These specialized metabolites occur naturally with a limited but heterogeneous distribution in  
53 the plant kingdom (Rivière et al., 2012). Stilbenoids can be divided in monomers and oligomers.  
54 There are two main hypotheses dealing with the biosynthesis of oligomers. The first approach  
55 is chemical, while the second involves chiral intermediates and possibly enzymes. Given the  
56 different structures of existing dimers, it seems that both possibilities are present. In any case,  
57 it is the ability of this type of compounds, like most polyphenols, to form and trap radicals,  
58 which makes it possible to obtain such diversity by radical coupling. Indeed, they are  
59 mechanisms of the Sequential Proton Loss Electron Transfer (SPLET) and Hydrogen Atom  
60 Transfer (HAT) type which, by radical and proton transfer, would lead to such reactivity (Shang  
61 et al., 2009; Stojanović & Brede, 2002). It was shown that some peroxidases from grapevine  
62 are capable to form the  $\delta$ -viniferin and other dimers (Calderón et al., 1992; Morales & Barceló,

63 1997; Barceló et al., 2003). Despite numerous attempts using Horseradish peroxidase (HRP) or  
64 other peroxidases, even from the grapevine, none data have been published, showing that these  
65 enzymes are involved in the formation of the *E-ε*-viniferin (Barceló et al., 2003). The presence  
66 of a chiral intermediate, however, is strongly assumed, as the plants seem able to produce  
67 specifically the (+)-*E-ε*-viniferin, as in Vitaceae and Dipterocarpaceae or (-)-*E-ε*-viniferin as  
68 in some Cyperaceae (Yoshiaki & Masatake, 2001). Laccase from *Botrytis cinerea* was  
69 considered capable to catalyze the reaction of resveratrol toward the (+)-*E-ε*-viniferin (Pezet,  
70 1998), but subsequent studies have refuted this hypothesis (Breuil et al., 1998; Cichewicz et al.,  
71 2000).

72 Structurally, *E-ε*- and *E-ω*-viniferins are resveratrol dimers belonging to the group A  
73 according to the natural stilbenes classification with two resveratrol units linked by two C-C  
74 and C-O-C connection (Shen and Lou, 2009). This structure has two stereogenic carbons on the  
75 benzofuran unit with four possible stereoisomers (**Figure 1**). As observed for drugs, it is  
76 possible that enantiomers of viniferins can have different activities. Recently, research carried  
77 out on the characterization of the molecular determinants responsible for the taste of wines  
78 showed how stereochemistry could influence taste properties. Thus, taste properties of  
79 lyoniresinol stereoisomers were evaluated and only one lyoniresinol enantiomer were strongly  
80 bitter whereas the other one was tasteless and the diastereoisomer is slightly sweet (Cretin et  
81 al., 2015). In order to better understand the different properties of each stereoisomer of *E-ε*- and  
82 *E-ω*-viniferins, it is crucial to isolate and characterize them.

83 This paper reports the chiroptical properties (vibrational and electronic circular  
84 dichroisms) of two stilbene dimers, *E-ε*-viniferin and *E-ω*-viniferin from stalks of grapevine in  
85 view to determine their absolute configurations. We have shown that the two dimers are present  
86 as a mixture of enantiomers, depending on the grape variety. All the stereoisomers were also

87 evaluated for their anti-inflammatory and anti-oxidant activities in Lipopolysaccharide (LPS)-  
88 stimulated macrophages.

89

## 90 **2. Material and Methods**

### 91 ***2.1. General Experimental Procedures.***

92 <sup>1</sup>H and <sup>13</sup>C NMR spectra were recorded on a Bruker Avance III 600 MHz NMR  
93 spectrometer and analyzed with Bruker Topspin software. Compounds were measured in 3 mm  
94 NMR tubes, using acetone-*d*<sub>6</sub> as the solvent. The specific optical rotations were determined in  
95 methanol at 20 °C on a JASCO P-2000 polarimeter using the sodium emission wavelength ( $\lambda$   
96 = 589 nm). The centrifugal partition chromatography (CPC) used in this study (FCPC200®)  
97 was provided by Kromaton Technologies (Sainte-Gemmes-sur-Loire, France). The solvents  
98 were pumped by a Gilson 321-H1 2-way binary high-pressure gradient pump. The samples  
99 were introduced into the CPC column via a high pressure injection valve (3725i-038 Rheodyne)  
100 equipped with a 20 mL sample loop. The CPC fractions were monitored with a Varian Prostar  
101 325 DAD detector (Victoria, Australia), at wavelengths of 306 and 280 nm. HPLC preparative  
102 separations were carried out using a Gilson PLC 2050 Purification System equipped with a  
103 binary pump, a UV-VIS Detector, a fraction Collector, and a Phenomenex Kinetex XB-C18  
104 AXIA column (5  $\mu$ m, 150 x 21.2 mm). The mobile phase was composed of two solvents: (A)  
105 0.025% TFA in H<sub>2</sub>O and (B) MeCN. The preparative enantioseparations were performed using  
106 the same HPLC system as above equipped with a Phenomenex Lux Amylose-1 (5  $\mu$ m, 150 x  
107 10 mm) chiral column. The mobile phase consisted of n-Hexane/2-Propanol (85/15, v/v)  
108 acidified with 0.01% TFA.

### 109 ***2.2. Plant Material.***

110 Grapevine stalks (Merlot) were collected in the “Château Rochemorin” vineyard in the  
111 region of Bordeaux (44°43'17''N, -0°33'45''W, Martillac, France) in January 2017. They were

112 obtained from Riparia Gloire de Montpellier rootstocks which were planted in 1985. Stalks  
 113 specimens were deposited in the Molécules d'Intérêt Biologique (MIB) laboratory at ISVV  
 114 (Villenave d'Ornon, France). Grapevine stalks of three other grape varieties (Cabernet  
 115 Sauvignon, Sauvignon Blanc, and Merlot) were collected in the "Domaine Haut Dambert"  
 116 vineyard in the region of Bordeaux (44°38'58''N, - 0°10'48''W, Gornac, France) in January  
 117 2015. The accession numbers are listed in **Table 1**.

118 **Table 1.** Cultivar/rootstock combinations, deposit number, and origins

Cultivar	rootstock	Deposit number	Origin (city, region, country)
Merlot	101-14	MIB_M-2017	Martillac (region of Bordeaux, France)
Carbernet Sauvignon	101-14	MIB_CS-TB	Gornac (region of Bordeaux, France)
Merlot	420A	MIB_M-TB	Gornac (region of Bordeaux, France)
Sauvignon Blanc	101-14	MIB_SB-TB	Gornac (region of Bordeaux, France)

119

### 120 **2.3. Extraction and Isolation.**

121 Dried and finely powdered stalks of *Vitis vinifera* (100 g) were defatted with petroleum  
 122 (1 L) using soxhlet extractor, extracted with 60% aqueous acetone (1 L, 2 times) at room  
 123 temperature and filtered. This aqueous acetone extract was evaporated under reduced pressure.  
 124 The filtrate was concentrated at 35°C under reduced pressure. Aqueous residue (200 mL) was  
 125 partitioned with EtOAc (4 x 200 mL). The organic extract was concentrated and freeze-dried  
 126 to yield 3 g.

127 1 g of the organic extract was subjected to the centrifugal partition chromatography (CPC)  
 128 using the quaternary biphasic Arizona-K system n-Heptane/EtOAc/MeOH/Water (1:2:1:2,  
 129 v/v). The CPC rotor was entirely filled with the aqueous stationary phase in the descending  
 130 mode at 500 rpm. After injection of the organic extract, dissolved in 8 mL of the  
 131 organic/aqueous phase mixture (1:1, v/v), the aqueous mobile phase was pumped into the

132 column in descending mode at a flow-rate of 3 mL/min. Then the rotation speed was increased  
133 from 500 to 1200 rpm. The back pressure was 25 bars. The content of the outgoing organic  
134 phase was monitored by online UV absorbance measurement at 280 and 306 nm. Six fractions  
135 were collected (**Supplementary material** Figure S1). *E-ε*-viniferin and *E-ω*-viniferin, obtained  
136 as a white solid were purified from the fraction 6 (200 mg) by preparative HPLC with elution  
137 program: 17% B (0-1.12 min), 17-30% B (1.12 -13.12 min), 30-38% B (13.12-22.12 min), 38-  
138 100% B (22.12-27 min), 100% (27-30 min).

139 The enantiomeric excess of the two enantiomers of *E-ε*-viniferin, **1**, extracted from  
140 Cabernet Sauvignon, Merlot and Sauvignon Blanc grape varieties was measured by analytical  
141 chiral HPLC. The mixture of enantiomers of each compound was solubilized in mobile phase  
142 and filtered on PTFE 0.45 μm. The two enantiomers of **1** were separated using a chiral HPLC  
143 column (Chiralpak IF, 250 × 4.6 mm). The mobile phase consisted of n-Hexane/2-Propanol  
144 (90/10, v/v) acidified with 0.001 % TFA. Isocratic elution was performed at a flow-rate of 2  
145 mL/min. It was observed that the (-)-enantiomer of **1** was first eluted at 17.2 min, followed by  
146 the (+)-enantiomer at 30.8 min (**Supplementary material** Figure S2).

147 To obtain the two enantiomers of **1** and **2** in fair quantities, a preparative Phenomenex  
148 Lux Amylose-1 (150 × 10 mm, eluent: n-Hexane/2-Propanol 85/15 acidified with 0.01 % TFA,  
149 5 mL/min) was used. For **1**, the first enantiomer (**1a**) was collected at 21 min and the second  
150 one (**1b**) at 30 min, whereas for **2**, the first enantiomer (**2a**) was eluted at 17 min and the second  
151 one (**2b**) at 30 min (**Supplementary material** Figure S3).

#### 152 **2.4. ECD measurements.**

153 ECD spectra of compounds **1** and **2** were recorded in EtOH at 20 °C with a 0.2 cm path  
154 length quartz cell. The concentration of the two compounds was taken in the range  $1 \cdot 10^{-4} - 1.5$   
155  $10^{-4}$  M. Spectra were recorded in the 210 – 400 nm wavelength range with a 0.5 nm increment  
156 and a 1s integration time. Spectra were processed with standard spectrometer software, baseline

157 corrected and slightly smoothed by using a third order least square polynomial fit. Spectral units  
158 were expressed in difference of molar extinction coefficients ( $\Delta\epsilon$  in L/mol/cm).

### 159 **2.5. VCD measurements.**

160 IR and VCD spectra were recorded with a ThermoNicolet Nexus 670 FTIR spectrometer  
161 equipped with a VCD optical bench (Buffeteau et al., 2005). In this optical bench, the light  
162 beam was focused by a BaF<sub>2</sub> lens (191 mm focal length) to the sample, passing an optical filter,  
163 a BaF<sub>2</sub> wire grid polarizer (Specac), and a ZnSe photoelastic modulator (Hinds Instruments,  
164 Type II/ZS50). The light was then focused by a ZnSe lens (38.1 mm focal length) onto a 1x1  
165 mm<sup>2</sup> HgCdTe (ThermoNicolet, MCTA\* E6032) detector. IR and VCD spectra were recorded  
166 at a resolution of 4 cm<sup>-1</sup>, by coadding 50 scans and 36000 scans (12h acquisition time),  
167 respectively. The sample was held in a fixed path length (100  $\mu$ m) cell with BaF<sub>2</sub> windows. IR  
168 and VCD spectra of the two enantiomers *E*- $\epsilon$ -viniferin **1** and *E*- $\omega$ -viniferin **2** were measured in  
169 DMSO-*d*<sub>6</sub> at a concentration of 40 mM. Baseline correction of the VCD spectrum was  
170 performed by subtracting the two enantiomer VCD spectra of **1** and **2** (recorded under the same  
171 experimental concentration), with division by two. In all experiments, the photoelastic  
172 modulator was adjusted for a maximum efficiency at 1400 cm<sup>-1</sup>. Calculations were done with  
173 the standard ThermoNicolet software, using Happ and Genzel apodization, de-Haseth phase-  
174 correction and a zero-filling factor of one. Calibration spectra were recorded using a  
175 birefringent plate (CdSe) and a second BaF<sub>2</sub> wire grid polarizer, following the experimental  
176 procedure previously published (Nafie & Vidrine, 1982). Finally, in the presented IR spectra,  
177 the solvent absorption was subtracted out.

### 178 **2.6. DFT calculations.**

179 All DFT calculations were carried out with Gaussian 09 (Frisch et al., 2009). The  
180 calculation of the IR and VCD spectra began by a conformational analysis of (7a*S*,8a*S*)- and  
181 (7a*R*,8a*S*)-viniferin (**1a** and **2b**), considering a *trans* conformation of the C=C bond.

182 Preliminary conformer distribution search of **1a** and **2b** was performed at the molecular  
183 mechanics level of theory, employing MMFF94 force fields incorporated in ComputeVOA  
184 software package. 290 conformers of **1a** (305 conformers for **2b**) were found within roughly 4  
185 kcal/mol of the lowest energy conformer. Their geometries were optimized at the DFT level  
186 using B3LYP functional and 6-31G\*\* basis set, leading to 74 (**1a**) and 61 (**2b**) different  
187 conformers within an energetic window of 3.25 (**1a**) and 2.87 (**2b**) kcal/mol. Finally, only the  
188 twenty four (**1a**) and twenty five (**1b**) lowest energetic geometries were kept, corresponding to  
189 Boltzmann population higher than 1%. Vibrational frequencies, IR and VCD intensities were  
190 calculated at the same level of theory. The spectra were calculated for the isolated molecule *in*  
191 *vacuo*. For comparison to experiment, the calculated frequencies were scaled by 0.968 and the  
192 calculated intensities were converted to Lorentzian bands with a full-width at half-maximum  
193 (FWHM) of 7 cm<sup>-1</sup>.

#### 194 **2.7. Macrophages cell culture.**

195 RAW 264.7 cells were obtained from the American Type Culture Collection (ATCC).  
196 They were cultured in 75 cm<sup>2</sup> flasks containing 20 mL of DMEM supplemented with 10% of  
197 FBS. Cells were maintained in a humidified incubator at 37°C and 5% of CO<sub>2</sub>. In order to  
198 perform the experiments, every 3 days cells were detached by scrapping and sub-cultured in 96  
199 transparent (for cytotoxicity and NO measurements) or black (ROS measurement) well plates  
200 with the same culture medium (200 µL) supplemented with 4 mM of glutamine at a density of  
201 40,000 cells per well.

#### 202 **2.8. MTT assay.**

203 The cytotoxicity of stereoisomers of viniferin (**1a**, **1b**, **2a** and **2b**) was carried out by using  
204 MTT that allows to measure the cellular metabolic activity of cells. After 24 hours of incubation  
205 in 96 well plates, cells were incubated with different concentrations of the four stereoisomers  
206 (0.5 to 100 µM) of viniferin (**1a**, **1b**, **2a** and **2b**). After 24 hours of treatment, cells were

207 incubated with 0.5 mg/mL of MTT during 3 hours at 37°C and 5% of CO<sub>2</sub>. Finally, the blue  
208 formazan crystals formed at the well bottom were dissolved with 100 µL of DMSO and, 30  
209 minutes after, the absorbance was measured with a microplate reader (FLUOstar Optima, BMG  
210 Labtech) set at 595 nm.

### 211 **2.9. Measurement of NO production.**

212 In order to evaluate the anti-inflammatory potential of the stereoisomers of viniferin (**1a**,  
213 **1b**, **2a** and **2b**), RAW 264.7 cells were incubated during 24 hours with all compounds at  
214 different non-cytotoxic concentrations (0.5, 1, 2.5, 5 and 10 µM) in the presence or absence of  
215 LPS (inflammatory triggering agent) in RPMI medium. Then, 70 µL of supernatant were mixed  
216 with 70 µL of Griess reagent and after an incubation of 15 minutes at room temperature, the  
217 absorbance was measured at 540 nm by using a microplate reader (FLUOstar Optima, BMG  
218 Labtech). NO concentration by using a calibration standard curve of sodium nitrite (0-100 µM).

### 219 **2.10. Intracellular ROS measurement.**

220 The intracellular generation of ROS in cells was analyzed using the fluorometric probe  
221 DCFH<sub>2</sub>-DA. After treatment with the stereoisomers of viniferin (**1a**, **1b**, **2a** and **2b**) at different  
222 concentrations (0.5, 1, 2.5, 5 and 10 µM) during 24 hours in 96 black well plates, cells were  
223 washed and 5 mM of DCFH<sub>2</sub>-DA diluted in PBS was added. After 30 minutes of incubation in  
224 the darkness at 37°C and 5% of CO<sub>2</sub>, the fluorescence intensity was measured using a  
225 microplate reader (FLUOstar Optima, BMG Labtech) set at 485 nm (excitation wavelength)  
226 and 520 nm (emission wavelength).

### 227 **2.11. Statistical Analysis.**

228 Data were subjected to one-way ANOVA followed by a Tukey's test ( $p < 0.05$ ) with  
229 Microsoft Excel® XLSTAT (Version 1.1.463) to explore significant differences for cell  
230 viability, NO and ROS measurements.

231

### 232 3. Results and Discussion

#### 233 3.1. Isolation of viniferin dimers and chiroptical properties in grape varieties

234 100 g of dry fine powder of *Vitis vinifera* cv. Merlot stalks, previously defatted with  
235 petroleum ether, was extracted two times with 60% aqueous acetone at room temperature. The  
236 extract was then filtered and the filtrate was concentrated *in vacuo*. The aqueous phase was  
237 further partitioned between EtOAc and water. The organic extract was separated by  
238 combination of centrifugal partition chromatography (**Supplementary material** Figure S1) and  
239 preparative RP-18 HPLC to obtain *E-ε*-viniferin with  $[\alpha]_{589}^{20} = +10.4^\circ$  (c 0.2, MeOH) and *E-ω*-  
240 viniferin with  $[\alpha]_{589}^{20} = -103^\circ$  (c 0.15, MeOH). In addition, the *E-ε*-viniferin was purified from  
241 three different grape varieties (Cabernet Sauvignon, Merlot, and Sauvignon Blanc). The  
242 specific optical rotation values of *E-ε*-viniferin varied between -12 and +46° (**Supplementary**  
243 **material** Table S1), indicating that *E-ε*-viniferin is not enantiopure. This could be related to the  
244 fact that the enantiomeric ratio of *E-ε*-viniferin could be different due to the grape varieties. For  
245 example, Cabernet Sauvignon variety gives the dextrorotatory form of *E-ε*-viniferin whereas  
246 the Merlot variety gives preferentially the levorotatory form. On the other hand, Sauvignon  
247 Blanc exhibits a lower value of specific rotation that probably means the presence of rather  
248 racemic mixture (**Supplementary material** Table S1). These values are in agreement with  
249 those reported in the literature from *V. vinifera* (Vitaceae) and others plant families, as shown  
250 in **Table 2**. The proportion of the two enantiomers of *E-ε*-viniferin and the enantiomeric excess  
251 (ee) for the three grape varieties are given in **Supplementary material** Table S2. The  
252 enantiomeric excess (ee) extracted from Cabernet Sauvignon, Merlot and Sauvignon Blanc  
253 grape varieties was measured by analytical chiral HPLC (**Supplementary material** Figure S2).  
254 **Table 2.** Optical rotation values of *E-ε*-viniferin measured in this study and found in the  
255 literature.

Species	Family	$[\alpha]_{589}^{20}$	Conditions	Reference
---------	--------	-----------------------	------------	-----------

<i>Vitis vinifera</i>	Vitaceae	+10.4°	0.13, MeOH	This study
cv. Merlot				
<i>Vitis vinifera</i>	Vitaceae	+46.4°	0.064, MeOH	This study
cv. Cabernet Sauvignon				
<i>Vitis vinifera</i>	Vitaceae	-12.1°	0.07, MeOH	This study
cv. Merlot				
<i>Vitis vinifera</i>	Vitaceae	+5.9°	0.083, MeOH	This study
cv. Sauvignon Blanc				
<i>Vitis amurensis</i>	Vitaceae	+41°	0.13, MeOH	(Pawlus et al., 2013)
<i>Vitis vinifera</i>	Vitaceae	+34°	0.32, MeOH	(Mattivi et al., 2011)
<i>Vitis heyneana</i>	Vitaceae	+39°	0.40, MeOH	(Li et al., 1996)
<i>Vitis chunganensis</i>	Vitaceae	+32°	0.27, MeOH	(He et al., 2009)
<i>Carex pumila</i>	Cyperaceae	-27,9°	0.843, MeOH	(Kurihara et al., 1990)
<i>Carex kobomugi</i>	Cyperaceae	-46°	0.5, MeOH	(Kurihara et al., 1991)
Rhubarb	Polygonaceae	-47°	0.5, MeOH	(Ngoc et al., 2008)
<i>Paeonia lactiflora</i>	Paeoniaceae	+59°	0.2, MeOH	(Yuk et al., 2013)

256

### 257 3.2. Absolute configuration of viniferin stereoisomers using NMR, VCD and ECD

258 According to the above observations, *E-ε*-viniferin (mixture of enantiomers) was then  
259 purified by chiral HPLC to separate the two enantiomers (**Supplementary material** Figure S3).  
260 The first eluted compound showed a specific optical rotation value  $[\alpha]_{589}^{20} = -43.4^\circ$  (c 0.06,  
261 MeOH) whereas a value  $[\alpha]_{589}^{20} = +46^\circ$  (c 0.06, MeOH) was measured for the second eluted  
262 compound. Accordingly, we have shown that *E-ω*-viniferin was also a mixture of enantiomers  
263 and it was purified by chiral HPLC as mentioned above to yield  $[\alpha]_{589}^{20} = +107^\circ$  (c 0.07, MeOH)  
264 for the first eluted compound and  $[\alpha]_{589}^{20} = -155^\circ$  (c 0.14, MeOH) for the second eluted  
265 compound. The NMR data ( $^1\text{H}$  and  $^{13}\text{C}$ ) of *E-ε*- and *E-ω*-viniferin were found to be similar to  
266 those previously obtained in our laboratory and in literature (**Supplementary material** Table  
267 S3, Figures S4 and S6) (Pawlus et al., 2013; Mattivi et al., 2011). The relative configuration

268 was established by ROESY. For *E-ε*-viniferin, the absence of NOE correlation between protons  
269 H7a/H8a (**Supplementary material** Figure S5) indicated that these protons were *trans*-  
270 orientated whereas for *E-ω*-viniferin, the cross peak between H7a/H8a (**Supplementary**  
271 **material** Figure S7), indicated these protons were cofacial (*cis*-orientation). In addition, the IR  
272 spectra of *E-ε*- and *E-ω*-viniferin allow the discrimination of the two diastereoisomers, using  
273 the intensity of the band at 1148 cm<sup>-1</sup>. Indeed, the *E-ω*-viniferin compound exhibits a high  
274 intensity for this band, whereas the 1148 cm<sup>-1</sup> band is weak for the *E-ε*-viniferin compound  
275 (**Supplementary material** Figure S8).

276 The absolute configurations of the chiral centers (C7a and C8a) of *E-ε*-viniferin and *E*-  
277 *ω*-viniferin were deduced in the same manner as for the two enantiomers of (-)-*E*-gnetin C  
278 (Buffeteau et al., 2014), using vibrational circular dichroism (VCD) associated with theoretical  
279 calculations. VCD spectra of the two enantiomers of compounds **1** and **2** were recorded in  
280 DMSO-*d*<sub>6</sub> at a concentration of 40 mM and the raw and baseline corrected VCD spectra are  
281 reported in **Supplementary material** Figures S9 and S10. For each compound, opposite VCD  
282 spectra were measured for the two enantiomers, as expected for enantiopure compounds.

283 The theoretical calculations began by a conformational analysis of (7a*S*,8a*S*)-*E-ε*-  
284 viniferin (**1a**) and (7a*R*,8a*S*)-*E-ω*-viniferin (**2b**). Preliminary conformer distribution search of  
285 **1a** and **2b** was performed at the molecular mechanics level of theory, employing MMFF94  
286 force fields incorporated in ComputeVOA software package. 290 conformers of **1a** (305  
287 conformers for **2b**) were found within roughly 4 kcal/mol of the lowest energy conformer. Their  
288 geometries were optimized at the DFT level using B3LYP functional and 6-31G\*\* basis set,  
289 leading to 74 (**1a**) and 61 (**2b**) different conformers within an energetic window of 3.25 (**1a**)  
290 and 2.87 (**2b**) kcal/mol. Finally, only the twenty four (**1a**) and twenty five (**1b**) lowest energetic  
291 geometries were kept, corresponding to Boltzmann population higher than 1%. Calculations  
292 were performed for the isolated molecule *in vacuo*. Harmonic vibrational frequencies were

293 calculated at the same level to confirm that all structures were stable conformations and to  
294 enable free energies to be calculated. The predicted VCD spectra, taking into account the  
295 relative populations of (7a*S*,8a*S*)-*E*- $\epsilon$ -viniferin and (7a*R*,8a*S*)-*E*- $\omega$ -viniferin, were compared to  
296 the experimental VCD spectra of the second eluted compound of **1** and **2** in **Figure 2**. The  
297 predicted VCD spectra of (7a*S*,8a*S*)-*E*- $\epsilon$ -viniferin and (7a*R*,8a*S*)-*E*- $\omega$ -viniferin reproduced  
298 fairly well the intensity and the sign of most bands observed in the experimental VCD spectra,  
299 allowing the definitive determination of the 8a*S* configuration of the beta stereogenic carbon of  
300 the benzofuran group. The determination of the configuration of the alpha stereogenic carbon  
301 was less obvious from VCD data, even though a better agreement between theoretical and  
302 experimental spectra in the 1550-1400 cm<sup>-1</sup> spectral range was obtained with the 7a*S*  
303 configuration for the second eluted compound of **1** and with the 7a*R* configuration for the  
304 second eluted compound of **2**. The 7a*S* configuration of the alpha stereogenic carbon of  
305 benzofuran group for the second eluted compound of **1** was confirmed by the absence of a cross-  
306 peak between the protons H7a ( $\delta$ =5.41 ppm) and H8a ( $\delta$ =4.47 ppm) in the ROESY spectrum  
307 (**Supplementary material** Figure S5), indicating the opposite orientation of these two protons.  
308 Similarly, the 7a*R* configuration of the alpha stereogenic carbon of benzofuran group for the  
309 second eluted compound of **2** was confirmed by the presence of a cross-peak between the  
310 protons H7a ( $\delta$ =5.86 ppm) and H8a ( $\delta$ =4.70 ppm) in the ROESY spectrum (**Supplementary**  
311 **material** Figure S7), indicating the cofacial orientation of these two protons. Thus, this VCD  
312 analysis, associated with NMR results, unambiguously established the (+)-(7a*S*,8a*S*)  
313 configuration for *E*- $\epsilon$ -viniferin and the (+)-(7a*R*,8a*S*) configuration for *E*- $\omega$ -viniferin. This  
314 result confirm the first proposition of the absolute configuration, (-)-(7a*R*,8a*R*), for *E*- $\epsilon$ -  
315 viniferin isolated from *Carex pumila* (Cyperaceae) by Kurihara et al. (1990).

316 The experimental VCD spectra measured for *E*- $\epsilon$ -viniferin extracted from different  
317 grape varieties are compared in **Figure 3** with the VCD spectrum of the enantiopure second

318 eluted compound purified by chiral HPLC. The VCD spectrum of *E-ε*-viniferin extracted from  
319 Cabernet Sauvignon stalks is quasi identical to the VCD spectrum of the enantiopure  
320 compound, revealing that this grape variety allows the extraction of *E-ε*-viniferin with an  
321 enantiomeric excess close to 1. Chiral HPLC measurements on this compound revealed an  
322 enantiomeric excess of 98.34% (**Supplementary material** Table S2). This feature is very  
323 interesting since the enantiopure (+)-(7*aS*,8*aS*)-*E-ε*-viniferin compound can be obtained  
324 directly by extraction from Cabernet Sauvignon. The VCD spectrum of *E-ε*-viniferin extracted  
325 from Merlot is opposite with an intensity divided by almost 4, as expected by the enantiomeric  
326 excess measured by chiral HPLC (ca. 23.32%). Finally, the VCD spectrum of *E-ε*-viniferin  
327 extracted from Sauvignon Blanc exhibits a very weak intensity, with the same sign than the one  
328 of Cabernet Sauvignon, as expected by chiral HPLC measurements.

329 As electronic circular dichroism (ECD) experiments are currently used in the structural  
330 studies of stilbenes, ECD spectra of the second eluted compound of **1** and **2** are reported in  
331 **Supplementary material** Figures S11 and S12, respectively. The ECD spectrum of (+)-*E-ε*-  
332 viniferin exhibits a positive band at 236 nm (+22.7) and a broad negative band around 300 nm  
333 (-3.8), in agreement with the ECD spectrum reported in the literature (Ito et al., 2009). The ECD  
334 spectrum of (+)-*E-ω*-viniferin is slightly different, with a positive band at 227.5 nm (+17), a  
335 negative band at 250 nm (-3.3) and a broad negative band around 310 nm (-7).

### 336 *3.3. Antioxidant and anti-inflammatory activities of viniferin stereoisomers in LPS-stimulated* 337 *macrophages*

338 The four stereoisomers of viniferin (**1a**, **1b**, **2a** and **2b**) were evaluated for their anti-  
339 inflammatory and anti-oxidant activities in LPS-stimulated macrophages. Firstly, the MTT  
340 assay was performed in order to evaluate the cytotoxicity of all stereoisomers. Thus, cells were  
341 treated with different concentrations of viniferin **1a**, **1b**, **2a** and **2b** (0.5-100 μM) during 24  
342 hours. **Figure 4a** displays the cell viability expressed as percentage relative to the non-treated

343 cells. As expected, the LPS did not affect the cell viability. Concerning viniferin stereoisomers,  
344 it can be observed that at low concentrations, between 0.5 to 10  $\mu\text{M}$ , the metabolic activity of  
345 cells was not affected. However, from 25  $\mu\text{M}$ , all compounds presented a significant cytotoxic  
346 effect, by killing between 40-70% of cells (**Figure 4a**). It can be also observed that compound  
347 **2a** presents a more slight toxic effect at 25  $\mu\text{M}$  comparing with the others compounds at the  
348 same concentrations. No significant differences were observed between all stereoisomers at the  
349 highest concentrations (50-100  $\mu\text{M}$ ). Based on these results, the concentrations ranging between  
350 0.5 to 10  $\mu\text{M}$  were selected to further evaluate the potential effect of viniferin stereoisomers to  
351 diminish the nitric oxide (NO) and reactive oxygen species (ROS) production.

352 RAW 264.7 cells were activated with LPS (0.1  $\mu\text{g/mL}$ ) in the presence of the four  
353 stereoisomers of viniferin at 0.5, 1, 2.5, 5 and 10  $\mu\text{M}$  during 24 hours. Afterwards, the  $\text{NO}_2$  in  
354 culture media were measured by the Griess reaction. The NO content ( $\mu\text{M}$ ) of cells treated with  
355 only LPS (positive control) increased more than tenfold (26.9  $\mu\text{M}$ ) in comparison with the  
356 negative control (2.4  $\mu\text{M}$ ) (cells without LPS treatment) (**Figure 4b**). A significant diminution  
357 of NO was observed at all concentrations of **1a** and **1b**. However, this effect is significant for  
358 **2a** and **2b** only from 2.5  $\mu\text{M}$ . Regarding differences between compounds, at the highest  
359 concentration tested (10  $\mu\text{M}$ ) it can be seen a more potent effect of **1a** with a diminution of 60%  
360 of NO production while for **1b** this decrease is 41%. By contrast, at this concentration the **2a**  
361 and **2b** exhibited the same effect (52 and 55%, respectively) (**Figure 4b**).

362 In addition, the intracellular ROS production induced by LPS was investigated by using  
363 the fluorometric probe DCFH<sub>2</sub>-DA, which permits the detection and quantification of ROS. The  
364 results show that **1a** is significantly the most active stereoisomer diminishing the intracellular  
365 ROS from the lowest concentration and reaching a reduction of 63% comparing with LPS alone.  
366 We can also observe differences between **2a** and **2b**, being this last significantly more anti-

367 oxidant, and diminishing the ROS production on 48% while only a 21% was observed for **2a**  
368 in comparison with control (**Figure 4c**).

369 Based on these results it can be concluded that viniferin stereoisomers possess *in vitro*  
370 anti-inflammatory and anti-oxidant properties in macrophages cells and that their activity varies  
371 according to their spatial configuration. Apart from resveratrol, other oligomeric stilbenes, as  
372 different viniferins, are showing promising results as anti-inflammatory, anti-oxidant,  
373 neuroprotective, anti-obesity, anticancer agents (Nassra et al., 2013; Ohara et al., 2015; Ficarra  
374 et al., 2016; Caillaud et al., 2019; Nivellet et al., 2018; Vion et al., 2018; Sergi et al., 2021).

375 Our results demonstrate that the four stereoisomers are toxic from 10  $\mu$ M concentration  
376 in RAW 264.7 cells. The same observation has been described for viniferin compounds in the  
377 same cellular model (Ha et al., 2018), but also in other cellular models as BV2 or Caco-2 cells  
378 (Nassra et al., 2013; Medrano-Padial et al., 2020).

379 Concerning anti-inflammatory properties, Nassra and co-workers showed that viniferins  
380 (*E*- $\delta$ -viniferin, *E*- $\epsilon$ -viniferin and *E*- $\omega$ -viniferin present very similar inhibitory capacity to reduce  
381 LPS-induced NO production in BV2 microglial cells. They showed that *E*- $\epsilon$ -viniferin is the  
382 most active compound (IC<sub>50</sub>: 8.6) presenting even better results than *E*-resveratrol (IC<sub>50</sub>: 13.1)  
383 (Nassra et al., 2013). Additionally, other more recent published article has demonstrated that  
384 *E*- $\epsilon$ -viniferin, also at low concentrations, is able to counteract the inflammation induced by  
385 LPS-activated microglia in N9 cells (Sergi et al., 2021). Only one recent article has  
386 demonstrated in our same cellular model (RAW 264.7 macrophage cells) that *E*- $\epsilon$ -viniferin  
387 decreased NO, PGE<sub>2</sub>, iNOS, and COX-2 productions after LPS stimulation and that this activity  
388 is may be mediated by the NF- $\kappa$ B activation (Ha et al., 2018). The present findings demonstrate  
389 for the first time that viniferin stereoisomers possess anti-inflammatory and anti-oxidant  
390 activities. Moreover and even though their structures are quite similar, this paper proved that  
391 these bioactivities are different according to their configuration.

## 392 **4. Conclusion**

393 In summary, this work demonstrated for the first time the presence of four stereoisomers  
394 of viniferin stilbene (*7aS,8aS*)-*E-ε*-viniferin, (*7aR,8aR*)-*E-ε*-viniferin, (*7aS,8aR*)-*E-ω*-viniferin,  
395 and (*7aR,8aS*)-*E-ω*-viniferin in grapevine branches. The absolute configurations were clearly  
396 established by vibrational circular dichroism (VCD) spectroscopy in combination with density  
397 functional theory (DFT) calculations. Moreover, the anti-inflammatory and anti-oxidant  
398 activities of the four identified viniferin stereoisomers revealed that viniferin stereoisomers  
399 possess different bioactivities according to their configuration. In addition, for the first time,  
400 the two enantiomers of *E-ε*-viniferin in grapevine are present and the enantiomeric excess are  
401 grape variety-dependent. Overall, the present study extends our knowledge of absolute  
402 stereochemistry of viniferin dimers present in grapevine and paves the way for further  
403 investigation related to their structure-activity relationship.

404

## 405 **ASSOCIATED CONTENT**

### 406 **Supporting Information**

407 The following data are available as supplementary material: Specific optical rotation values of  
408 *E-ε*-viniferin (Table S1), enantiomeric excess for the three grape varieties (Table S2), NMR  
409 data of *E-ε*-viniferin and *E-ω*-viniferin (Table S3), CPC chromatogram (Figure S1), analytical  
410 (Figure S2) and preparative (Figure S3) chiral HPLC chromatograms, <sup>1</sup>H NMR and <sup>1</sup>H-<sup>1</sup>H-  
411 ROESY NMR spectra of *E-ε*-viniferin (Figure S4 and S5), <sup>1</sup>H NMR and <sup>1</sup>H-<sup>1</sup>H-ROESY NMR  
412 spectra of *E-ω*-viniferin (Figure S6 and S7), IR spectra of *E-ε*-viniferin and *E-ω*-viniferin  
413 (Figure S8), VCD spectra of *E-ε*-viniferin and *E-ω*-viniferin (Figures S9 and S10), ECD spectra  
414 of *E-ε*-viniferin and *E-ω*-viniferin (Figures S11 and S12).

## 415 **ACKNOWLEDGMENTS**

416 The authors thank R. Cooke for proofreading the manuscript.

417 **FUNDING**

418 Research support was provided by the French Ministry of Higher Education and Research.  
419 NMR experiments were performed at the Bordeaux Metabolome Facility and MetaboHUB  
420 (ANR-11-INBS-0010 project).

421 **REFERENCES**

- 422 Alkadi, H., & Jbeily, R. (2018). Role of chirality in drugs: an overview. *Infectious Disorders*  
423 *Drug Targets*, 18(2), 88–95. <https://doi.org/10.2174/1871526517666170329123845>
- 424 Barceló, A. R., Pomar, F., López-Serrano, M., & Pedreño, M. A. (2003). Peroxidase: a  
425 multifunctional enzyme in grapevines. *Functional Plant Biology*, 30(6), 577–591.  
426 <https://doi.org/10.1071/fp02096>
- 427 Breuil, A. C., Adrian, M., Pirio, N., Meunier, P., Bessis, R., & Jeandet, P. (1998). Metabolism  
428 of stilbene phytoalexins by *Botrytis cinerea*: 1. Characterization of a resveratrol  
429 dehydrodimer. *Tetrahedron Letters*, 39(7), 537–540. [https://doi.org/10.1016/S0040-](https://doi.org/10.1016/S0040-4039(97)10622-0)  
430 [4039\(97\)10622-0](https://doi.org/10.1016/S0040-4039(97)10622-0)
- 431 Buffeteau, T., Cavagnat, D., Bisson, J., Marchal, A., Kapche, G. D., Battistini, I., Da Costa, G.,  
432 Badoc, A., Monti, J.-P., Mérillon, J.-M., & Waffo-Téguo, P. (2014). Unambiguous  
433 determination of the absolute configuration of dimeric stilbene glucosides from the  
434 rhizomes of *Gnetum africanum*. *Journal of Natural Products*, 77(8), 1981–1985.  
435 <https://doi.org/10.1021/np500427v>
- 436 Buffeteau, T., Lagugné-Labarthe, F., & Sourisseau, C. (2005). Vibrational circular dichroism  
437 in general anisotropic thin solid films: measurement and theoretical approach. *Applied*  
438 *Spectroscopy*, 59(6), 732–745. <https://doi.org/10.1366/0003702054280568>
- 439 Caillaud, M., Guillard, J., Richard, D., Milin, S., Chassaing, D., Paccalin, M., Page, G., & Bilan,  
440 A. R. (2019). *Trans*  $\epsilon$  viniferin decreases amyloid deposits and inflammation in a mouse

441 transgenic Alzheimer model. *PLoS ONE*, *14*(2) : e0212663.  
442 <https://doi.org/10.1371/journal.pone.0212663>

443 Calderón, A. A., Zapata, J. M., Pedreño, M. A., Muñoz, R., & Barceló, A. R. (1992). Levels of  
444 4-hydroxystilbene-oxidizing isoperoxidases related to constitutive disease resistance in  
445 *in vitro*-cultured grapevine. *Plant Cell, Tissue and Organ Culture*, *29*(2), 63–70.

446 Cichewicz, R. H., Kouzi, S. A., & Hamann, M. T. (2000). Dimerization of resveratrol by the  
447 grapevine pathogen *Botrytis cinerea*. *Journal of Natural Products*, *63*(1), 29–33.  
448 <https://doi.org/10.1021/np990266n>

449 Cretin, B. N., Sallembien, Q., Sindt, L., Daugey, N., Buffeteau, T., Waffo-Teguo, P.,  
450 Dubourdieu, D., & Marchal, A. (2015). How stereochemistry influences the taste of  
451 wine: isolation, characterization and sensory evaluation of lyoniresinol stereoisomers.  
452 *Analytica Chimica Acta*, *888*, 191-198. <https://doi.org/10.1016/j.aca.2015.06.061>

453 Ficarra, S., Tellone, E., Pirolli, D., Russo, A., Barreca, D., Galtieri, A., Giardina, B., Gavezzotti,  
454 P., Riva, S., & Rosa, M. C. D. (2016). Insights into the properties of the two enantiomers  
455 of *trans*- $\delta$ -viniferin, a resveratrol derivative: antioxidant activity, biochemical and  
456 molecular modeling studies of its interactions with hemoglobin. *Molecular BioSystems*,  
457 *12*, 1276-1286. <https://doi.org/10.1039/c5mb00897b>

458 Frisch, M. J., Trucks, G. W., Schlegel, H. B., Scuseria, G. E., Robb, M. A., Cheeseman, J. R.,  
459 Scalmani, G., Barone, V., Mennucci, B., Petersson, G. A., Nakatsuji, H., Caricato, M.,  
460 Li, X., Hratchian, H. P., Izmaylov, A. F., Bloino, J., Zheng, G., Sonnenberg, J. L., Hada,  
461 M.; Ehara, M., Toyota, K., Fukuda, R., Hasegawa, J., Ishida, M., Nakajima, T., Honda,  
462 Y., Kitao, O., Nakai, H., Vreven, T., Montgomery, J. A. Jr., Peralta, J. E., Ogliaro, F.,  
463 Bearpark, M., Heyd, J. J., Brothers, E., Kudin, K. N., Staroverov, V. N., Kobayashi, R.,  
464 Normand, J., Raghavachari, K., Rendell, A., Burant, J. C., Iyengar, S. S., Tomasi, J.,

465 Cossi, M., Rega, N., Millam, J. M., Klene, M., Knox, J. E., Cross, J. B., Bakken, V.,  
466 Adamo, C., Jaramillo, J., Gomperts, R., Stratmann, R. E., Yazyev, O., Austin, A. J.,  
467 Cammi, R., Pomelli, C., Ochterski, J. W., Martin, R. L., Morokuma, K., Zakrzewski, V.  
468 G., Voth, G. A., Salvador, P., Dannenberg, J. J., Dapprich, S., Daniels, A. D., Farkas, Ö  
469 ., Foresman, J. B., Ortiz, J. V., Cioslowski, J., Fox, D. J. Gaussian 09, Revision A.01;  
470 Gaussian Inc.: Wallingford, CT, 2009. Retrieved September 25, 2021, from  
471 <https://gaussian.com/glossary/g09/>

472 Ha, D. T., Long, P. T., Hien, T. T., Tuan, D. T., An, N. T. T., Khoi, N. M., Van Oanh, H., &  
473 Hung, T. M. (2018). Anti-inflammatory effect of oligostilbenoids from *Vitis heyneana*  
474 in LPS-stimulated RAW 264.7 macrophages via suppressing the NF-κB activation.  
475 *Chemistry Central Journal*, 12(1), 14. <https://doi.org/10.1186/s13065-018-0386-5>

476 He, S., Jiang, L., Wu, B., Li, C., & Pan, Y. (2009). Chunganenol: an unusual antioxidative  
477 resveratrol hexamer from *Vitis chunganensis*. *The Journal of Organic Chemistry*,  
478 74(20), 7966–7969. <https://doi.org/10.1021/jo901354p>

479 Ito, T., Abe, N., Oyama, M., & Iinuma, M. (2009). Absolute structures of C-glucosides of  
480 resveratrol oligomers from *Shorea uliginosa*. *Tetrahedron Letters*, 50, 2516–2520.  
481 <https://doi.org/10.1016/j.tetlet.2009.03.043>

482 Keylor, M. H., Matsuura, B. S., & Stephenson, C. R. J. (2015). Chemistry and biology of  
483 resveratrol-derived natural products. *Chemical Reviews*, 115(17), 8976–9027.  
484 <https://doi.org/10.1021/cr500689b>

485 Ko, J.-H., Sethi, G., Um, J.-Y., Shanmugam, M. K., Arfuso, F., Kumar, A. P., Bishayee, A., &  
486 Ahn, K. S. (2017). The role of resveratrol in cancer therapy. *International Journal of*  
487 *Molecular Sciences*, 18(12). <https://doi.org/10.3390/ijms18122589>

488 Kurihara, H., Kawabata, J., Ichikawa, S., Mishima, M., & Mizutani, J. (1991). Oligostilbenes  
489 from *Carex kobomugi*. *Phytochemistry*, 30(2), 649–653. <https://doi.org/10.1016/0031->  
490 9422(91)83745-7

491 Kurihara, H., Kawabata, J., Ichikawa, S., & Mizutani, J. (1990). (-)-e-Viniferin and related  
492 oligostilbenes from *Carex pumila* Thunb. (Cyperaceae). *Agricultural and Biological*  
493 *Chemistry*, 54(4), 1097–1099.

494 Li, W. W., Ding, L. S. eng, Li, B. G. ng, & Chen, Y. Z. (1996). Oligostilbenes from *Vitis*  
495 *heyneana*. *Phytochemistry*, 42(4), 1163–1165. <https://doi.org/10.1016/0031->  
496 9422(96)00069-6

497 Mattivi, F., Vrhovsek, U., Malacarne, G., Masuero, D., Zulini, L., Stefanini, M., Moser, C.,  
498 Velasco, R., & Guella, G. (2011). Profiling of resveratrol oligomers, important stress  
499 metabolites, accumulating in the leaves of hybrid *Vitis vinifera* (Merzling × Teroldego)  
500 genotypes infected with *Plasmopara viticola*. *Journal of Agricultural and Food*  
501 *Chemistry*, 59(10), 5364–5375. <https://doi.org/10.1021/jf200771y>

502 Medrano-Padial, C., Puerto, M., Merchán-Gragero, M. D. M., Moreno, F. J., Richard, T.,  
503 Cantos-Villar, E., & Pichardo, S. (2020). Cytotoxicity studies of a stilbene extract and  
504 its main components intended to be used as preservative in the wine industry. *Food*  
505 *Research International*, 137, 109738. <https://doi.org/10.1016/j.foodres.2020.109738>

506 Morales, M., & Barceló, A. R. (1997). A basic peroxidase isoenzyme from vacuoles and cell  
507 walls of *Vitis vinifera*. *Phytochemistry*, 45(2), 229–232. <https://doi.org/10.1016/S0031->  
508 9422(96)00825-4

509 Nafie, L. A., Vidrine, D. W. In *Fourier Transform Infrared Spectroscopy*; Ferraro, J. R.; Basile,  
510 L. J., Eds.; Academic Press: New York, 1982; Vol. 3, pp 83–123.

511 Nassra, M., Krisa, S., Papastamoulis, Y., Kapche, G. D., Bisson, J., André, C., Konsman, J.-P.,  
512 Schmitter, J.-M., Mérillon, J.-M., & Waffo-Téguo, P. (2013). Inhibitory activity of plant  
513 stilbenoids against nitric oxide production by lipopolysaccharide-activated microglia.  
514 *Planta Medica*, 79(11), 966–970. <https://doi.org/10.1055/s-0032-1328651>

515 Ngoc, T. M., Hung, T. M., Thuong, P. T., Na, M., Kim, H., Ha, D. T., Min, B.-S., Minh, P. T.  
516 H., & Bae, K. (2008). Inhibition of human low density lipoprotein and high density  
517 lipoprotein oxidation by oligostilbenes from rhubarb. *Biological & Pharmaceutical*  
518 *Bulletin*, 31(9), 1809–1812. <https://doi.org/10.1248/bpb.31.1809>.

519 Nivelles, L., Aires, V., Rioult, D., Martiny, L., Tarpin, M., & Delmas, D. (2018). Molecular  
520 analysis of differential antiproliferative activity of resveratrol, epsilon viniferin and  
521 labruscol on melanoma cells and normal dermal cells. *Food and Chemical Toxicology*,  
522 116(Pt B), 323–334. <https://doi.org/10.1016/j.fct.2018.04.043>

523 Ohara, K., Kusano, K., Kitao, S., Yanai, T., Takata, R., & Kanauchi, O. (2015). ε-Viniferin, a  
524 resveratrol dimer, prevents diet-induced obesity in mice. *Biochemical and Biophysical*  
525 *Research Communications*, 468(4), 877–882.  
526 <https://doi.org/10.1016/j.bbrc.2015.11.047>

527 Pawlus, A. D., Sahli, R., Bisson, J., Rivière, C., Delaunay, J.-C., Richard, T., Gomès, E.,  
528 Bordenave, L., Waffo-Téguo, P., & Mérillon, J.-M. (2013). Stilbenoid profiles of canes  
529 from *Vitis* and *Muscadinia* species. *Journal of Agricultural and Food Chemistry*, 61(3),  
530 501–511. <https://doi.org/10.1021/jf303843z>

531 Pezet, R. (1998). Purification and characterization of a 32-kDa laccase-like stilbene oxidase  
532 produced by *Botrytis cinerea* Pers.:Fr. *FEMS Microbiology Letters*, 167(2), 203–208.

533 Richard, T., Pawlus, A. D., Iglesias, M.-L., Pedrot, E., Waffo-Teguo, P., Merillon, J.-M., &  
534 Monti, J.-P. (2011). Neuroprotective properties of resveratrol and derivatives. *Annals of*  
535 *the New York Academy of Sciences*, 1215(1), 103–108. <https://doi.org/10.1111/j.1749->  
536 [6632.2010.05865.x](https://doi.org/10.1111/j.1749-6632.2010.05865.x)

537 Rivière, C., Pawlus, A. D., & Mérillon, J.-M. (2012). Natural stilbenoids: distribution in the  
538 plant kingdom and chemotaxonomic interest in Vitaceae. *Natural Product Reports*,  
539 29(11), 1317–1333. Scopus. <https://doi.org/10.1039/c2np20049j>

540 Saiko, P., Szakmary, A., Jaeger, W., & Szekeres, T. (2008). Resveratrol and its analogs: defense  
541 against cancer, coronary disease and neurodegenerative maladies or just a fad? *Mutation*  
542 *Research*, 658(1–2), 68–94. <https://doi.org/10.1016/j.mrrev.2007.08.004>

543 Sergi, D., Gélinas, A., Beaulieu, J., Renaud, J., Tardif-Pellerin, E., Guillard, J., & Martinoli,  
544 M.-G. (2021). Anti-apoptotic and anti-inflammatory role of *trans*  $\epsilon$ -viniferin in a  
545 neuron-glia co-culture cellular model of Parkinson's disease. *Foods*, 10(3), 586.  
546 <https://doi.org/10.3390/foods10030586>

547 Shang, Y.-J., Qian, Y.-P., Liu, X.-D., Dai, F., Shang, X.-L., Jia, W.-Q., Liu, Q., Fang, J.-G., &  
548 Zhou, B. (2009). Radical-scavenging activity and mechanism of resveratrol-oriented  
549 analogues: influence of the solvent, radical, and substitution. *The Journal of Organic*  
550 *Chemistry*, 74(14), 5025–5031. <https://doi.org/10.1021/jo9007095>

551 Shen, T., Wang, X.-N., & Lou, H.-X. (2009). Natural stilbenes: an overview. *Natural Product*  
552 *Reports*, 26(7), 916–935. <https://doi.org/10.1039/B905960A>

553 Stojanović, S., & Brede, O. (2002). Elementary reactions of the antioxidant action of *trans*-  
554 stilbene derivatives: resveratrol, pinosylvin and 4-hydroxystilbene. *Physical Chemistry*  
555 *Chemical Physics*, 4(5), 757–764. <https://doi.org/10.1039/b109063c>

556 Vion, E., Page, G., Bourdeaud, E., Paccalin, M., Guillard, J., & Rioux Bilan, A. (2018). *Trans*  
557  $\epsilon$ -viniferin is an amyloid- $\beta$  disaggregating and anti-inflammatory drug in a mouse  
558 primary cellular model of Alzheimer's disease. *Molecular and Cellular Neuroscience*,  
559 88, 1–6. <https://doi.org/10.1016/j.mcn.2017.12.003>

560 Yoshiaki, T., & Masatake, N. (2001). Oligostilbenes from Vitaceaeous plants. *Trends in*  
561 *Heterocyclic Chemistry*, 7, 41–54.

562 Yuk, H. J., Ryu, H. W., Jeong, S. H., Curtis-Long, M. J., Kim, H. J., Wang, Y., Song, Y. H., &  
563 Park, K. H. (2013). Profiling of neuraminidase inhibitory polyphenols from the seeds of  
564 *Paeonia lactiflora*. *Food and Chemical Toxicology*, 55, 144–149.  
565 <https://doi.org/10.1016/j.fct.2012.12.053>

566

567

568

569

## FIGURES CAPTIONS

**Figure 1.** Chemical structures of viniferins (only the **1a** and **2a** compounds are reported).

**Figure 2.** Comparison of experimental VCD spectra for the second eluted compound of **1** and **2** recorded in DMSO-*d*<sub>6</sub> solution (40 mM, 100 μm path length) with the predicted spectra of (7*aS*,8*aS*)-*E*-ε-viniferin and (7*aR*,8*aS*)-*E*-ω-viniferin.

**Figure 3.** Comparison of experimental VCD spectra for the second eluted compound of **1** recorded in DMSO-*d*<sub>6</sub> solution (40 mM, 100 μm path length) with the VCD spectra of *E*-ε-viniferin extracted from different grape varieties.

**Figure 4.** (A) Cell viability (%) (B) NO (μM) (C) ROS (fluorescence intensity) in LPS-stimulated RAW 264.7 cells. Cells were treated for 24 hours with LPS (0.1 μg/mL; + control) or LPS with **1a**, **1b**, **2a** and **2b** at different concentrations (from 0.5-100 μM for cell viability and between 0.5-10 μM for NO and ROS measurements). Results are expressed as mean SEM of eight replicates (*n*=8). Different letters mean significant differences (*p*<0.5).

**Figure 1.**

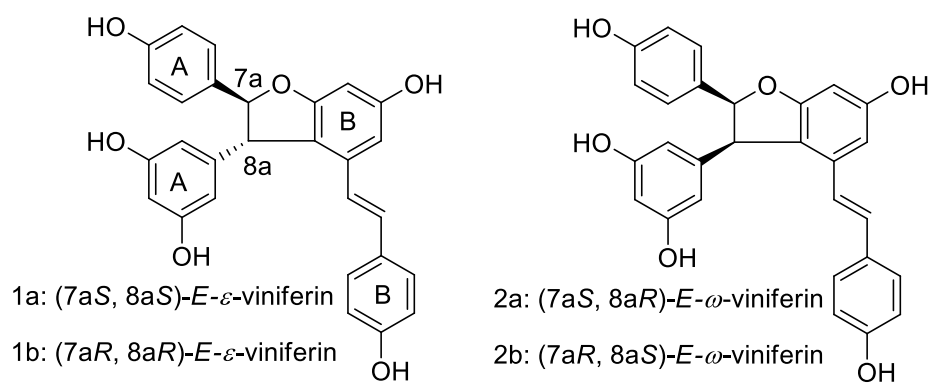


Figure 2.

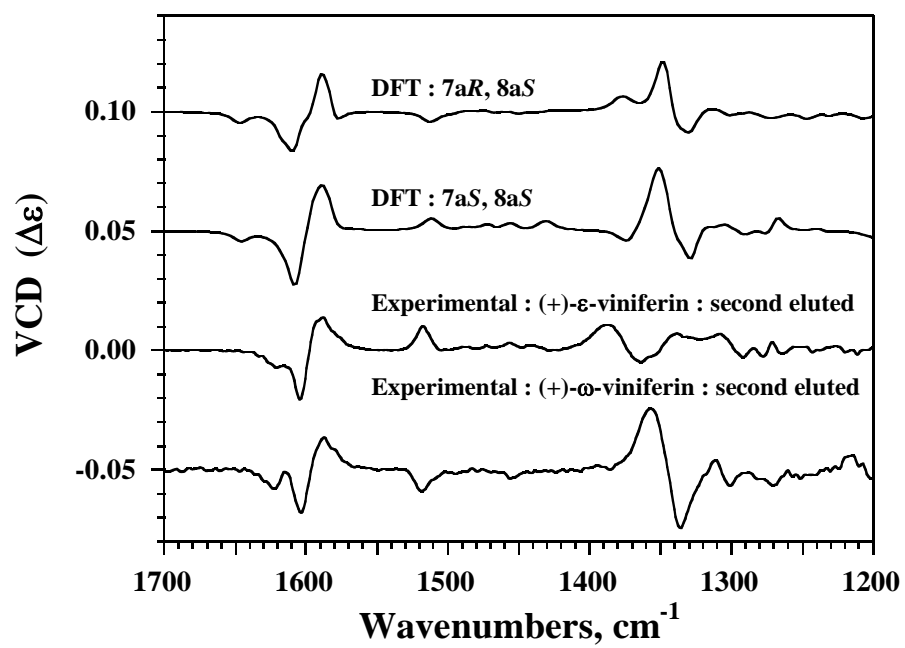
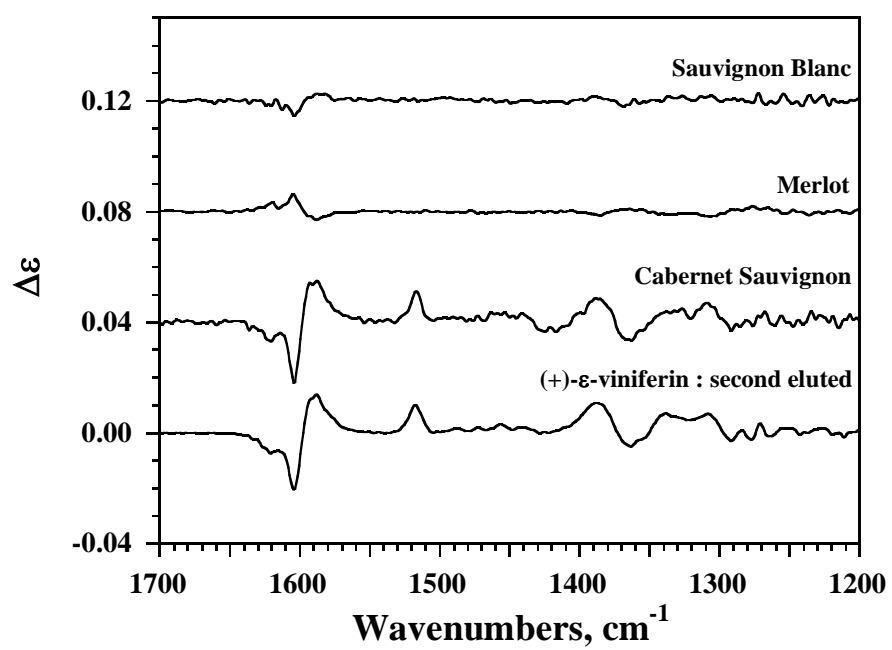
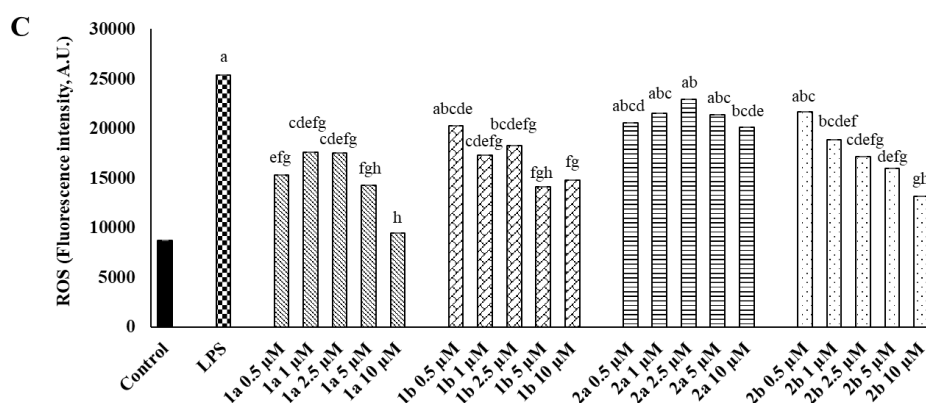
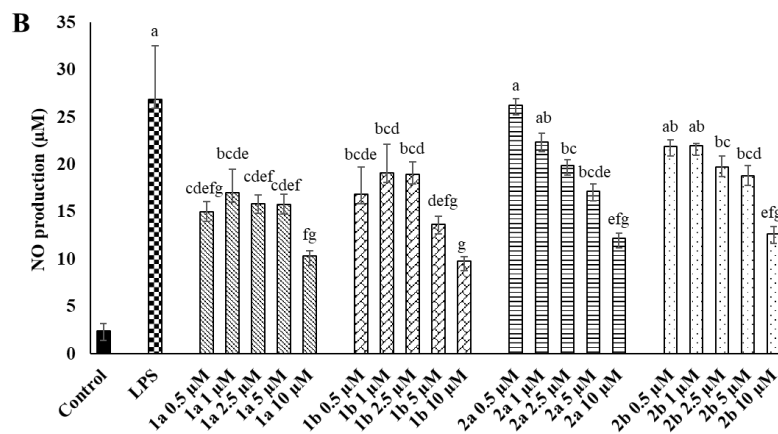
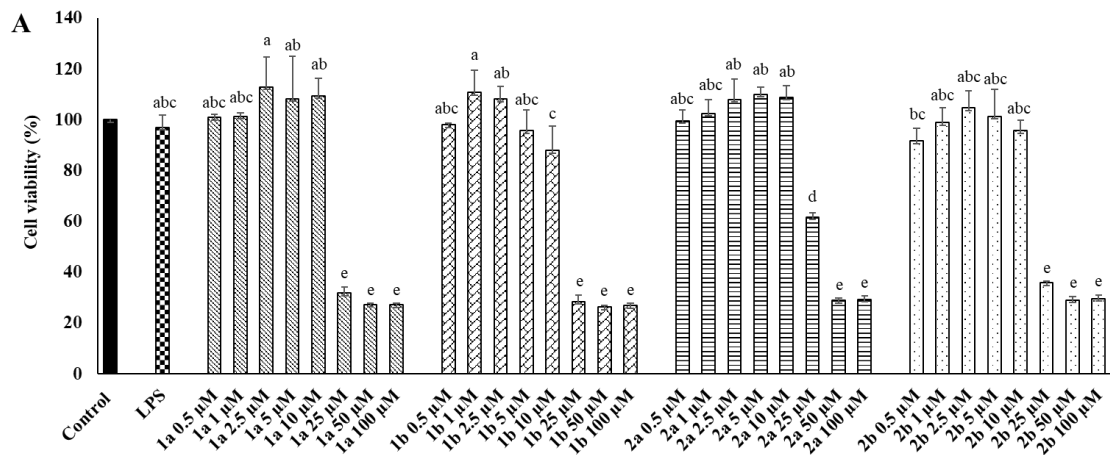


Figure 3.



**Figure 4.**

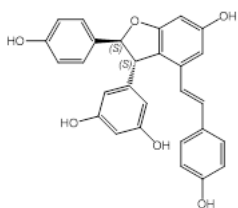


## For TOC Graphic only



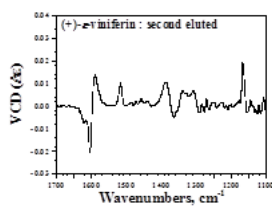
Cabernet Sauvignon stalks

Extraction  
CPC, HPLC



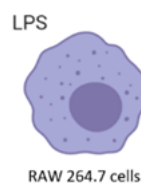
(7aS,8aS)-E-ε-viniferin

Absolute configuration  
determination



ee = 98.3%

Bioactivity



RAW 264.7 cells

anti-inflammatory and  
anti-oxidant activities

## Supporting Information

### Chiroptical and Potential *In Vitro* Anti-Inflammatory Properties of Viniferin Stereoisomers from Grapevine (*Vitis vinifera* L.)

Guillaume Buffeteau,<sup>a</sup> Ruth Hornedo-Ortega,<sup>a</sup> Julien Gabaston,<sup>a</sup> Nicolas Daugey,<sup>b</sup> Antonio Palos-Pinto,<sup>a</sup> Anne Thienpont,<sup>b</sup> Thierry Brotin,<sup>c</sup> Jean-Michel Mérillon,<sup>a</sup> Thierry Buffeteau<sup>b,\*</sup> and Pierre Waffo-Teguo<sup>a,\*</sup>

<sup>a</sup>Univ. Bordeaux, UFR des Sciences Pharmaceutiques, Unité OENO UMR 1366 INRAE, Bordeaux INP - Institut des Sciences de la Vigne et du Vin, CS 50008 - 210, chemin de Leysotte, 33882 Villenave d'Ornon, France.

<sup>b</sup>Univ. Bordeaux, Institut des Sciences Moléculaires, UMR 5255 - CNRS, 351 Cours de la Libération, F-33405 Talence, France.

<sup>c</sup>Université Lyon 1, Ecole Normale Supérieure de Lyon, CNRS UMR 5182, Laboratoire de Chimie, 69364 Lyon, France.

#### Corresponding Author:

\*Tel.: +33-55-757-5955. Fax: +33-55-757-5952. E-mail: [pierre.waffo-teguo@u-bordeaux.fr](mailto:pierre.waffo-teguo@u-bordeaux.fr)

Univ. Bordeaux, UFR des Sciences Pharmaceutiques, Unité OENO UMR 1366 INRAE, Bordeaux INP - Institut des Sciences de la Vigne et du Vin, CS 50008 - 210, chemin de Leysotte, 33882 Villenave d'Ornon, France.

## List of Contents

<b>Table S1:</b> Origin of the plants used in this study, the deposit number of a representative sample and optical rotation values.	S3
<b>Table S2:</b> Proportions of the two enantiomers of <i>E-ε</i> -viniferin and the enantiomeric excess (ee) for the three grape varieties.	S3
<b>Table S3:</b> NMR data of <i>E-ε</i> -viniferin ( <b>1</b> ) and <i>E-ω</i> -viniferin ( <b>2</b> ) in acetone- <i>d</i> <sub>6</sub> at 293°K	S4
<b>Figure S1:</b> CPC chromatogram of the organic extract of stalks of <i>Vitis vinifera</i> . Experimental conditions: rotation speed, 1200 rpm/min solvent system; Arizona-K system n-Heptane/EtOAc/MeOH/Water (1:2:1:2, v/v), in descending mode at a flow-rate of 3 mL/min.	S5
<b>Figure S2.</b> Chromatograms of analytical chiral HPLC for separation of <i>E-ε</i> -viniferin for the Cabernet Sauvignon (a), Merlot (b) and Sauvignon Blanc (c) grape varieties.	S6
<b>Figure: S3.</b> Chromatograms of chiral HPLC for separation of <i>E-ε</i> -viniferin enantiomers (A) and <i>E-ω</i> -viniferin enantiomers (B) from Merlot stalks. Experimental conditions: preparative Phenomenex Lux Amylose-1 column (150 × 10 mm); eluent: n-Hexane/2-Propanol 85/15 acidified with 0.01 % TFA; isocratic elution at flow-rate 5 mL/min; detection (UV 280 nm).	S7
<b>Figure S4.</b> <sup>1</sup> H NMR spectrum of <i>E-ε</i> -viniferin in acetone- <i>d</i> <sub>6</sub> at 293°K.	S8
<b>Figure S5.</b> <sup>1</sup> H- <sup>1</sup> H-ROESY NMR spectrum of <i>E-ε</i> -viniferin in acetone- <i>d</i> <sub>6</sub> at 293°K.	S8
<b>Figure S6.</b> <sup>1</sup> H NMR spectrum of <i>E-ω</i> -viniferin in acetone- <i>d</i> <sub>6</sub> at 293°K.	S9
<b>Figure S7.</b> <sup>1</sup> H- <sup>1</sup> H-ROESY NMR spectrum of <i>E-ω</i> -viniferin in acetone- <i>d</i> <sub>6</sub> at 293°K.	S9
<b>Figure S8.</b> IR spectra of <i>E-ε</i> -viniferin (black) and <i>E-ω</i> -viniferin (red) in DMSO- <i>d</i> <sub>6</sub> at 293°K	S10
<b>Figure S9.</b> Raw (top) and baseline corrected (bottom) VCD spectra of the two eluted compounds of <i>E-ε</i> -viniferin in DMSO- <i>d</i> <sub>6</sub> at 293°K.	S11
<b>Figure S10.</b> Raw (top) and baseline corrected (bottom) VCD spectra of the two eluted compounds of <i>E-ω</i> -viniferin in DMSO- <i>d</i> <sub>6</sub> at 293°K.	S12
<b>Figure S11.</b> ECD spectrum of the second eluted compound of <i>E-ε</i> -viniferin in MeOH at 293°K.	S13
<b>Figure S12.</b> ECD spectrum of the second eluted compound of <i>E-ω</i> -viniferin in MeOH at 293°K.	S13

**Table S1.** Origin of the plants used in this study, the deposit number of a representative sample and optical rotation values.

<i>Vitis vinifera</i> variety	Deposit number	Origin <sup>a</sup>	Optical rotation
Merlot	MIB_CS2017	Martillac	41°
Cabernet Sauvignon	MIB_CS-TB	Gornac	46.4°
Merlot	MIB_M-TB	Gornac	-12.1°
Sauvignon Blanc	MIB_SB-TB	Gornac	5.9°

<sup>a</sup>Domaine Haut Dambert, Gornac, France (cadastral number: ZH0099 for Cabernet Sauvignon and Merlot and ZH0054 for Sauvignon Blanc). Cabernet Sauvignon and Sauvignon Blanc were planted on a rootstock 101-14 whereas Merlot was planted on a rootstock 420A.

**Table S2.** Proportions of the two enantiomers of *E-ε*-viniferin and the enantiomeric excess (ee) for the three grape varieties.

<i>Vitis vinifera</i> variety	% enantiomer 1	% enantiomer 2	ee (%)
Cabernet Sauvignon	0.83	99.17	98.34
Merlot	61.66	38.34	23.32
Sauvignon Blanc	40.87	59.13	18.26

**Table S3.** NMR data of *E-ε*-viniferin (**1**) and *E-ω*-viniferin (**2**) in acetone-*d*<sub>6</sub> at 293°K

position	<i>E-ε</i> -viniferin ( <b>1</b> )		<i>E-ω</i> -viniferin ( <b>2</b> )	
	δ <sub>C</sub>	δ <sub>H</sub> (J in Hz)	δ <sub>C</sub>	δ <sub>H</sub> (J in Hz)
1a	133, C		135.7, C	
2a/6a	128.2, CH	7.17 <i>d</i> (8.6)	128.1, CH	7.02 <i>d</i> (8.4)
3a/5a	115.5, CH	6.72 <i>d</i> (8.6)	115.5, CH	6.61 <i>d</i> (8.4)
4a	157.3, C		157.4, C	
7a	93, CH	5.41 <i>d</i> (5.4)	89.5, CH	5.86 <i>d</i> (8.1)
8a	56.2, CH	4.47 <i>d</i> (5.4)	51.9, CH	4.70 <i>d</i> (8.1)
9a	146.7 C		142.5 C	
10a/14a	106.2, CH	6.23 <i>brd</i>	107.6, CH	5.80 <i>d</i> (2.2)
11a/13a	159.04, C		157.9, C	
12a	101.22, CH	6.23 <i>brd</i>	100.7, CH	5.96 <i>t</i> (2.2)
1b	133, C		135.5, C	
2b/6b	127.1, CH	7.19 <i>d</i> (8.6)	127.1, CH	7.23 <i>d</i> (8.7)
3b/5b	115.2, CH	6.82 <i>d</i> (8.6)	115.2, CH	6.75 <i>d</i> (8.7)
4b	157.3, C		156.4, C	
7b	129.2, CH	6.90 <i>d</i> (16.3)	129.4, CH	6.95 <i>d</i> (16.3)
8b	122.5	6.70 <i>d</i> (16.3)	122.6	6.76 <i>d</i> (16.3)
9b	135.5, C		135.4, C	
10b	118.9, C		121, C	
11b	161.5, C		161.4, C	
12b	95.9, CH	6.31 <i>d</i> (2.1)	96.3, CH	6.36 <i>d</i> (2.2)
13b	158.7, C		158.7, C	
14b	103.2	6.71 <i>brd</i>	103.2	6.72 <i>d</i> (2.2)

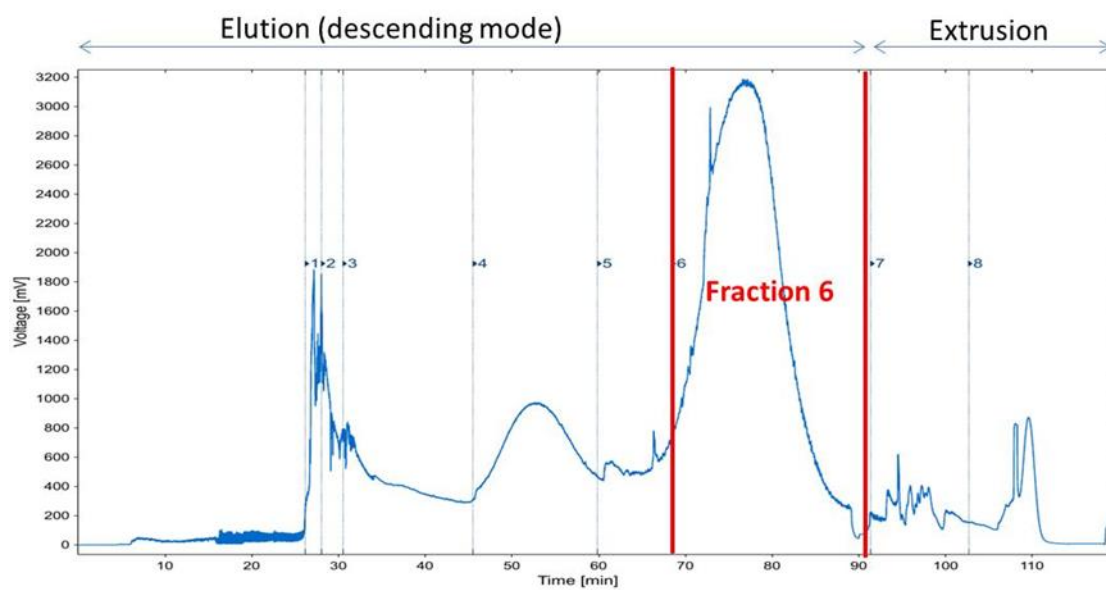


**Figure S1.** CPC chromatogram of the organic extract of stalks of *Vitis vinifera*. Experimental conditions: rotation speed, 1200 rpm/min solvent system; Arizona-K system n-Heptane/EtOAc/MeOH/Water (1:2:1:2, v/v), in descending mode at a flow-rate of 3 mL/min.

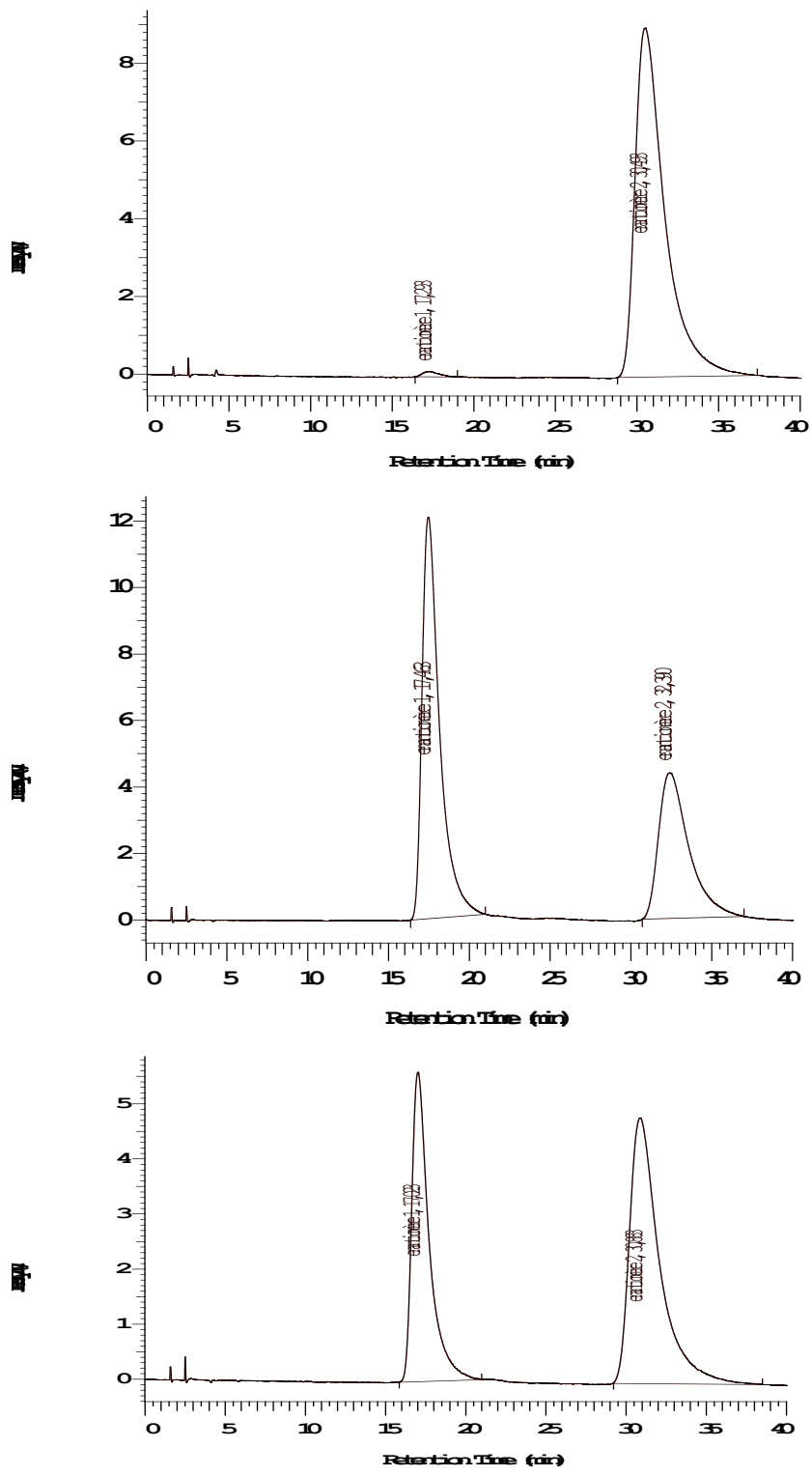


**Figure S2.** Chromatograms of analytical chiral HPLC for separation of *E-ε*-viniferin for the Cabernet Sauvignon (a), Merlot (b) and Sauvignon Blanc (c) grape varieties.

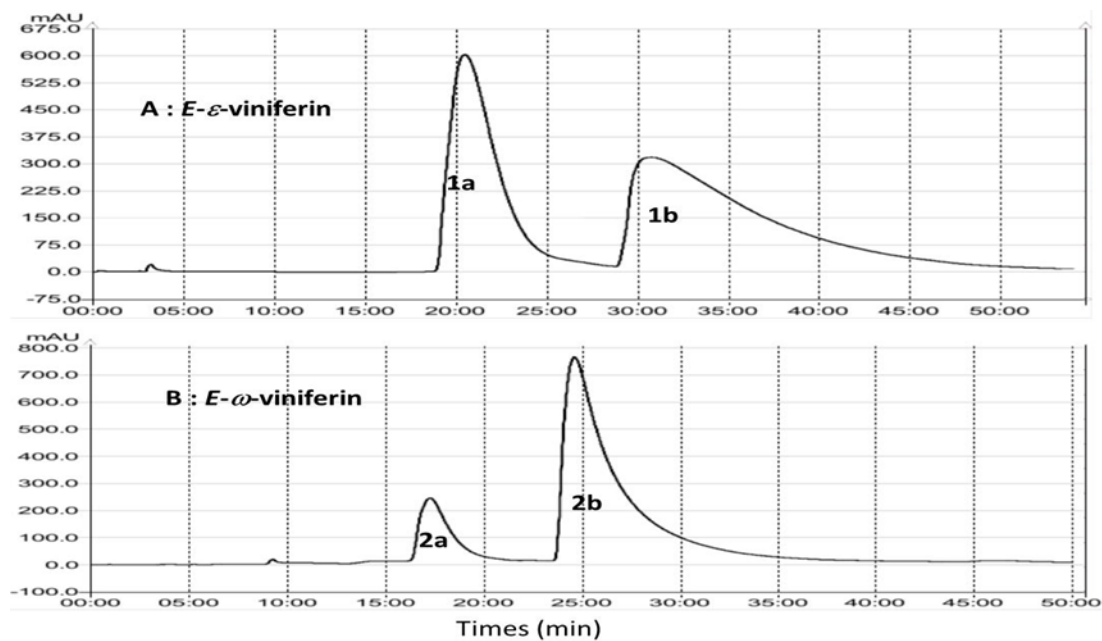


**Figure S3.** Chromatograms of chiral HPLC for separation of *E-ε*-viniferin enantiomers (A) and *E-ω*-viniferin enantiomers (B) from Merlot stalks. Experimental conditions: preparative Phenomenex Lux Amylose-1 column (150 × 10 mm); eluent: n-Hexane/2-Propanol 85/15 acidified with 0.01 % TFA; isocratic elution at flow-rate 5 mL/min; detection (UV 280 nm).

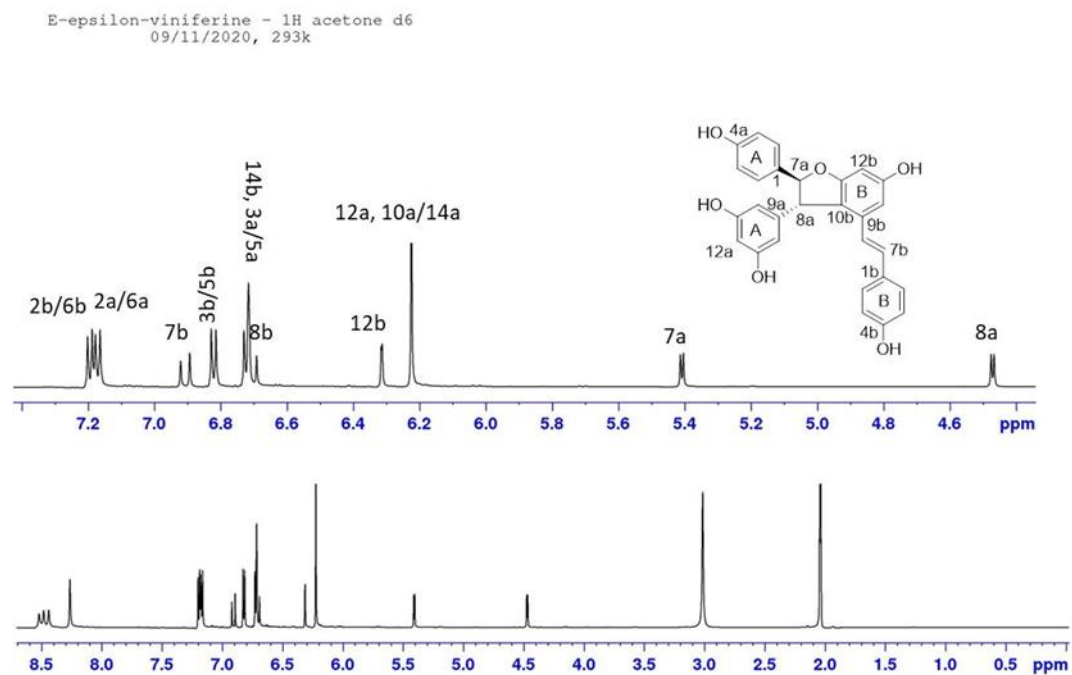


**Figure S4.**  $^1\text{H}$  NMR spectrum of *E*- $\epsilon$ -viniferin in acetone-*d*<sub>6</sub> at 293°K.

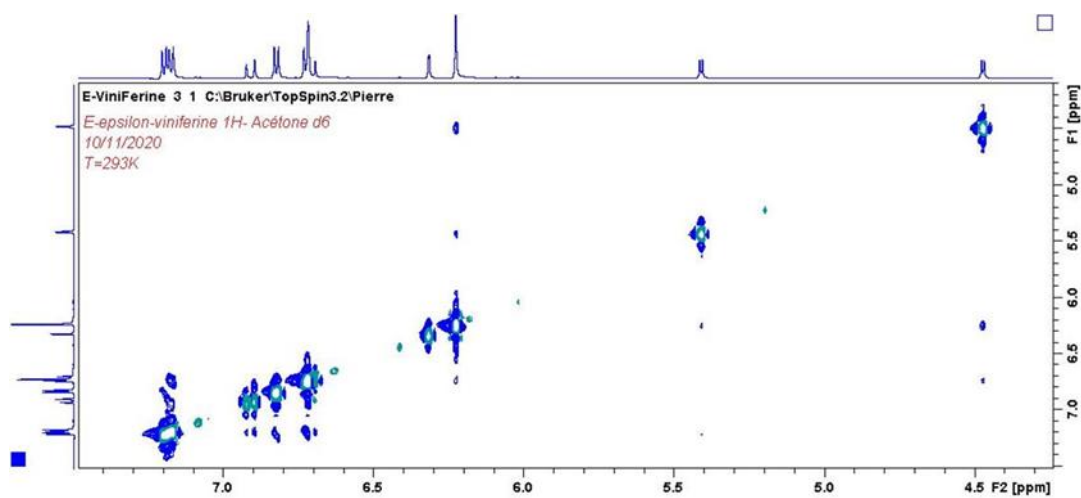


**Figure S5.**  $^1\text{H}$ - $^1\text{H}$ -ROESY NMR spectrum of *E*- $\epsilon$ -viniferin in acetone-*d*<sub>6</sub> at 293°K.

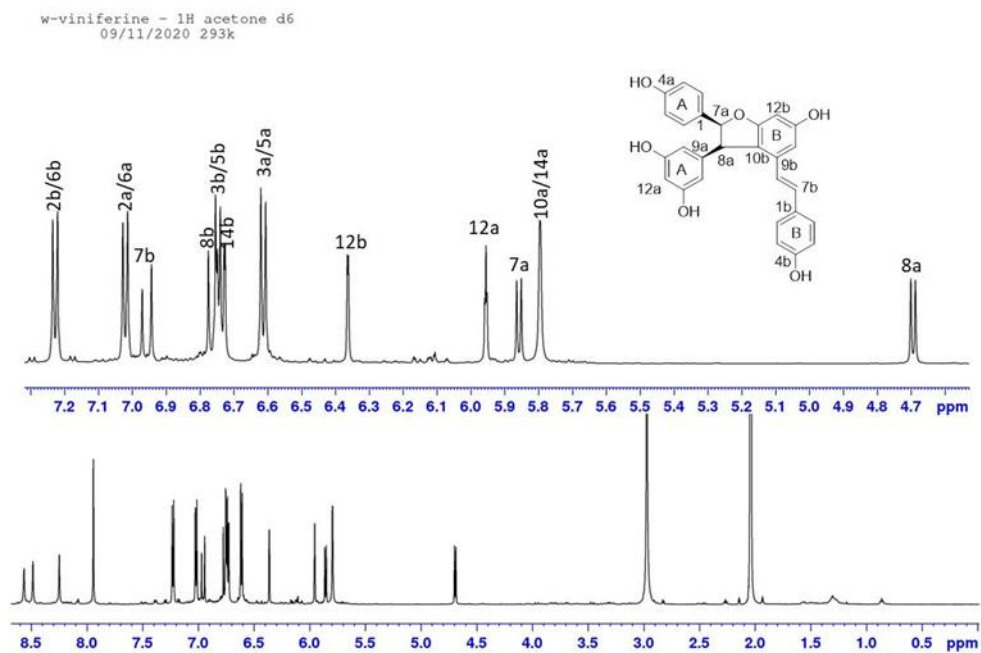


**Figure S6.**  $^1\text{H}$  NMR spectrum of *E*- $\omega$ -viniferin in acetone-*d*<sub>6</sub> at 293°K.

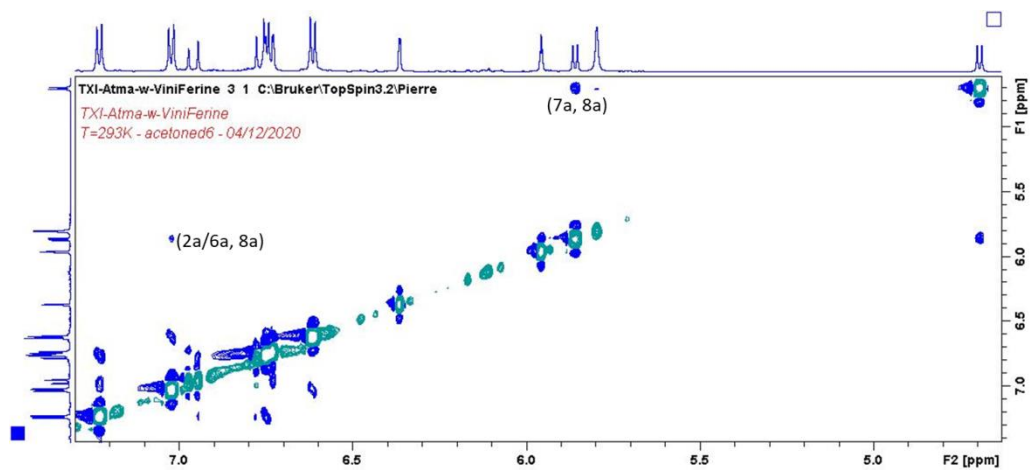


**Figure S7.**  $^1\text{H}$ - $^1\text{H}$ -ROESY NMR spectrum of *E*- $\omega$ -viniferin in acetone-*d*<sub>6</sub> at 293°K.

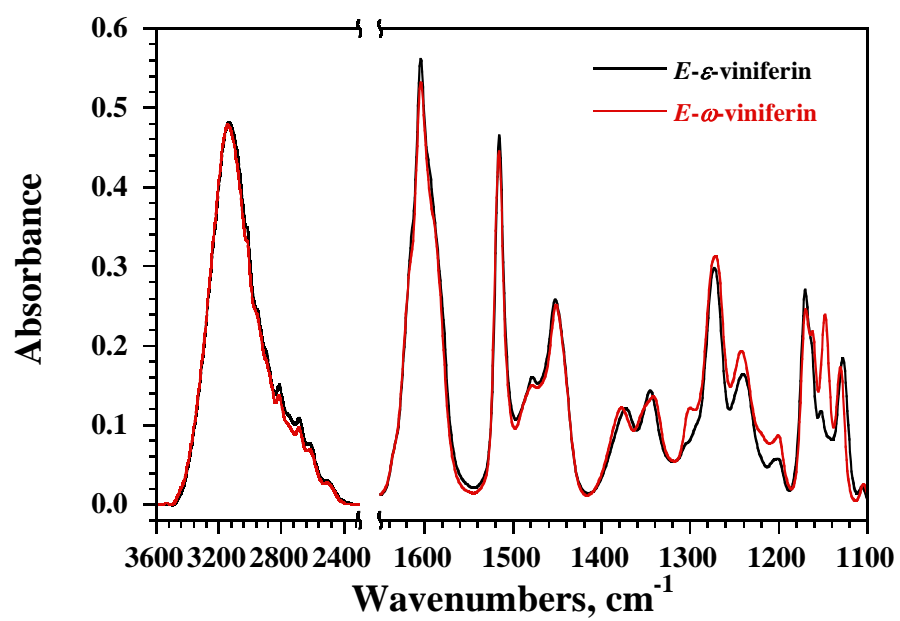


**Figure S8.** IR spectra of *E-ε*-viniferin (black) and *E-ω*-viniferin (red) in DMSO-*d*<sub>6</sub> at 293°K.

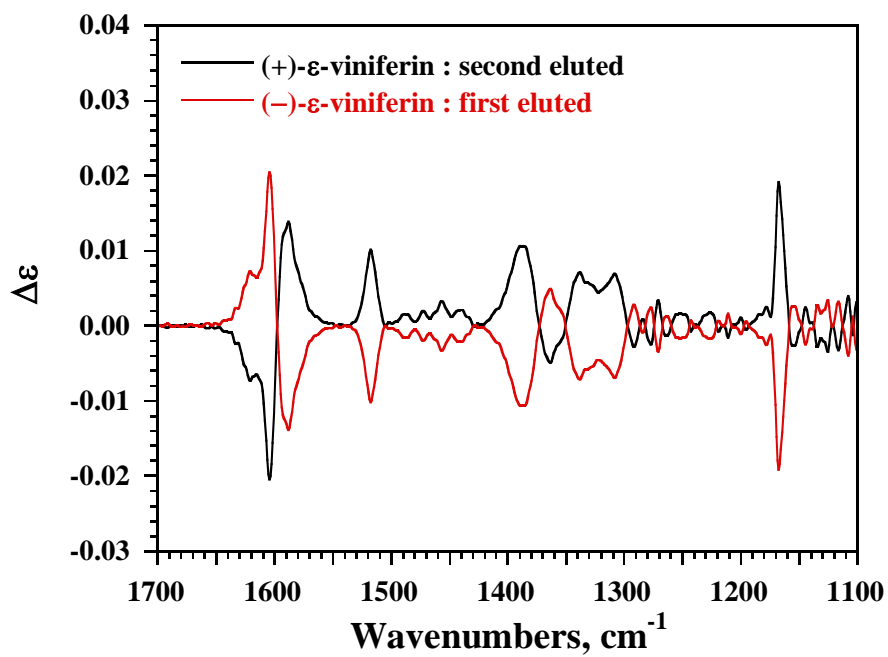
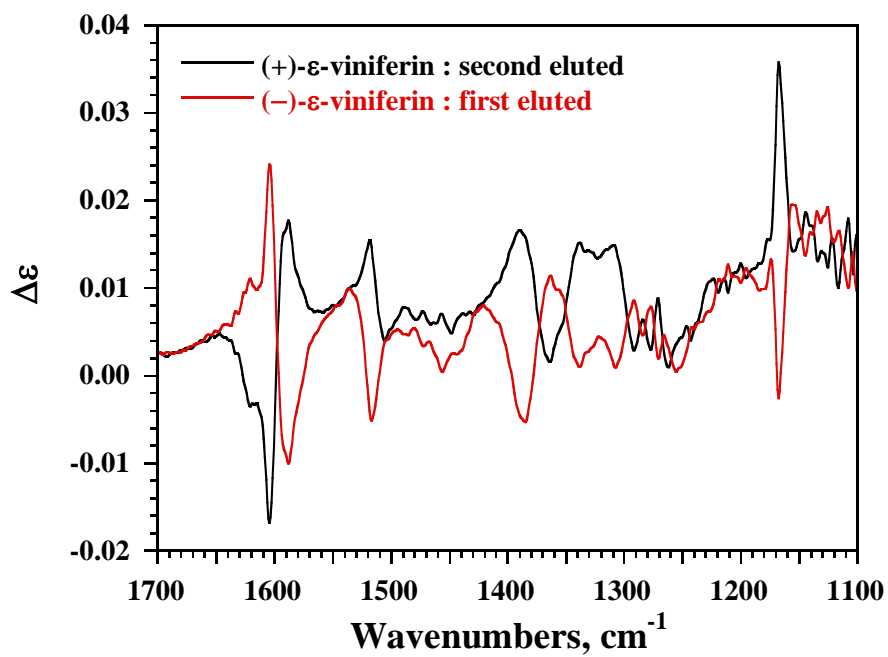


**Figure S9.** Raw (top) and baseline corrected (bottom) VCD spectra of the two eluted compounds of *E*- $\epsilon$ -viniferin in  $\text{DMSO-}d_6$  at 293°K.

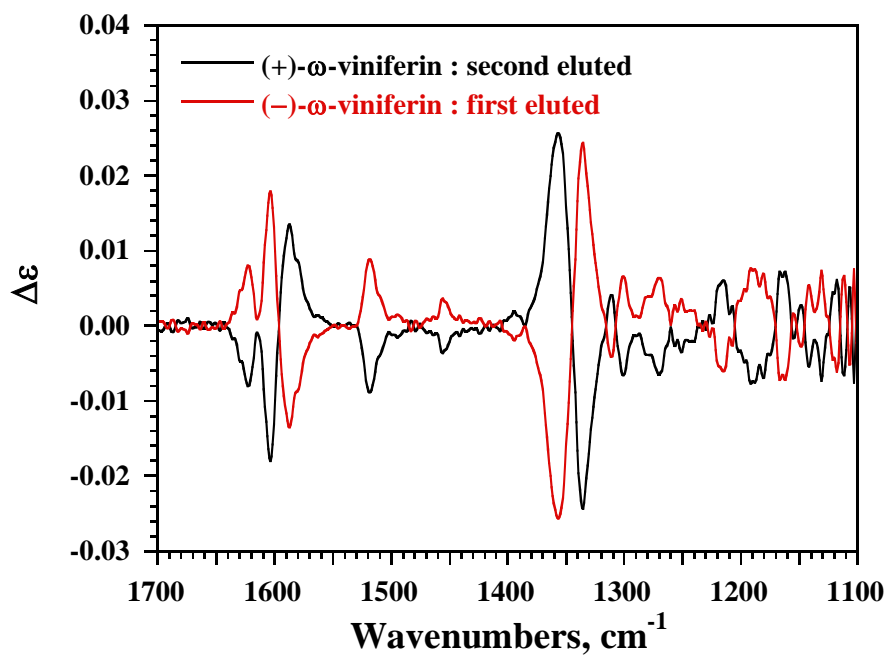
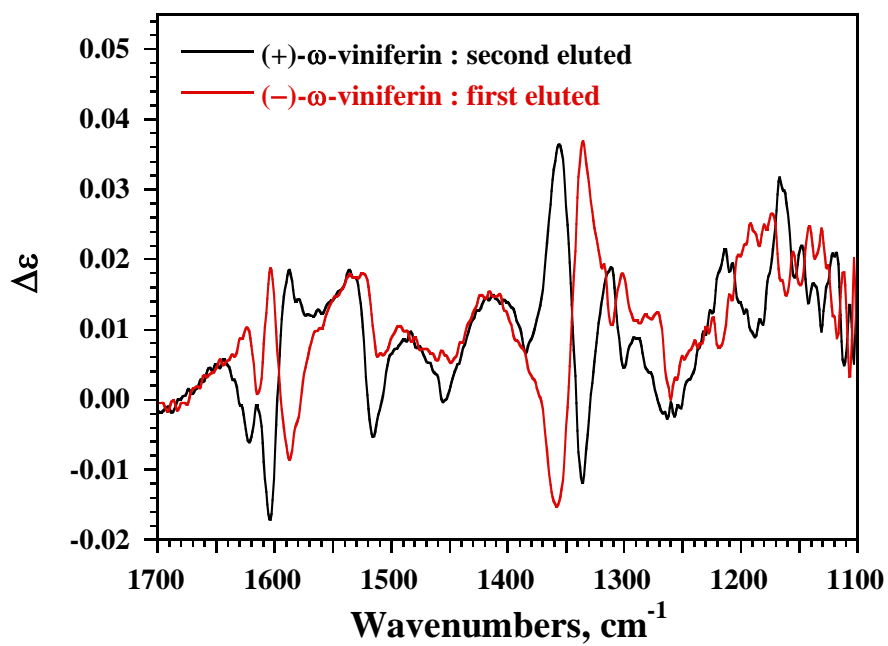


**Figure S10.** Raw (top) and baseline corrected (bottom) VCD spectra of the two eluted compounds of *E*- $\omega$ -viniferin in DMSO-*d*<sub>6</sub> at 293°K.

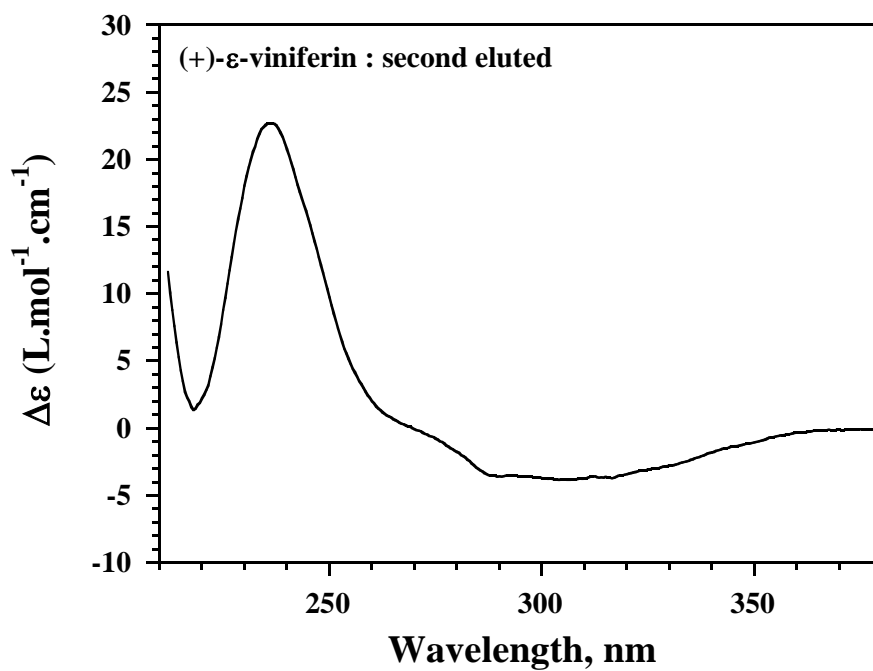


**Figure S11.** ECD spectrum of the second eluted compound of *E*- $\epsilon$ -viniferin in MeOH at 293°K.

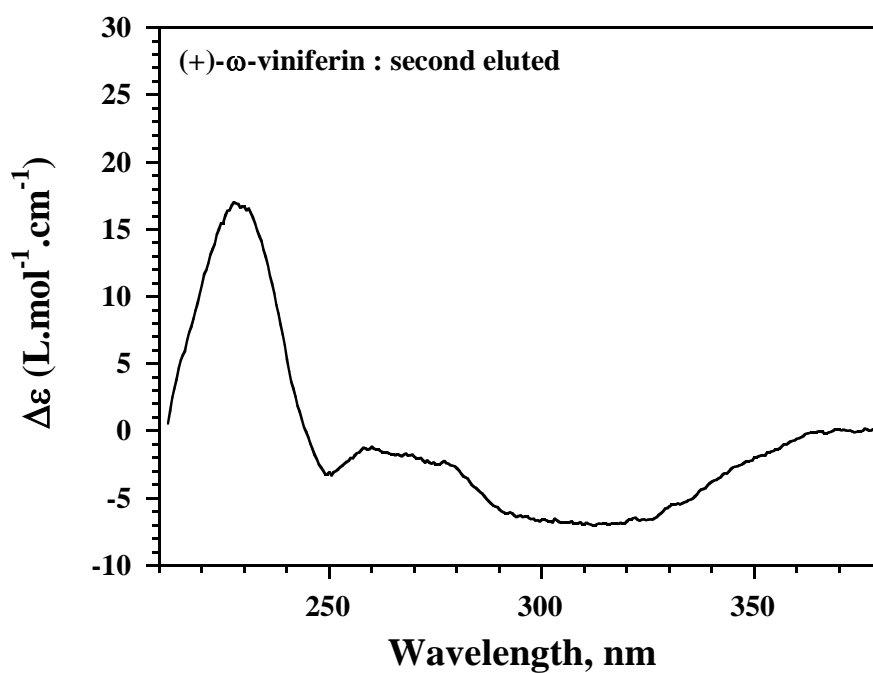


**Figure S12.** ECD spectrum of the second eluted compound of *E*- $\omega$ -viniferin in MeOH at 293°K.

July 26, 2022

Dr Sian Astley  
Receiving Editor  
*Food Chemistry*

Dear Dr. Sian,

We have submitted electronically for publication in *Food Chemistry* the revised version of the manuscript entitled "Chiroptical and Potential In Vitro Anti-Inflammatory Properties of Viniferin Stereoisomers from Grapevine" by Buffeteau *et al.* (Manuscript ID: FOODCHEM-D-22-01901). All the comments of the reviewers and editor have been addressed. We hope that the modifications made (marked changes in RED in the revised version of the manuscript) as well as our responses to the reviewers and editor will make our manuscript acceptable for publication in *Food Chemistry*

Thank you very much for your consideration of our manuscript.

Yours sincerely,



Pr P. WAFFO TEGUO

July 26, 2022

Dr Sian Astley  
Receiving Editor  
*Food Chemistry*

Dear Dr. Sian,

We have submitted electronically for publication in *Food Chemistry* the revised version of the manuscript entitled "Chiroptical and Potential In Vitro Anti-Inflammatory Properties of Viniferin Stereoisomers from Grapevine" by Guillaume Buffeteau et al. (Manuscript ID: FOODCHEM-D-22-01901). All the comments of the reviewers have been addressed. We hope that the modifications made (marked changes in RED in the revised version of the manuscript) as well as our responses to the reviewers and editor will make our manuscript acceptable for publication in *Food Chemistry*

Thank you very much for your consideration of our manuscript.

Yours sincerely,



Pr P. WAFFO TEGUO

## Response to the reviewers and Editor

### Reviewer: 1

In this study the authors extracted, purified and unambiguously identified four stereoisomers of viniferin from grapevine stalks. They further assessed the antioxidant and anti-inflammatory activities using cell models and found the activities depended on the configuration of the stereoisomers. The findings are important because as the mechanisms of these bioactivities become better understood, the stereospecificity of these bioactive components also becomes critically important for future research and applications.

The paper was generally acceptable. The experiments were conducted properly, and the data were collected and analyzed correctly. However, I have a few comments before it can be accepted.

1. The authors should provide quantitative data for the purified stereoisomers in addition to the 3 g crude extract/100 g grapevine stalks (Section 2.3)

*Author reply: As suggested by reviewer 1, we have provided quantitative data of stilbene content and purified stereoisomers for the three grape varieties.*

2. Additional information and discussion should be provided in terms of how to acquire large amount of pure stereoisomers of viniferin for future research e.g. in vivo experiment

*Author reply: The amount of pure stereoisomers of viniferin is very dependent on the investigated plant material. For grapevine, E- $\epsilon$ - and E- $\omega$ -viniferins can be extracted from grape berries, leaves, stalks and roots with different efficiencies. We have chosen their extraction from stalks of grapevine because the amount (0.1 – 0.5 % of dried weight) is one hundred higher than the one obtained by extraction from grape berries. This information has been added in the introduction.*

3. Tables should be listed separately from the main text.

*Author reply: Tables can be placed either next to the relevant text in the article, or on separate page at the end (Guide for authors, Food Chemistry).*

4. Spell out ECD for first mention in the text (pg 7, ln 153)

*Author reply: This modification has been made.*

5. No Arabic numbers to start a sentence (pg 6, ln 127; pg. 11, ln 234)

*Author reply: These modifications have been made.*

6. Concentration of LPS should be pointed out first in the methods section (move related content on ln 352 to pg 10, Ln 215)

*Author reply: This information has been mentioned in the manuscript (line 227).*

7. The manuscript needs some English improvement (abstract: allows to extract...; pg 4, ln 64, non data...; pg 4, ln 85: in view to... etc)

*Author reply: These modifications have been made. Moreover, our manuscript has been proofread by a native English speaker.*

## Reviewer: 2

The manuscript deals with elucidating the chemical structures of the enantiomers of two stilbene dimers present in grapevine stalks. Although the work is well-structured, in my opinion, it is out of the scope of the Food Chemistry Journal. No relation with foods is reported; the four stereoisomers are isolated from a non-food part of the grapevine; moreover, some biological properties are studied for these compounds but it is not demonstrated their relevance to food or food chemistry. I think that this manuscript should be submitted to other journals dealing with organic or medicinal chemistry.

*Author reply: The determination of stereochemistry and enantiomeric excess in chiral natural molecules is a research of great interest in food chemistry. Indeed, the two enantiomers of a chiral natural molecule could interact in different ways with receptors, transport systems and enzymes, leading to diverse effects such as dissimilar taste or aroma, or different biological activities. Viniferin stilbene dimers are natural molecules present in food (grape berries) and beverage (wine) but also, in larger amount, in stalks of grapevine. We have chosen the extraction of E- $\epsilon$ - and E- $\omega$ -viniferins from stalks of grapevine because the amount (0.1 – 0.5 % of dried weight) is one hundred higher than the one obtained by extraction from grape berries. We have mentioned this point in the introduction to show the relation of viniferin stilbene dimers and food.*

## Editor comments

Highlights should showcase your results without the need to read the manuscript first and must have context and interest for readers; they must focus on the outcomes of your work.

- Viniferins were isolated from vine stalks using a combination of CPC and Prep. HPLC
- Enantiomers of E- $\epsilon$ -viniferins and E- $\omega$ -viniferins were purified by chiral HPLC
- Stereochemistry was investigated by NMR and VCD associated to DFT calculations  
What you did rather than what you found.
- Enantiomeric excess of E- $\epsilon$ -viniferin were grape variety-dependent – I'm not sure what "Enantiomeric excess of E- $\epsilon$ -viniferin" means in the context. Please clarify.
- Stereoisomers of viniferins showed anti-inflammatory and antioxidant activities – bit generic. Something more specific to your outcomes?

*Author reply: As suggested by Editor, the highlights have been modified:*

- *Viniferins were isolated from vine stalks using a combination of CPC and Prep. HPLC*
- *Enantiomers of E- $\epsilon$ -viniferins and E- $\omega$ -viniferins were purified by chiral HPLC*
- *NMR and VCD associated to DFT calculations establish the (+)-(7aS,8aS) and (+)-(7aR,8aS) configurations for E- $\epsilon$ -viniferin and E- $\omega$ -viniferin, respectively.*
- *Cabernet Sauvignon grape variety provides the quasi enantiopure (+)-(7aS,8aS)-E- $\epsilon$ -viniferin compound.*
- *(+)-(7aS,8aS)-E- $\epsilon$ -viniferin was the most efficient compound diminishing NO and ROS*

22 Four stereoisomers of viniferin stilbene dimers (7aS,8aS)-E- $\epsilon$ -viniferin (1a), (7aR,8aR)-E- $\epsilon$ - 23 viniferin (1b), (7aS,8aR)-E- $\omega$ -viniferin (2a), and (7aR,8aS)-E- $\omega$ -viniferin (2b) were isolated 24 from grapevine stalks of various varieties (Cabernet Sauvignon, Merlot, Sauvignon Blanc) 25 using a combination of centrifugal partition chromatography (CPC), preparative HPLC and 26 chiral HPLC.

- The abstract should introduce your hypothesis, which can be further elaborated in the introduction. You launch in with what you did, not really explaining why.

*Author reply: As suggested by Editor, the abstract has been totally rewritten in order to introduce our hypothesis.*

39-45 are of scope for Food Chemistry

*Author reply: The first paragraph of the introduction has been totally rewritten to be in the scope of Food Chemistry.*

84 dichroisms) of two stilbene dimers, E- $\epsilon$ -viniferin and E- $\omega$ -viniferin from stalks of grapevine in – we don't eat grapevine vine stalks, so you are going to have to justify their use for the paper to be in scope, e.g., easier to obtain from stalks but still relevant to grapes etc.

*Author reply: Viniferin stilbene dimers are natural molecules present in food (grape berries) and beverage (wine) but also, in larger amount, in stalks of grapevine. We have chosen the extraction of E- $\epsilon$ - and E- $\omega$ -viniferins from stalks of grapevine because the amount (0.1 – 0.5 % of dried weight) is one hundred higher than the one obtained by extraction from grape berries. We have mentioned this point in the introduction to show the relation of viniferin stilbene dimers and food.*

92 C NMR spectra were recorded on a Bruker Avance III 600 MHz NMR 93 spectrometer and analyzed with Bruker Topspin software.

- Ensure all sources of reagents and equipment are included and compliant with the Guide for Authors, i.e., company name, city and country

*Author reply: All sources of reagents and equipment are included and compliant with the Guide for Authors.*

Details such as numbers of biological and technical replicates are missing.

*Author reply: As suggested by Editor, numbers of replicates have been mentioned in the manuscript (lines 222, 231 and 239).*

133 The back pressure was 25 bars. – bars are not an SI unit

*Author reply: As suggested by Editor, bar pressure unit has been converted in Pa*

There are issues with the English (syntax, grammar, etc.) throughout the manuscript. These must be addressed with the help of a native speaker or English language editing service, such as that provided by Elsevier <https://webshop.elsevier.com/language-editing-services/>

*Author reply: To improve its quality, our manuscript has been proofread by a native English speaker.*

# Chiroptical and Potential *In Vitro* Anti-Inflammatory Properties of Viniferin Stereoisomers from Grapevine (*Vitis vinifera* L.)

Guillaume Buffeteau,<sup>a</sup> Ruth Hornedo-Ortega,<sup>a</sup> Julien Gabaston,<sup>a</sup> Nicolas Daugey,<sup>b</sup> Antonio Palos-Pinto,<sup>a</sup> Anne Thienpont,<sup>b</sup> Thierry Brotin,<sup>c</sup> Jean-Michel Mérellon,<sup>a</sup> Thierry Buffeteau<sup>b,\*</sup> and Pierre Waffo-Teguo<sup>a,\*</sup>

<sup>a</sup>Univ. Bordeaux, UFR des Sciences Pharmaceutiques, Unité OENO UMR 1366 INRAE, Bordeaux INP - Institut des Sciences de la Vigne et du Vin, CS 50008 - 210, chemin de Leysotte, 33882 Villenave d'Ornon, France..

<sup>b</sup>Univ. Bordeaux, Institut des Sciences Moléculaires, UMR 5255 - CNRS, 351 Cours de la Libération, F-33405 Talence, France.

<sup>c</sup>Université Lyon 1, Ecole Normale Supérieure de Lyon, CNRS UMR 5182, Laboratoire de Chimie, 69364 Lyon, France.

## Highlights

- Viniferins were isolated from vine stalks using a combination of CPC and Prep. HPLC
- The enantiomers of *E-ε*-viniferins and *E-ω*-viniferins were purified by chiral HPLC
- NMR and VCD associated to DFT calculations establish the (+)-(7*a*S,8*a*S) and (+)-(7*a*R,8*a*S) configurations for *E-ε*-viniferin and *E-ω*-viniferin, respectively
- Cabernet Sauvignon grape variety provides the quasi enantiopure (+)-(7*a*S,8*a*S)-*E-ε*-viniferin compound.
- (+)-(7*a*S,8*a*S)-*E-ε*-viniferin was the most efficient compound diminishing NO and ROS

1           **Chiroptical and Potential *In Vitro* Anti-Inflammatory Properties of**  
2           **Viniferin Stereoisomers from Grapevine (*Vitis vinifera* L.)**

3  
4 Guillaume Buffeteau,<sup>a</sup> Ruth Hornedo-Ortega,<sup>a</sup> Julien Gabaston,<sup>a</sup> Nicolas Daugey,<sup>b</sup> Antonio  
5 Palos-Pinto,<sup>a</sup> Anne Thienpont,<sup>b</sup> Thierry Brotin,<sup>c</sup> Jean-Michel Mérillon,<sup>a</sup> Thierry Buffeteau<sup>b,\*</sup>  
6 and Pierre Waffo-Teguo<sup>a,\*</sup>

7  
8 <sup>a</sup>Univ. Bordeaux, UFR des Sciences Pharmaceutiques, Unité OENO UMR 1366 INRAE,  
9 Bordeaux INP - Institut des Sciences de la Vigne et du Vin, CS 50008 - 210, chemin de  
10 Leysotte, 33882 Villenave d'Ornon, France.

11 <sup>b</sup>Université de Bordeaux, Institut des Sciences Moléculaires, UMR 5255 - CNRS, 351 Cours  
12 de la Libération, F-33405 Talence, France.

13 <sup>c</sup>Université Lyon 1, Ecole Normale Supérieure de Lyon, CNRS UMR 5182, Laboratoire de  
14 Chimie, 69364 Lyon, France.

15  
16 **Corresponding Author:**

17 \*Tel.: +33-55-757-5955. Fax: +33-55-757-5952. E-mail: [pierre.waffo-teguo@u-bordeaux.fr](mailto:pierre.waffo-teguo@u-bordeaux.fr)

18 Univ. Bordeaux, UFR des Sciences Pharmaceutiques, Unité OENO UMR 1366 INRAE,  
19 Bordeaux INP - Institut des Sciences de la Vigne et du Vin, CS 50008 - 210, chemin de  
20 Leysotte, 33882 Villenave d'Ornon, France..

21 **Abstract**

22 Determination of stereochemistry and enantiomeric excess in chiral natural molecules is a  
23 research of great interest because enantiomers can exhibit different biological activities.  
24 Viniferin stilbene dimers are natural molecules present in grape berries and wine but also, in  
25 larger amount, in stalks of grapevine. Four stereoisomers of viniferin stilbene dimers (*7aS,8aS*)-  
26 *E-ε*-viniferin (**1a**), (*7aR,8aR*)-*E-ε*-viniferin (**1b**), (*7aS,8aR*)-*E-ω*-viniferin (**2a**), and (*7aR,8aS*)-  
27 *E-ω*-viniferin (**2b**) were isolated from grapevine stalks of Cabernet Sauvignon, Merlot and  
28 Sauvignon Blanc, using a combination of centrifugal partition chromatography (CPC),  
29 preparative and chiral HPLC. The structure elucidation of these molecules was achieved by  
30 NMR whereas the absolute configurations of the four stereoisomers were investigated by  
31 vibrational circular dichroism spectroscopy in combination with density functional theory  
32 (DFT) calculations. This study unambiguously established the (+)-(*7aS,8aS*) and (+)-(*7aR,8aS*)  
33 configurations for *E-ε*-viniferin and *E-ω*-viniferin, respectively. Finally, we show that Cabernet  
34 Sauvignon provided the quasi enantiopure (+)-(*7aS,8aS*)-*E-ε*-viniferin compound which  
35 presents the best anti-inflammatory and anti-oxidant activities.

36 **Keywords:** stilbene, viniferins, stereoisomers, chirality, vine, anti-inflammatory

37

## 38 **1. Introduction**

39 Chirality is omnipresent in chemistry and biology. It is not surprising that this  
40 phenomenon also plays a major role in food chemistry and natural products. Chirality is a  
41 geometric property of some molecules that are non-superposable with their mirror images. A  
42 chiral compound and its mirror image are called enantiomers, and could interact in different  
43 ways with receptors, transport systems and enzymes, leading to diverse effects such as  
44 dissimilar taste or aroma, or different biological activities. Therefore, the determination of  
45 enantiomeric excess in chiral natural molecules is a research of great interest in food chemistry.

46 The hydroxylated derivatives of stilbene, especially resveratrol and its congeners have  
47 attracted much attention owing to their various benefits in human health. It is now accepted that  
48 resveratrol possesses a large number of pharmacological properties including cardioprotective  
49 (Saiko et al., 2008), neuroprotective (Richard et al., 2011), and chemopreventive effects (Ko et  
50 al., 2017). More than one thousand stilbenoids have been identified until now, and several  
51 articles tried to make a catalog (Shen et al., 2009; Rivière et al., 2012; Keylor et al., 2015).  
52 These specialized metabolites occur naturally with a limited but heterogeneous distribution in  
53 the plant kingdom (Rivière et al., 2012). Stilbenoids can be divided in monomers and oligomers.  
54 There are two main hypotheses dealing with the biosynthesis of oligomers. The first approach  
55 is chemical, while the second involves chiral intermediates and possibly enzymes. Given the  
56 different structures of existing dimers, it seems that both possibilities are present. In any case,  
57 it is the ability of this type of compounds, like most polyphenols, to form and trap radicals,  
58 which makes it possible to obtain such diversity by radical coupling. Indeed, they are  
59 mechanisms of the Sequential Proton Loss Electron Transfer (SPLET) and Hydrogen Atom  
60 Transfer (HAT) type which, by radical and proton transfer, would lead to such reactivity (Shang  
61 et al., 2009; Stojanović & Brede, 2002). It was shown that some peroxidases from grapevine  
62 are capable to form the  $\delta$ -viniferin and other dimers (Calderón et al., 1992; Morales & Barceló,

63 1997; Barceló et al., 2003). Despite numerous attempts using Horseradish peroxidase (HRP) or  
64 other peroxidases, even from the grapevine, no data have been published, showing that these  
65 enzymes are involved in the formation of the *E-ε*-viniferin (Barceló et al., 2003). The presence  
66 of a chiral intermediate, however, is strongly assumed, as the plants seem able to produce  
67 specifically the (+)-*E-ε*-viniferin, as in Vitaceae and Dipterocarpaceae or (-)-*E-ε*-viniferin as  
68 in some Cyperaceae (Yoshiaki & Masatake, 2001). Laccase from *Botrytis cinerea* was  
69 considered capable to catalyze the reaction of resveratrol toward the (+)-*E-ε*-viniferin (Pezet,  
70 1998), but subsequent studies have refuted this hypothesis (Breuil et al., 1998; Cichewicz et al.,  
71 2000).

72 Structurally, *E-ε*- and *E-ω*-viniferins are resveratrol dimers belonging to the group A  
73 according to the natural stilbenes classification with two resveratrol units linked by two C-C  
74 and C-O-C connection (Shen and Lou, 2009). This structure has two stereogenic carbons on the  
75 benzofuran unit with four possible stereoisomers (**Figure 1**). As observed for drugs, it is  
76 possible that enantiomers of viniferins can have different activities. Recently, research carried  
77 out on the characterization of the molecular determinants responsible for the taste of wines  
78 showed how stereochemistry could influence taste properties. Thus, taste properties of  
79 lyoniresinol stereoisomers were evaluated and only one lyoniresinol enantiomer were strongly  
80 bitter whereas the other one was tasteless and the diastereoisomer is slightly sweet (Cretin et  
81 al., 2015). In order to better understand the different properties of each stereoisomer of *E-ε*- and  
82 *E-ω*-viniferins, it is crucial to isolate and characterize them.

83 To perform structural and biological measurements, it is necessary to acquire a large  
84 amount of pure stereoisomers of viniferin. However, this amount is very dependent on the  
85 investigated plant material. Thus, for grapevine, *E-ε*- and *E-ω*-viniferins can be extracted from  
86 grape berries, leaves, stalks and roots with different efficiencies. Indeed, their extraction

87 represents around 0.1 – 0.5 % of dried weight (DW) from stalks of grapevine whereas the  
88 amount is one hundred lower from grape berries (Gabaston et al, 2020).

89 This paper reports the chiroptical properties (vibrational and electronic circular  
90 dichroisms) of two stilbene dimers, *E-ε*-viniferin and *E-ω*-viniferin from stalks of grapevine in  
91 order to determine their absolute configurations. We have shown that the two dimers are present  
92 as a mixture of enantiomers, depending on the grape variety. All the stereoisomers were also  
93 evaluated for their anti-inflammatory and anti-oxidant activities in Lipopolysaccharide (LPS)-  
94 stimulated macrophages.

95

## 96 **2. Material and Methods**

### 97 **2.1. General Experimental Procedures.**

98 All <sup>1</sup>H and <sup>13</sup>C NMR spectra were recorded on a Bruker Avance III 600 MHz NMR  
99 spectrometer (Wissembourg, France) equipped with a 5-mm TXI probe. Compounds were  
100 measured in 3 mm NMR tubes, using acetone-*d*<sub>6</sub> (Euriso-Top, Gif-sur-Yvette, France) as the  
101 solvent at 27°C. <sup>1</sup>H and <sup>13</sup>C chemical shifts were referenced to solvent signals. Data were  
102 processed using Bruker software Topspin 3.2. The specific optical rotations were determined  
103 in methanol at 20 °C on a JASCO P-2000 polarimeter (Tokyo, Japan) using the sodium emission  
104 wavelength ( $\lambda = 589$  nm). The centrifugal partition chromatography (CPC) used in this study  
105 (FCPC200®) was provided by Kromaton Technologies (Sainte-Gemmes-sur-Loire, France).  
106 The solvents were pumped by a Gilson 321-H1 2-way binary high-pressure gradient pump. The  
107 samples were introduced into the CPC column via a high pressure injection valve (3725i-038  
108 Rheodyne) equipped with a 20 mL sample loop. The CPC fractions were monitored with a  
109 Varian Prostar 325 DAD detector (Victoria, Australia), at wavelengths of 306 and 280 nm.  
110 HPLC preparative separations were carried out using a Gilson PLC 2050 Purification System  
111 (Villiers-le-bel, France) equipped with a binary pump, a UV-VIS Detector, a fraction Collector,

112 and a Phenomenex Kinetex XB-C18 AXIA column (5  $\mu\text{m}$ , 150 x 21.2 mm). The mobile phase  
113 was composed of two solvents: (A) 0.025% TFA in H<sub>2</sub>O and (B) MeCN. The preparative  
114 enantioseparations were performed using the same HPLC system as above equipped with a  
115 Phenomenex Lux Amylose-1 (5  $\mu\text{m}$ , 250 x 10 mm) chiral column. The mobile phase consisted  
116 of n-Hexane/2-Propanol (85/15, v/v) acidified with 0.01% TFA.

## 117 **2.2. Plant Material.**

118 Grapevine stalks (Merlot) were collected in the “Château Rochemorin” vineyard in the  
119 region of Bordeaux (44°43’17’’N, - 0°33’45’’W, Martillac, France) in January 2017. They were  
120 obtained from Riparia Gloire de Montpellier rootstocks which were planted in 1985. Stalks  
121 specimens were deposited in the Molécules d’Intérêt Biologique (MIB) laboratory at ISVV  
122 (Villenave d’Ornon, France). Grapevine stalks of three other grape varieties (Cabernet  
123 Sauvignon, Sauvignon Blanc, and Merlot) were collected in the “Domaine Haut Dambert”  
124 vineyard in the region of Bordeaux (44°38’58’’N, - 0°10’48’’W, Gornac, France) in January  
125 2015. The accession numbers are listed in **Table 1**.

126 **Table 1.** Cultivar/rootstock combinations, deposit number, and origins

Cultivar	rootstock	Deposit number	Origin (city, region, country)
Merlot	101-14	MIB_M-2017	Martillac (region of Bordeaux, France)
Carbernet Sauvignon	101-14	MIB_CS-TB	Gornac (region of Bordeaux, France)
Merlot	420A	MIB_M-TB	Gornac (region of Bordeaux, France)
Sauvignon Blanc	101-14	MIB_SB-TB	Gornac (region of Bordeaux, France)

127

## 128 **2.3. Extraction and Isolation.**

129 Dried and finely powdered stalks of *Vitis vinifera* (100 g DW) were defatted with  
130 petroleum (1 L) using soxhlet extractor, extracted with 60% aqueous acetone (1 L, 2 times) at  
131 room temperature and filtered. This aqueous acetone extract was evaporated under reduced

132 pressure. The filtrate was concentrated at 35°C under reduced pressure. Aqueous residue (200  
133 mL) was partitioned with EtOAc (4 x 200 mL). The organic extract was concentrated and  
134 freeze-dried to yield 0.7 – 1.5 g depending on the grape variety. The highest concentration in  
135 stilbenes was found with the Merlot (14.3 g.kg<sup>-1</sup> DW), followed by Sauvignon Blanc (9.5 g.kg<sup>-1</sup>  
136 DW) and Cabernet Sauvignon (7.4 g.kg<sup>-1</sup> DW).

137 One g of the organic extract was subjected to the centrifugal partition chromatography  
138 (CPC) using the quaternary biphasic Arizona-K system n-Heptane/EtOAc/MeOH/Water  
139 (1:2:1:2, v/v). The CPC rotor was entirely filled with the aqueous stationary phase in the  
140 descending mode at 500 rpm. After injection of the organic extract, dissolved in 8 mL of the  
141 organic/aqueous phase mixture (1:1, v/v), the aqueous mobile phase was pumped into the  
142 column in descending mode at a flow-rate of 3 mL/min. Then the rotation speed was increased  
143 from 500 to 1200 rpm. The back pressure was 2.5 MPa. The content of the outgoing organic  
144 phase was monitored by online UV absorbance measurement at 280 and 306 nm. Six fractions  
145 were collected (**Supplementary material** Figure S1). *E-ε*-viniferin and *E-ω*-viniferin, obtained  
146 as a white solid were purified from the fraction 6 (around 200 mg) by preparative HPLC with  
147 elution program: 17% B (0-1.12 min), 17-30% B (1.12 -13.12 min), 30-38% B (13.12-22.12  
148 min), 38-100% B (22.12-27 min), 100% (27-30 min). The concentrations of *E-ε*-viniferin were  
149 found in the 0.23 – 0.35 % range (3.5 g.kg<sup>-1</sup> DW for Merlot, 2.6 g.kg<sup>-1</sup> DW for Sauvignon Blanc  
150 and 2.3 g.kg<sup>-1</sup> DW for Cabernet Sauvignon).

151 The enantiomeric excess of the two enantiomers of *E-ε*-viniferin, **1**, extracted from  
152 Cabernet Sauvignon, Merlot and Sauvignon Blanc grape varieties was measured by analytical  
153 chiral HPLC. The mixture of enantiomers of each compound was solubilized in mobile phase  
154 and filtered on PTFE 0.45 μm. The two enantiomers of **1** were separated using a chiral HPLC  
155 column (Chiralpak IF, 250 × 4.6 mm). The mobile phase consisted of n-Hexane/2-Propanol  
156 (90/10, v/v) acidified with 0.001 % TFA. Isocratic elution was performed at a flow-rate of 2

157 mL/min. It was observed that the (–)-enantiomer of **1** was first eluted at 17.2 min, followed by  
158 the (+)-enantiomer at 30.8 min (**Supplementary material** Figure S2).

159 To obtain the two enantiomers of **1** and **2** in fair quantities, a preparative Phenomenex  
160 Lux Amylose-1 (250 × 10 mm, eluent: n-Hexane/2-Propanol 85/15 acidified with 0.01 % TFA,  
161 5 mL/min) was used. For **1**, the first enantiomer (**1a**) was collected at 21 min and the second  
162 one (**1b**) at 30 min, whereas for **2**, the first enantiomer (**2a**) was eluted at 17 min and the second  
163 one (**2b**) at 30 min (**Supplementary material** Figure S3).

#### 164 **2.4. Electronic Circular Dichroism (ECD) measurements.**

165 ECD spectra of compounds **1** and **2** were recorded in EtOH at 20 °C with a 0.2 cm path  
166 length quartz cell. The concentration of the two compounds was taken in the range  $1 \cdot 10^{-4} - 1.5$   
167  $10^{-4}$  M. Spectra were recorded in the 210 – 400 nm wavelength range with a 0.5 nm increment  
168 and a 1s integration time. Spectra were processed with standard spectrometer software, baseline  
169 corrected and slightly smoothed by using a third order least square polynomial fit. Spectral units  
170 were expressed in difference of molar extinction coefficients ( $\Delta\epsilon$  in L/mol/cm).

#### 171 **2.5. Vibrational Circular Dichroism (VCD) measurements.**

172 IR and VCD spectra were recorded with a ThermoNicolet Nexus 670 FTIR spectrometer  
173 equipped with a VCD optical bench (Buffeteau et al., 2005). In this optical bench, the light  
174 beam was focused by a BaF<sub>2</sub> lens (191 mm focal length) to the sample, passing an optical filter,  
175 a BaF<sub>2</sub> wire grid polarizer (Specac), and a ZnSe photoelastic modulator (Hinds Instruments,  
176 Type II/ZS50). The light was then focused by a ZnSe lens (38.1 mm focal length) onto a 1x1  
177 mm<sup>2</sup> HgCdTe (ThermoNicolet, MCTA\* E6032) detector. IR and VCD spectra were recorded  
178 at a resolution of 4 cm<sup>-1</sup>, by coadding 50 scans and 36000 scans (12h acquisition time),  
179 respectively. The sample was held in a fixed path length (100 μm) cell with BaF<sub>2</sub> windows. IR  
180 and VCD spectra of the two enantiomers *E*- $\epsilon$ -viniferin **1** and *E*- $\omega$ -viniferin **2** were measured in  
181 DMSO-*d*<sub>6</sub> at a concentration of 40 mM. Baseline correction of the VCD spectrum was

182 performed by subtracting the two enantiomer VCD spectra of **1** and **2** (recorded under the same  
183 experimental concentration), with division by two. In all experiments, the photoelastic  
184 modulator was adjusted for a maximum efficiency at 1400 cm<sup>-1</sup>. Calculations were done with  
185 the standard ThermoNicolet software, using Happ and Genzel apodization, de-Haseth phase-  
186 correction and a zero-filling factor of one. Calibration spectra were recorded using a  
187 birefringent plate (CdSe) and a second BaF<sub>2</sub> wire grid polarizer, following the experimental  
188 procedure previously published (Nafie & Vidrine, 1982). Finally, in the presented IR spectra,  
189 the solvent absorption was subtracted out.

## 190 **2.6. DFT calculations.**

191 All DFT calculations were carried out with Gaussian 09 (Frisch et al., 2009). The  
192 calculation of the IR and VCD spectra began by a conformational analysis of (7a*S*,8a*S*)- and  
193 (7a*R*,8a*S*)-viniferin (**1a** and **2b**), considering a *trans* conformation of the C=C bond.  
194 Preliminary conformer distribution search of **1a** and **2b** was performed at the molecular  
195 mechanics level of theory, employing MMFF94 force fields incorporated in ComputeVOA  
196 software package. 290 conformers of **1a** (305 conformers for **2b**) were found within roughly 4  
197 kcal/mol of the lowest energy conformer. Their geometries were optimized at the DFT level  
198 using B3LYP functional and 6-31G\*\* basis set, leading to 74 (**1a**) and 61 (**2b**) different  
199 conformers within an energetic window of 3.25 (**1a**) and 2.87 (**2b**) kcal/mol. Finally, only the  
200 twenty four (**1a**) and twenty five (**1b**) lowest energetic geometries were kept, corresponding to  
201 Boltzmann population higher than 1%. Vibrational frequencies, IR and VCD intensities were  
202 calculated at the same level of theory. The spectra were calculated for the isolated molecule *in*  
203 *vacuo*. For comparison to experiment, the calculated frequencies were scaled by 0.968 and the  
204 calculated intensities were converted to Lorentzian bands with a full-width at half-maximum  
205 (FWHM) of 7 cm<sup>-1</sup>.

## 206 **2.7. Macrophages cell culture.**

207 RAW 264.7 cells were obtained from the American Type Culture Collection (ATCC).  
208 They were cultured in 75 cm<sup>2</sup> flasks containing 20 mL of DMEM supplemented with 10% of  
209 FBS. Cells were maintained in a humidified incubator at 37°C and 5% of CO<sub>2</sub>. In order to  
210 perform the experiments, every 3 days cells were detached by scrapping and sub-cultured in 96  
211 transparent (for cytotoxicity and NO measurements) or black (ROS measurement) well plates  
212 with the same culture medium (200 µL) supplemented with 4 mM of glutamine at a density of  
213 40,000 cells per well.

#### 214 **2.8. MTT assay.**

215 The cytotoxicity of stereoisomers of viniferin (**1a**, **1b**, **2a** and **2b**) was carried out by using  
216 MTT that allows to measure the cellular metabolic activity of cells. After 24 hours of incubation  
217 in 96 well plates, cells were incubated with different concentrations of the four stereoisomers  
218 (0.5 to 100 µM) of viniferin (**1a**, **1b**, **2a** and **2b**). After 24 hours of treatment, cells were  
219 incubated with 0.5 mg/mL of MTT during 3 hours at 37°C and 5% of CO<sub>2</sub>. Finally, the blue  
220 formazan crystals formed at the well bottom were dissolved with 100 µL of DMSO and, 30  
221 minutes after, the absorbance was measured with a microplate reader (FLUOstar Optima, BMG  
222 Labtech) set at 595 nm. **Results are expressed as mean of four replicates (n=4).**

#### 223 **2.9. Measurement of NO production.**

224 In order to evaluate the anti-inflammatory potential of the stereoisomers of viniferin (**1a**,  
225 **1b**, **2a** and **2b**), RAW 264.7 cells were incubated during 24 hours with all compounds at  
226 different non-cytotoxic concentrations (0.5, 1, 2.5, 5 and 10 µM) in the presence or absence of  
227 LPS (inflammatory triggering agent, **0.1 µg/mL**) in RPMI medium. Then, 70 µL of supernatant  
228 were mixed with 70 µL of Griess reagent and after an incubation of 15 minutes at room  
229 temperature, the absorbance was measured at 540 nm by using a microplate reader (FLUOstar  
230 Optima, BMG Labtech). NO concentration by using a calibration standard curve of sodium  
231 nitrite (0-100 µM). **Results are expressed as mean of four replicates (n=4).**

## 232 **2.10. Intracellular ROS measurement.**

233 The intracellular generation of ROS in cells was analyzed using the fluorometric probe  
234 DCFH<sub>2</sub>-DA. After treatment with the stereoisomers of viniferin (**1a**, **1b**, **2a** and **2b**) at different  
235 concentrations (0.5, 1, 2.5, 5 and 10 μM) during 24 hours in 96 black well plates, cells were  
236 washed and 5 mM of DCFH<sub>2</sub>-DA diluted in PBS was added. After 30 minutes of incubation in  
237 the darkness at 37°C and 5% of CO<sub>2</sub>, the fluorescence intensity was measured using a  
238 microplate reader (FLUOstar Optima, BMG Labtech) set at 485 nm (excitation wavelength)  
239 and 520 nm (emission wavelength). **Results are expressed as mean of four replicates (n=4).**

## 240 **2.11. Statistical Analysis.**

241 Data were subjected to one-way ANOVA followed by a Tukey's test ( $p < 0.05$ ) with  
242 Microsoft Excel® XLSTAT (Version 1.1.463) to explore significant differences for cell  
243 viability, NO and ROS measurements.

244

## 245 **3. Results and Discussion**

### 246 **3.1. Isolation of viniferin dimers and chiroptical properties in grape varieties**

247 **One hundred** g of dry fine powder of *Vitis vinifera* cv. Merlot stalks, previously defatted  
248 with petroleum ether, was extracted two times with 60% aqueous acetone at room temperature.  
249 The extract was then filtered and the filtrate was concentrated *in vacuo*. The aqueous phase was  
250 further partitioned between EtOAc and water. The organic extract was separated by  
251 combination of centrifugal partition chromatography (**Supplementary material** Figure S1) and  
252 preparative RP-18 HPLC to obtain *E-ε*-viniferin with  $[\alpha]_{589}^{20} = +10.4^\circ$  (c 0.2, MeOH) and *E-ω*-  
253 viniferin with  $[\alpha]_{589}^{20} = -103^\circ$  (c 0.15, MeOH). In addition, the *E-ε*-viniferin was purified from  
254 three different grape varieties (Cabernet Sauvignon, Merlot, and Sauvignon Blanc). The  
255 specific optical rotation values of *E-ε*-viniferin varied between -12 and +46° (**Supplementary**  
256 **material** Table S1), indicating that *E-ε*-viniferin is not enantiopure. This could be related to the

257 fact that the enantiomeric ratio of *E-ε*-viniferin could be different due to the grape varieties. For  
 258 example, Cabernet Sauvignon variety gives the dextrorotatory form of *E-ε*-viniferin whereas  
 259 the Merlot variety gives preferentially the levorotatory form. On the other hand, Sauvignon  
 260 Blanc exhibits a lower value of specific rotation that probably means the presence of rather  
 261 racemic mixture (**Supplementary material** Table S1). These values are in agreement with  
 262 those reported in the literature from *V. vinifera* (Vitaceae) and others plant families, as shown  
 263 in **Table 2**. The proportion of the two enantiomers of *E-ε*-viniferin and the enantiomeric excess  
 264 (ee) for the three grape varieties are given in **Supplementary material** Table S2. The  
 265 enantiomeric excess (ee) extracted from Cabernet Sauvignon, Merlot and Sauvignon Blanc  
 266 grape varieties was measured by analytical chiral HPLC (**Supplementary material** Figure S2).  
 267 **Table 2.** Optical rotation values of *E-ε*-viniferin measured in this study and found in the  
 268 literature.

Species	Family	$[\alpha]_{589}^{20}$	Conditions	Reference
<i>Vitis vinifera</i> cv. Merlot	Vitaceae	+10.4°	0.13, MeOH	This study
<i>Vitis vinifera</i> cv. Cabernet Sauvignon	Vitaceae	+46.4°	0.064, MeOH	This study
<i>Vitis vinifera</i> cv. Merlot	Vitaceae	-12.1°	0.07, MeOH	This study
<i>Vitis vinifera</i> cv. Sauvignon Blanc	Vitaceae	+5.9°	0.083, MeOH	This study
<i>Vitis amurensis</i>	Vitaceae	+41°	0.13, MeOH	(Pawlus et al., 2013)
<i>Vitis vinifera</i>	Vitaceae	+34°	0.32, MeOH	(Mattivi et al., 2011)
<i>Vitis heyneana</i>	Vitaceae	+39°	0.40, MeOH	(Li et al., 1996)
<i>Vitis chunganensis</i>	Vitaceae	+32°	0.27, MeOH	(He et al., 2009)
<i>Carex pumila</i>	Cyperaceae	-27,9°	0.843, MeOH	(Kurihara et al., 1990)
<i>Carex kobomugi</i>	Cyperaceae	-46°	0.5, MeOH	(Kurihara et al., 1991)
Rhubarb	Polygonaceae	-47°	0.5, MeOH	(Ngoc et al., 2008)

269

## 270 3.2. Absolute configuration of viniferin stereoisomers using NMR, VCD and ECD

271 According to the above observations, *E-ε*-viniferin (mixture of enantiomers) was then  
272 purified by chiral HPLC to separate the two enantiomers (**Supplementary material** Figure S3).  
273 The first eluted compound showed a specific optical rotation value  $[\alpha]_{589}^{20} = -43.4^\circ$  (c 0.06,  
274 MeOH) whereas a value  $[\alpha]_{589}^{20} = +46^\circ$  (c 0.06, MeOH) was measured for the second eluted  
275 compound. Accordingly, we have shown that *E-ω*-viniferin was also a mixture of enantiomers  
276 and it was purified by chiral HPLC as mentioned above to yield  $[\alpha]_{589}^{20} = +107^\circ$  (c 0.07, MeOH)  
277 for the first eluted compound and  $[\alpha]_{589}^{20} = -155^\circ$  (c 0.14, MeOH) for the second eluted  
278 compound. The NMR data ( $^1\text{H}$  and  $^{13}\text{C}$ ) of *E-ε*- and *E-ω*-viniferin were found to be similar to  
279 those previously obtained in our laboratory and in literature (**Supplementary material** Table  
280 S3, Figures S4 and S6) (Pawlus et al., 2013; Mattivi et al., 2011). The relative configuration  
281 was established by ROESY. For *E-ε*-viniferin, the absence of NOE correlation between protons  
282 H7a/H8a (**Supplementary material** Figure S5) indicated that these protons were *trans*-  
283 orientated whereas for *E-ω*-viniferin, the cross peak between H7a/H8a (**Supplementary**  
284 **material** Figure S7), indicated these protons were cofacial (*cis*-orientation). In addition, the IR  
285 spectra of *E-ε*- and *E-ω*-viniferin allow the discrimination of the two diastereoisomers, using  
286 the intensity of the band at  $1148\text{ cm}^{-1}$ . Indeed, the *E-ω*-viniferin compound exhibits a high  
287 intensity for this band, whereas the  $1148\text{ cm}^{-1}$  band is weak for the *E-ε*-viniferin compound  
288 (**Supplementary material** Figure S8).

289 The absolute configurations of the chiral centers (C7a and C8a) of *E-ε*-viniferin and *E*-  
290 *ω*-viniferin were deduced in the same manner as for the two enantiomers of (–)-*E*-gnetin C  
291 (Buffeteau et al., 2014), using vibrational circular dichroism (VCD) associated with theoretical  
292 calculations. VCD spectra of the two enantiomers of compounds **1** and **2** were recorded in

293 DMSO-*d*<sub>6</sub> at a concentration of 40 mM and the raw and baseline corrected VCD spectra are  
294 reported in **Supplementary material** Figures S9 and S10. For each compound, opposite VCD  
295 spectra were measured for the two enantiomers, as expected for enantiopure compounds.

296 The theoretical calculations began by a conformational analysis of (7*aS*,8*aS*)-*E-ε*-  
297 viniferin (**1a**) and (7*aR*,8*aS*)-*E-ω*-viniferin (**2b**). Preliminary conformer distribution search of  
298 **1a** and **2b** was performed at the molecular mechanics level of theory, employing MMFF94  
299 force fields incorporated in ComputeVOA software package. 290 conformers of **1a** (305  
300 conformers for **2b**) were found within roughly 4 kcal/mol of the lowest energy conformer. Their  
301 geometries were optimized at the DFT level using B3LYP functional and 6-31G\*\* basis set,  
302 leading to 74 (**1a**) and 61 (**2b**) different conformers within an energetic window of 3.25 (**1a**)  
303 and 2.87 (**2b**) kcal/mol. Finally, only the twenty four (**1a**) and twenty five (**1b**) lowest energetic  
304 geometries were kept, corresponding to Boltzmann population higher than 1%. Calculations  
305 were performed for the isolated molecule *in vacuo*. Harmonic vibrational frequencies were  
306 calculated at the same level to confirm that all structures were stable conformations and to  
307 enable free energies to be calculated. The predicted VCD spectra, taking into account the  
308 relative populations of (7*aS*,8*aS*)-*E-ε*-viniferin and (7*aR*,8*aS*)-*E-ω*-viniferin, were compared to  
309 the experimental VCD spectra of the second eluted compound of **1** and **2** in **Figure 2**. The  
310 predicted VCD spectra of (7*aS*,8*aS*)-*E-ε*-viniferin and (7*aR*,8*aS*)-*E-ω*-viniferin reproduced  
311 fairly well the intensity and the sign of most bands observed in the experimental VCD spectra,  
312 allowing the definitive determination of the 8*aS* configuration of the beta stereogenic carbon of  
313 the benzofuran group. The determination of the configuration of the alpha stereogenic carbon  
314 was less obvious from VCD data, even though a better agreement between theoretical and  
315 experimental spectra in the 1550-1400 cm<sup>-1</sup> spectral range was obtained with the 7*aS*  
316 configuration for the second eluted compound of **1** and with the 7*aR* configuration for the  
317 second eluted compound of **2**. The 7*aS* configuration of the alpha stereogenic carbon of

318 benzofuran group for the second eluted compound of **1** was confirmed by the absence of a cross-  
319 peak between the protons H7a ( $\delta=5.41$  ppm) and H8a ( $\delta=4.47$  ppm) in the ROESY spectrum  
320 (**Supplementary material** Figure S5), indicating the opposite orientation of these two protons.  
321 Similarly, the *7aR* configuration of the alpha stereogenic carbon of benzofuran group for the  
322 second eluted compound of **2** was confirmed by the presence of a cross-peak between the  
323 protons H7a ( $\delta=5.86$  ppm) and H8a ( $\delta=4.70$  ppm) in the ROESY spectrum (**Supplementary**  
324 **material** Figure S7), indicating the cofacial orientation of these two protons. Thus, this VCD  
325 analysis, associated with NMR results, unambiguously established the (+)-(*7aS,8aS*)  
326 configuration for *E-ε*-viniferin and the (+)-(*7aR,8aS*) configuration for *E-ω*-viniferin. This  
327 result confirm the first proposition of the absolute configuration, (-)-(*7aR,8aR*), for *E-ε*-  
328 viniferin isolated from *Carex pumila* (Cyperaceae) by Kurihara et al. (1990).

329 The experimental VCD spectra measured for *E-ε*-viniferin extracted from different  
330 grape varieties are compared in **Figure 3** with the VCD spectrum of the enantiopure second  
331 eluted compound purified by chiral HPLC. The VCD spectrum of *E-ε*-viniferin extracted from  
332 Cabernet Sauvignon stalks is quasi identical to the VCD spectrum of the enantiopure  
333 compound, revealing that this grape variety allows the extraction of *E-ε*-viniferin with an  
334 enantiomeric excess close to 1. Chiral HPLC measurements on this compound revealed an  
335 enantiomeric excess of 98.34% (**Supplementary material** Table S2). This feature is very  
336 interesting since the enantiopure (+)-(*7aS,8aS*)-*E-ε*-viniferin compound can be obtained  
337 directly by extraction from Cabernet Sauvignon. The VCD spectrum of *E-ε*-viniferin extracted  
338 from Merlot is opposite with an intensity divided by almost 4, as expected by the enantiomeric  
339 excess measured by chiral HPLC (ca. 23.32%). Finally, the VCD spectrum of *E-ε*-viniferin  
340 extracted from Sauvignon Blanc exhibits a very weak intensity, with the same sign than the one  
341 of Cabernet Sauvignon, as expected by chiral HPLC measurements.

342 As electronic circular dichroism (ECD) experiments are currently used in the structural  
343 studies of stilbenes, ECD spectra of the second eluted compound of **1** and **2** are reported in  
344 **Supplementary material** Figures S11 and S12, respectively. The ECD spectrum of (+)-*E-ε*-  
345 viniferin exhibits a positive band at 236 nm (+22.7) and a broad negative band around 300 nm  
346 (-3.8), in agreement with the ECD spectrum reported in the literature (Ito et al., 2009). The ECD  
347 spectrum of (+)-*E-ω*-viniferin is slightly different, with a positive band at 227.5 nm (+17), a  
348 negative band at 250 nm (-3.3) and a broad negative band around 310 nm (-7).

### 349 *3.3. Antioxidant and anti-inflammatory activities of viniferin stereoisomers in LPS-stimulated* 350 *macrophages*

351 The four stereoisomers of viniferin (**1a**, **1b**, **2a** and **2b**) were evaluated for their anti-  
352 inflammatory and anti-oxidant activities in LPS-stimulated macrophages. Firstly, the MTT  
353 assay was performed in order to evaluate the cytotoxicity of all stereoisomers. Thus, cells were  
354 treated with different concentrations of viniferin **1a**, **1b**, **2a** and **2b** (0.5-100 μM) during 24  
355 hours. **Figure 4a** displays the cell viability expressed as percentage relative to the non-treated  
356 cells. As expected, the LPS did not affect the cell viability. Concerning viniferin stereoisomers,  
357 it can be observed that at low concentrations, between 0.5 to 10 μM, the metabolic activity of  
358 cells was not affected. However, from 25 μM, all compounds presented a significant cytotoxic  
359 effect, by killing between 40-70% of cells (**Figure 4a**). It can be also observed that compound  
360 **2a** presents a more slight toxic effect at 25 μM comparing with the others compounds at the  
361 same concentrations. No significant differences were observed between all stereoisomers at the  
362 highest concentrations (50-100 μM). Based on these results, the concentrations ranging between  
363 0.5 to 10 μM were selected to further evaluate the potential effect of viniferin stereoisomers to  
364 diminish the nitric oxide (NO) and reactive oxygen species (ROS) production.

365 RAW 264.7 cells were activated with LPS (0.1 μg/mL) in the presence of the four  
366 stereoisomers of viniferin at 0.5, 1, 2.5, 5 and 10 μM during 24 hours. Afterwards, the NO<sub>2</sub> in

367 culture media were measured by the Griess reaction. The NO content ( $\mu\text{M}$ ) of cells treated with  
368 only LPS (positive control) increased more than tenfold ( $26.9 \mu\text{M}$ ) in comparison with the  
369 negative control ( $2.4 \mu\text{M}$ ) (cells without LPS treatment) (**Figure 4b**). A significant diminution  
370 of NO was observed at all concentrations of **1a** and **1b**. However, this effect is significant for  
371 **2a** and **2b** only from  $2.5 \mu\text{M}$ . Regarding differences between compounds, at the highest  
372 concentration tested ( $10 \mu\text{M}$ ) it can be seen a more potent effect of **1a** with a diminution of 60%  
373 of NO production while for **1b** this decrease is 41%. By contrast, at this concentration the **2a**  
374 and **2b** exhibited the same effect (52 and 55%, respectively) (**Figure 4b**).

375 In addition, the intracellular ROS production induced by LPS was investigated by using  
376 the fluorometric probe DCFH<sub>2</sub>-DA, which permits the detection and quantification of ROS. The  
377 results show that **1a** is significantly the most active stereoisomer diminishing the intracellular  
378 ROS from the lowest concentration and reaching a reduction of 63% comparing with LPS alone.  
379 We can also observe differences between **2a** and **2b**, being this last significantly more anti-  
380 oxidant, and diminishing the ROS production on 48% while only a 21% was observed for **2a**  
381 in comparison with control (**Figure 4c**).

382 Based on these results it can be concluded that viniferin stereoisomers possess *in vitro*  
383 anti-inflammatory and anti-oxidant properties in macrophages cells and that their activity varies  
384 according to their spatial configuration. Apart from resveratrol, other oligomeric stilbenes, as  
385 different viniferins, are showing promising results as anti-inflammatory, anti-oxidant,  
386 neuroprotective, anti-obesity, anticancer agents (Nassra et al., 2013; Ohara et al., 2015; Ficarra  
387 et al., 2016; Caillaud et al., 2019; Nivellet et al., 2018; Vion et al., 2018; Sergi et al., 2021).

388 Our results demonstrate that the four stereoisomers are toxic from  $10 \mu\text{M}$  concentration  
389 in RAW 264.7 cells. The same observation has been described for viniferin compounds in the  
390 same cellular model (Ha et al., 2018), but also in other cellular models as BV2 or Caco-2 cells  
391 (Nassra et al., 2013; Medrano-Padial et al., 2020).

392 Concerning anti-inflammatory properties, Nassra and co-workers showed that viniferins  
393 (*E*- $\delta$ -viniferin, *E*- $\epsilon$ -viniferin and *E*- $\omega$ -viniferin present very similar inhibitory capacity to reduce  
394 LPS-induced NO production in BV2 microglial cells. They showed that *E*- $\epsilon$ -viniferin is the  
395 most active compound (IC<sub>50</sub>: 8.6) presenting even better results than *E*-resveratrol (IC<sub>50</sub>: 13.1)  
396 (Nassra et al., 2013). Additionally, other more recent published article has demonstrated that  
397 *E*- $\epsilon$ -viniferin, also at low concentrations, is able to counteract the inflammation induced by  
398 LPS-activated microglia in N9 cells (Sergi et al., 2021). Only one recent article has  
399 demonstrated in our same cellular model (RAW 264.7 macrophage cells) that *E*- $\epsilon$ -viniferin  
400 decreased NO, PGE<sub>2</sub>, iNOS, and COX-2 productions after LPS stimulation and that this activity  
401 is may be mediated by the NF- $\kappa$ B activation (Ha et al., 2018). The present findings demonstrate  
402 for the first time that viniferin stereoisomers possess anti-inflammatory and anti-oxidant  
403 activities. Moreover and even though their structures are quite similar, this paper proved that  
404 these bioactivities are different according to their configuration.

#### 405 **4. Conclusion**

406 In summary, this work demonstrated for the first time the presence of four stereoisomers  
407 of viniferin stilbene (*7aS,8aS*)-*E*- $\epsilon$ -viniferin, (*7aR,8aR*)-*E*- $\epsilon$ -viniferin, (*7aS,8aR*)-*E*- $\omega$ -viniferin,  
408 and (*7aR,8aS*)-*E*- $\omega$ -viniferin in grapevine branches. The absolute configurations were clearly  
409 established by vibrational circular dichroism (VCD) spectroscopy in combination with density  
410 functional theory (DFT) calculations. Moreover, the anti-inflammatory and anti-oxidant  
411 activities of the four identified viniferin stereoisomers revealed that viniferin stereoisomers  
412 possess different bioactivities according to their configuration. In addition, for the first time,  
413 the two enantiomers of *E*- $\epsilon$ -viniferin in grapevine are present and the enantiomeric excess are  
414 grape variety-dependent. Overall, the present study extends our knowledge of absolute  
415 stereochemistry of viniferin dimers present in grapevine and paves the way for further  
416 investigation related to their structure-activity relationship.

417

## 418 ASSOCIATED CONTENT

### 419 Supporting Information

420 The following data are available as supplementary material: Specific optical rotation values of  
421 *E-ε*-viniferin (Table S1), enantiomeric excess for the three grape varieties (Table S2), NMR  
422 data of *E-ε*-viniferin and *E-ω*-viniferin (Table S3), CPC chromatogram (Figure S1), analytical  
423 (Figure S2) and preparative (Figure S3) chiral HPLC chromatograms, <sup>1</sup>H NMR and <sup>1</sup>H-<sup>1</sup>H-  
424 ROESY NMR spectra of *E-ε*-viniferin (Figure S4 and S5), <sup>1</sup>H NMR and <sup>1</sup>H-<sup>1</sup>H-ROESY NMR  
425 spectra of *E-ω*-viniferin (Figure S6 and S7), IR spectra of *E-ε*-viniferin and *E-ω*-viniferin  
426 (Figure S8), VCD spectra of *E-ε*-viniferin and *E-ω*-viniferin (Figures S9 and S10), ECD spectra  
427 of *E-ε*-viniferin and *E-ω*-viniferin (Figures S11 and S12).

### 428 ACKNOWLEDGMENTS

429 The authors thank R. Cooke for proofreading the manuscript.

### 430 FUNDING

431 Research support was provided by the French Ministry of Higher Education and Research.  
432 NMR experiments were performed at the Bordeaux Metabolome Facility and MetaboHUB  
433 (ANR-11-INBS-0010 project).

### 434 REFERENCES

435 **Barceló**, A. R., Pomar, F., López-Serrano, M., & Pedreño, M. A. (2003). Peroxidase: a  
436 multifunctional enzyme in grapevines. *Functional Plant Biology*, 30(6), 577–591.  
437 <https://doi.org/10.1071/fp02096>

438 Breuil, A. C., Adrian, M., Pirio, N., Meunier, P., Bessis, R., & Jeandet, P. (1998). Metabolism  
439 of stilbene phytoalexins by *Botrytis cinerea*: 1. Characterization of a resveratrol  
440 dehydrodimer. *Tetrahedron Letters*, 39(7), 537–540. [https://doi.org/10.1016/S0040-](https://doi.org/10.1016/S0040-4039(97)10622-0)  
441 [4039\(97\)10622-0](https://doi.org/10.1016/S0040-4039(97)10622-0)

442 Buffeteau, T., Cavagnat, D., Bisson, J., Marchal, A., Kapche, G. D., Battistini, I., Da Costa, G.,  
443 Badoc, A., Monti, J.-P., Mérillon, J.-M., & Waffo-Téguo, P. (2014). Unambiguous  
444 determination of the absolute configuration of dimeric stilbene glucosides from the  
445 rhizomes of *Gnetum africanum*. *Journal of Natural Products*, 77(8), 1981–1985.  
446 <https://doi.org/10.1021/np500427v>

447 Buffeteau, T., Lagugn -Labarthe, F., & Sourisseau, C. (2005). Vibrational circular dichroism  
448 in general anisotropic thin solid films: measurement and theoretical approach. *Applied*  
449 *Spectroscopy*, 59(6), 732–745. <https://doi.org/10.1366/0003702054280568>

450 Caillaud, M., Guillard, J., Richard, D., Milin, S., Chassaing, D., Paccalin, M., Page, G., & Bilan,  
451 A. R. (2019). *Trans*  $\epsilon$  viniferin decreases amyloid deposits and inflammation in a mouse  
452 transgenic Alzheimer model. *PLoS ONE*, 14(2) : e0212663.  
453 <https://doi.org/10.1371/journal.pone.0212663>

454 Calder n, A. A., Zapata, J. M., Pedre o, M. A., Mu oz, R., & Barcel , A. R. (1992). Levels of  
455 4-hydroxystilbene-oxidizing isoperoxidases related to constitutive disease resistance in  
456 *in vitro*-cultured grapevine. *Plant Cell, Tissue and Organ Culture*, 29(2), 63–70.

457 Cichewicz, R. H., Kouzi, S. A., & Hamann, M. T. (2000). Dimerization of resveratrol by the  
458 grapevine pathogen *Botrytis cinerea*. *Journal of Natural Products*, 63(1), 29–33.  
459 <https://doi.org/10.1021/np990266n>

460 Cretin, B. N., Sallembien, Q., Sindt, L., Daugey, N., Buffeteau, T., Waffo-Tegu, P.,  
461 Dubourdiu, D., & Marchal, A. (2015). How stereochemistry influences the taste of  
462 wine: isolation, characterization and sensory evaluation of lyoniresinol stereoisomers.  
463 *Analytica Chimica Acta*, 888, 191-198. <https://doi.org/10.1016/j.aca.2015.06.061>

464 Ficarra, S., Tellone, E., Pirolli, D., Russo, A., Barreca, D., Galtieri, A., Giardina, B., Gavezzotti,  
465 P., Riva, S., & Rosa, M. C. D. (2016). Insights into the properties of the two enantiomers  
466 of *trans*- $\delta$ -viniferin, a resveratrol derivative: antioxidant activity, biochemical and  
467 molecular modeling studies of its interactions with hemoglobin. *Molecular BioSystems*,  
468 12, 1276-1286. <https://doi.org/10.1039/c5mb00897b>

469 Frisch, M. J., Trucks, G. W., Schlegel, H. B., Scuseria, G. E., Robb, M. A., Cheeseman, J. R.,  
470 Scalmani, G., Barone, V., Mennucci, B., Petersson, G. A., Nakatsuji, H., Caricato, M.,  
471 Li, X., Hratchian, H. P., Izmaylov, A. F., Bloino, J., Zheng, G., Sonnenberg, J. L., Hada,  
472 M.; Ehara, M., Toyota, K., Fukuda, R., Hasegawa, J., Ishida, M., Nakajima, T., Honda,  
473 Y., Kitao, O., Nakai, H., Vreven, T., Montgomery, J. A. Jr., Peralta, J. E., Ogliaro, F.,  
474 Bearpark, M., Heyd, J. J., Brothers, E., Kudin, K. N., Staroverov, V. N., Kobayashi, R.,  
475 Normand, J., Raghavachari, K., Rendell, A., Burant, J. C., Iyengar, S. S., Tomasi, J.,  
476 Cossi, M., Rega, N., Millam, J. M., Klene, M., Knox, J. E., Cross, J. B., Bakken, V.,  
477 Adamo, C., Jaramillo, J., Gomperts, R., Stratmann, R. E., Yazyev, O., Austin, A. J.,  
478 Cammi, R., Pomelli, C., Ochterski, J. W., Martin, R. L., Morokuma, K., Zakrzewski, V.  
479 G., Voth, G. A., Salvador, P., Dannenberg, J. J., Dapprich, S., Daniels, A. D., Farkas, Ö  
480 ., Foresman, J. B., Ortiz, J. V., Cioslowski, J., Fox, D. J. Gaussian 09, Revision A.01;  
481 Gaussian Inc.: Wallingford, CT, 2009. Retrieved September 25, 2021, from  
482 <https://gaussian.com/glossary/g09/>

483 Gabaston, J., Valls Fonayet, J., Franc, C., Waffo-Teguo, P., de Revel, G., Hilbert, G., Gomès,  
484 E., Richard, T., Mérillon, J.-M. (2020). Characterization of stilbene composition in  
485 grape berries from wild *Vitis* species in year-to-year harvest. *Journal of Agricultural*  
486 *and Food Chemistry*, 68(47), 13408-13417. <https://doi.org/10.1021/acs.jafc.0c04907>

487 Ha, D. T., Long, P. T., Hien, T. T., Tuan, D. T., An, N. T. T., Khoi, N. M., Van Oanh, H., &  
488 Hung, T. M. (2018). Anti-inflammatory effect of oligostilbenoids from *Vitis heyneana*  
489 in LPS-stimulated RAW 264.7 macrophages via suppressing the NF- $\kappa$ B activation.  
490 *Chemistry Central Journal*, 12(1), 14. <https://doi.org/10.1186/s13065-018-0386-5>

491 He, S., Jiang, L., Wu, B., Li, C., & Pan, Y. (2009). Chunganenol: an unusual antioxidative  
492 resveratrol hexamer from *Vitis chunganensis*. *The Journal of Organic Chemistry*,  
493 74(20), 7966–7969. <https://doi.org/10.1021/jo901354p>

494 Ito, T., Abe, N., Oyama, M., & Iinuma, M. (2009). Absolute structures of C-glucosides of  
495 resveratrol oligomers from *Shorea uliginosa*. *Tetrahedron Letters*, 50, 2516–2520.  
496 <https://doi.org/10.1016/j.tetlet.2009.03.043>

497 Keylor, M. H., Matsuura, B. S., & Stephenson, C. R. J. (2015). Chemistry and biology of  
498 resveratrol-derived natural products. *Chemical Reviews*, 115(17), 8976–9027.  
499 <https://doi.org/10.1021/cr500689b>

500 Ko, J.-H., Sethi, G., Um, J.-Y., Shanmugam, M. K., Arfuso, F., Kumar, A. P., Bishayee, A., &  
501 Ahn, K. S. (2017). The role of resveratrol in cancer therapy. *International Journal of*  
502 *Molecular Sciences*, 18(12). <https://doi.org/10.3390/ijms18122589>

503 Kurihara, H., Kawabata, J., Ichikawa, S., Mishima, M., & Mizutani, J. (1991). Oligostilbenes  
504 from *Carex kobomugi*. *Phytochemistry*, 30(2), 649–653. [https://doi.org/10.1016/0031-](https://doi.org/10.1016/0031-9422(91)83745-7)  
505 [9422\(91\)83745-7](https://doi.org/10.1016/0031-9422(91)83745-7)

506 Kurihara, H., Kawabata, J., Ichikawa, S., & Mizutani, J. (1990). (-)-e-Viniferin and related  
507 oligostilbenes from *Carex pumila* Thunb. (Cyperaceae). *Agricultural and Biological*  
508 *Chemistry*, 54(4), 1097–1099.

509 Li, W. W., Ding, L. S. eng, Li, B. G. ng, & Chen, Y. Z. (1996). Oligostilbenes from *Vitis*  
510 *heyneana*. *Phytochemistry*, 42(4), 1163–1165. <https://doi.org/10.1016/0031->  
511 9422(96)00069-6

512 Mattivi, F., Vrhovsek, U., Malacarne, G., Masuero, D., Zulini, L., Stefanini, M., Moser, C.,  
513 Velasco, R., & Guella, G. (2011). Profiling of resveratrol oligomers, important stress  
514 metabolites, accumulating in the leaves of hybrid *Vitis vinifera* (Merzling × Teroldego)  
515 genotypes infected with *Plasmopara viticola*. *Journal of Agricultural and Food*  
516 *Chemistry*, 59(10), 5364–5375. <https://doi.org/10.1021/jf200771y>

517 Medrano-Padial, C., Puerto, M., Merchán-Gragero, M. D. M., Moreno, F. J., Richard, T.,  
518 Cantos-Villar, E., & Pichardo, S. (2020). Cytotoxicity studies of a stilbene extract and  
519 its main components intended to be used as preservative in the wine industry. *Food*  
520 *Research International*, 137, 109738. <https://doi.org/10.1016/j.foodres.2020.109738>

521 Morales, M., & Barceló, A. R. (1997). A basic peroxidase isoenzyme from vacuoles and cell  
522 walls of *Vitis vinifera*. *Phytochemistry*, 45(2), 229–232. <https://doi.org/10.1016/S0031->  
523 9422(96)00825-4

524 Nafie, L. A., Vidrine, D. W. In *Fourier Transform Infrared Spectroscopy*; Ferraro, J. R.; Basile,  
525 L. J., Eds.; Academic Press: New York, 1982; Vol. 3, pp 83–123.

526 Nassra, M., Krisa, S., Papastamoulis, Y., Kapche, G. D., Bisson, J., André, C., Konsman, J.-P.,  
527 Schmitter, J.-M., Mérillon, J.-M., & Waffo-Téguo, P. (2013). Inhibitory activity of plant  
528 stilbenoids against nitric oxide production by lipopolysaccharide-activated microglia.  
529 *Planta Medica*, 79(11), 966–970. <https://doi.org/10.1055/s-0032-1328651>

530 Ngoc, T. M., Hung, T. M., Thuong, P. T., Na, M., Kim, H., Ha, D. T., Min, B.-S., Minh, P. T.  
531 H., & Bae, K. (2008). Inhibition of human low density lipoprotein and high density

532 lipoprotein oxidation by oligostilbenes from rhubarb. *Biological & Pharmaceutical*  
533 *Bulletin*, 31(9), 1809–1812. <https://doi.org/10.1248/bpb.31.1809>.

534 Nivelles, L., Aires, V., Rioult, D., Martiny, L., Tarpin, M., & Delmas, D. (2018). Molecular  
535 analysis of differential antiproliferative activity of resveratrol, epsilon viniferin and  
536 labruscol on melanoma cells and normal dermal cells. *Food and Chemical Toxicology*,  
537 116(Pt B), 323–334. <https://doi.org/10.1016/j.fct.2018.04.043>

538 Ohara, K., Kusano, K., Kitao, S., Yanai, T., Takata, R., & Kanauchi, O. (2015). ε-Viniferin, a  
539 resveratrol dimer, prevents diet-induced obesity in mice. *Biochemical and Biophysical*  
540 *Research Communications*, 468(4), 877–882.  
541 <https://doi.org/10.1016/j.bbrc.2015.11.047>

542 Pawlus, A. D., Sahli, R., Bisson, J., Rivière, C., Delaunay, J.-C., Richard, T., Gomès, E.,  
543 Bordenave, L., Waffo-Téguo, P., & Mérillon, J.-M. (2013). Stilbenoid profiles of canes  
544 from *Vitis* and *Muscadinia* species. *Journal of Agricultural and Food Chemistry*, 61(3),  
545 501–511. <https://doi.org/10.1021/jf303843z>

546 Pezet, R. (1998). Purification and characterization of a 32-kDa laccase-like stilbene oxidase  
547 produced by *Botrytis cinerea* Pers.:Fr. *FEMS Microbiology Letters*, 167(2), 203–208.

548 Richard, T., Pawlus, A. D., Iglesias, M.-L., Pedrot, E., Waffo-Teguo, P., Merillon, J.-M., &  
549 Monti, J.-P. (2011). Neuroprotective properties of resveratrol and derivatives. *Annals of*  
550 *the New York Academy of Sciences*, 1215(1), 103–108. <https://doi.org/10.1111/j.1749->  
551 [6632.2010.05865.x](https://doi.org/10.1111/j.1749-6632.2010.05865.x)

552 Rivière, C., Pawlus, A. D., & Mérillon, J.-M. (2012). Natural stilbenoids: distribution in the  
553 plant kingdom and chemotaxonomic interest in Vitaceae. *Natural Product Reports*,  
554 29(11), 1317–1333. Scopus. <https://doi.org/10.1039/c2np20049j>

555 Saiko, P., Szakmary, A., Jaeger, W., & Szekeres, T. (2008). Resveratrol and its analogs: defense  
556 against cancer, coronary disease and neurodegenerative maladies or just a fad? *Mutation*  
557 *Research*, 658(1–2), 68–94. <https://doi.org/10.1016/j.mrrev.2007.08.004>

558 Sergi, D., Gélinas, A., Beaulieu, J., Renaud, J., Tardif-Pellerin, E., Guillard, J., & Martinoli,  
559 M.-G. (2021). Anti-apoptotic and anti-inflammatory role of *trans*  $\epsilon$ -viniferin in a  
560 neuron-glia co-culture cellular model of Parkinson's disease. *Foods*, 10(3), 586.  
561 <https://doi.org/10.3390/foods10030586>

562 Shang, Y.-J., Qian, Y.-P., Liu, X.-D., Dai, F., Shang, X.-L., Jia, W.-Q., Liu, Q., Fang, J.-G., &  
563 Zhou, B. (2009). Radical-scavenging activity and mechanism of resveratrol-oriented  
564 analogues: influence of the solvent, radical, and substitution. *The Journal of Organic*  
565 *Chemistry*, 74(14), 5025–5031. <https://doi.org/10.1021/jo9007095>

566 Shen, T., Wang, X.-N., & Lou, H.-X. (2009). Natural stilbenes: an overview. *Natural Product*  
567 *Reports*, 26(7), 916–935. <https://doi.org/10.1039/B905960A>

568 Stojanović, S., & Brede, O. (2002). Elementary reactions of the antioxidant action of *trans*-  
569 stilbene derivatives: resveratrol, pinosylvin and 4-hydroxystilbene. *Physical Chemistry*  
570 *Chemical Physics*, 4(5), 757–764. <https://doi.org/10.1039/b109063c>

571 Vion, E., Page, G., Bourdeaud, E., Paccalin, M., Guillard, J., & Rioux Bilan, A. (2018). *Trans*  
572  $\epsilon$ -viniferin is an amyloid- $\beta$  disaggregating and anti-inflammatory drug in a mouse  
573 primary cellular model of Alzheimer's disease. *Molecular and Cellular Neuroscience*,  
574 88, 1–6. <https://doi.org/10.1016/j.mcn.2017.12.003>

575 Yoshiaki, T., & Masatake, N. (2001). Oligostilbenes from Vitaceaeous plants. *Trends in*  
576 *Heterocyclic Chemistry*, 7, 41–54.

577 Yuk, H. J., Ryu, H. W., Jeong, S. H., Curtis-Long, M. J., Kim, H. J., Wang, Y., Song, Y. H., &  
578 Park, K. H. (2013). Profiling of neuraminidase inhibitory polyphenols from the seeds of  
579 *Paeonia lactiflora*. *Food and Chemical Toxicology*, 55, 144–149.  
580 <https://doi.org/10.1016/j.fct.2012.12.053>

581

582

583

584

## FIGURES CAPTIONS

**Figure 1.** Chemical structures of viniferins (only the **1a** and **2a** compounds are reported).

**Figure 2.** Comparison of experimental VCD spectra for the second eluted compound of **1** and **2** recorded in DMSO-*d*<sub>6</sub> solution (40 mM, 100 μm path length) with the predicted spectra of (7*aS*,8*aS*)-*E*-ε-viniferin and (7*aR*,8*aS*)-*E*-ω-viniferin.

**Figure 3.** Comparison of experimental VCD spectra for the second eluted compound of **1** recorded in DMSO-*d*<sub>6</sub> solution (40 mM, 100 μm path length) with the VCD spectra of *E*-ε-viniferin extracted from different grape varieties.

**Figure 4.** (A) Cell viability (%) (B) NO (μM) (C) ROS (fluorescence intensity) in LPS-stimulated RAW 264.7 cells. Cells were treated for 24 hours with LPS (0.1 μg/mL; + control) or LPS with **1a**, **1b**, **2a** and **2b** at different concentrations (from 0.5-100 μM for cell viability and between 0.5-10 μM for NO and ROS measurements). Results are expressed as mean SEM of eight replicates (*n*=8). Different letters mean significant differences (*p*<0.5).

**Figure 1.**

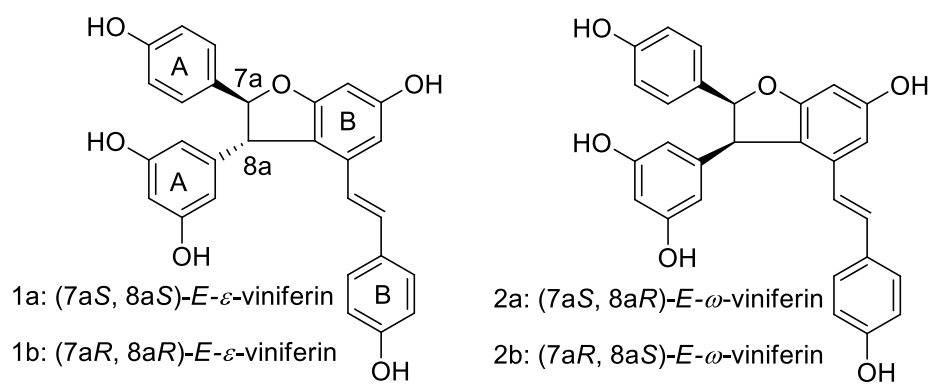


Figure 2.

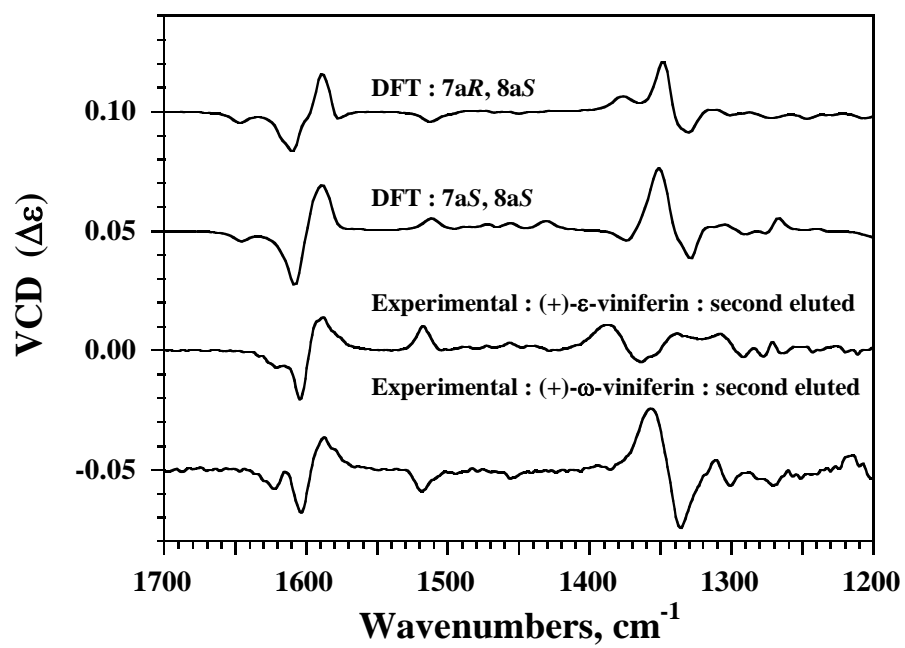
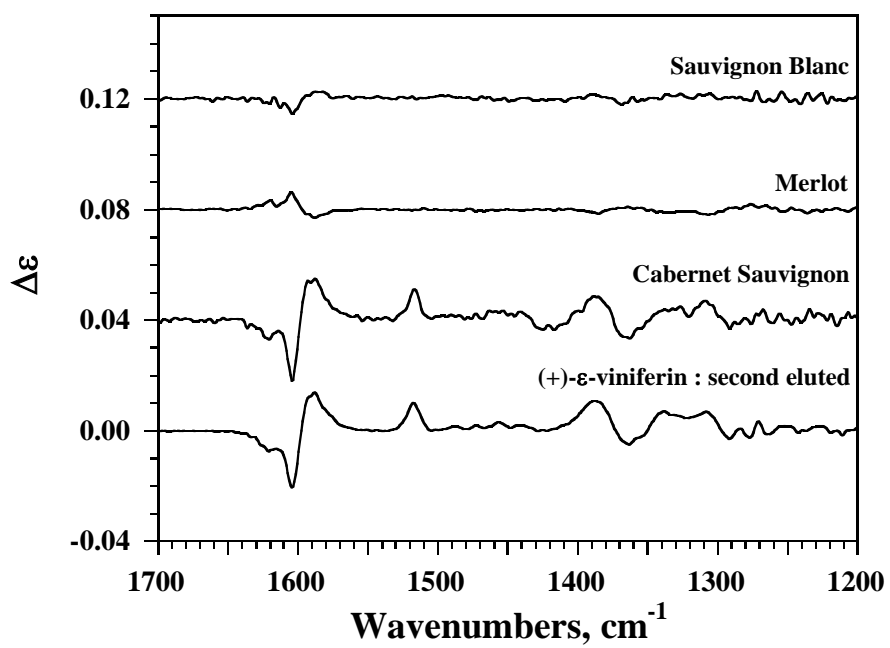
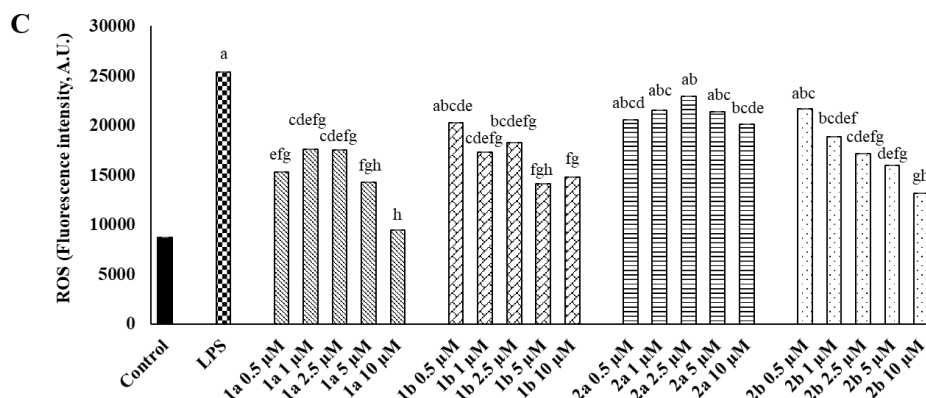
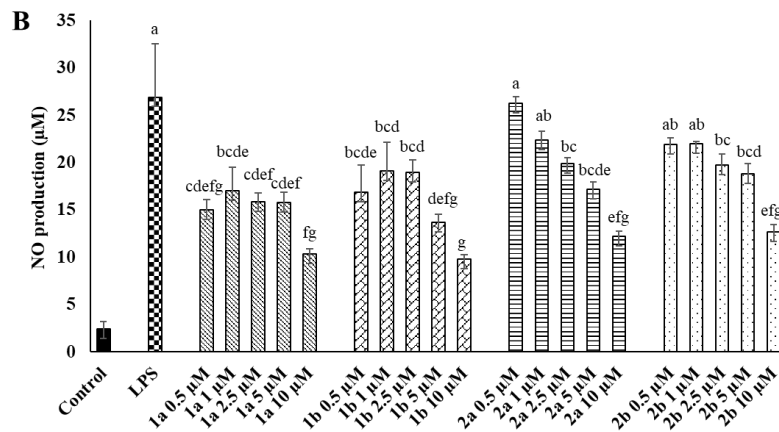
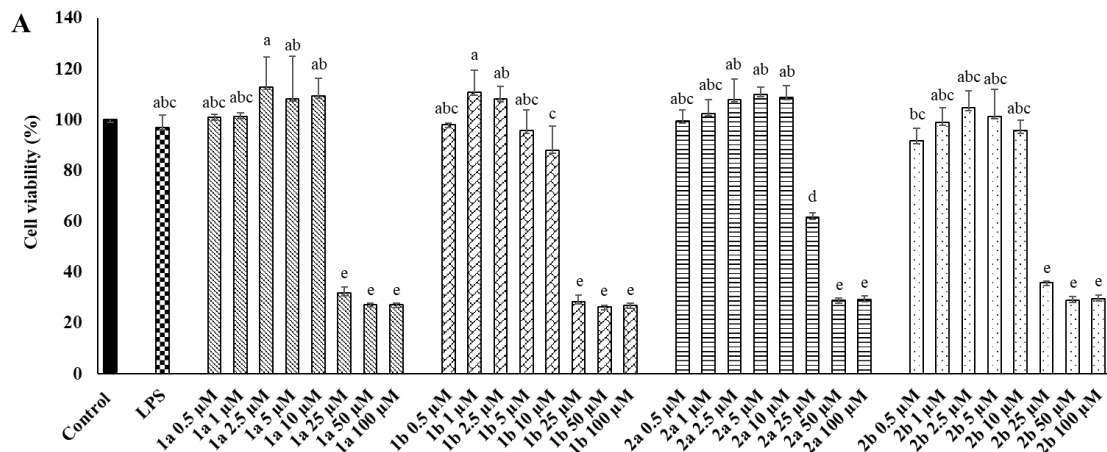


Figure 3.



**Figure 4.**

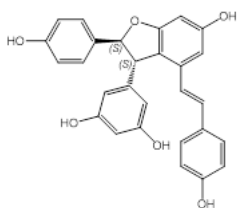


## For TOC Graphic only



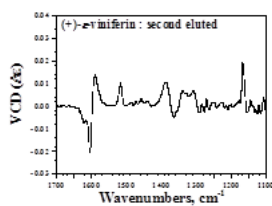
Cabernet Sauvignon stalks

Extraction  
CPC, HPLC



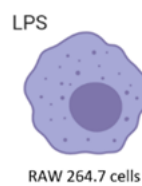
(7aS,8aS)-E-ε-viniferin

Absolute configuration  
determination



ee = 98.3%

Bioactivity



RAW 264.7 cells

anti-inflammatory and  
anti-oxidant activities

1           **Chiroptical and Potential *In Vitro* Anti-Inflammatory Properties of**  
2           **Viniferin Stereoisomers from Grapevine (*Vitis vinifera* L.)**

3  
4 Guillaume Buffeteau,<sup>a</sup> Ruth Hornedo-Ortega,<sup>a</sup> Julien Gabaston,<sup>a</sup> Nicolas Daugey,<sup>b</sup> Antonio  
5 Palos-Pinto,<sup>a</sup> Anne Thienpont,<sup>b</sup> Thierry Brotin,<sup>c</sup> Jean-Michel Mérillon,<sup>a</sup> Thierry Buffeteau<sup>b,\*</sup>  
6 and Pierre Waffo-Teguo<sup>a,\*</sup>

7  
8 <sup>a</sup>Univ. Bordeaux, UFR des Sciences Pharmaceutiques, Unité OENO UMR 1366 INRAE,  
9 Bordeaux INP - Institut des Sciences de la Vigne et du Vin, CS 50008 - 210, chemin de  
10 Leysotte, 33882 Villenave d'Ornon, France.

11 <sup>b</sup>Université de Bordeaux, Institut des Sciences Moléculaires, UMR 5255 - CNRS, 351 Cours  
12 de la Libération, F-33405 Talence, France.

13 <sup>c</sup>Université Lyon 1, Ecole Normale Supérieure de Lyon, CNRS UMR 5182, Laboratoire de  
14 Chimie, 69364 Lyon, France.

15  
16 **Corresponding Author:**

17 \*Tel.: +33-55-757-5955. Fax: +33-55-757-5952. E-mail: [pierre.waffo-teguo@u-bordeaux.fr](mailto:pierre.waffo-teguo@u-bordeaux.fr)

18 Univ. Bordeaux, UFR des Sciences Pharmaceutiques, Unité OENO UMR 1366 INRAE,  
19 Bordeaux INP - Institut des Sciences de la Vigne et du Vin, CS 50008 - 210, chemin de  
20 Leysotte, 33882 Villenave d'Ornon, France..

21 **Abstract**

22 Determination of stereochemistry and enantiomeric excess in chiral natural molecules is a  
23 research of great interest because enantiomers can exhibit different biological activities.  
24 Viniferin stilbene dimers are natural molecules present in grape berries and wine but also, in  
25 larger amount, in stalks of grapevine. Four stereoisomers of viniferin stilbene dimers (7a*S*,8a*S*)-  
26 *E*- $\epsilon$ -viniferin (**1a**), (7a*R*,8a*R*)-*E*- $\epsilon$ -viniferin (**1b**), (7a*S*,8a*R*)-*E*- $\omega$ -viniferin (**2a**), and (7a*R*,8a*S*)-  
27 *E*- $\omega$ -viniferin (**2b**) were isolated from grapevine stalks of Cabernet Sauvignon, Merlot and  
28 Sauvignon Blanc, using a combination of centrifugal partition chromatography (CPC),  
29 preparative and chiral HPLC. The structure elucidation of these molecules was achieved by  
30 NMR whereas the absolute configurations of the four stereoisomers were investigated by  
31 vibrational circular dichroism spectroscopy in combination with density functional theory  
32 (DFT) calculations. This study unambiguously established the (+)-(7a*S*,8a*S*) and (+)-(7a*R*,8a*S*)  
33 configurations for *E*- $\epsilon$ -viniferin and *E*- $\omega$ -viniferin, respectively. Finally, we show that Cabernet  
34 Sauvignon provided the quasi enantiopure (+)-(7a*S*,8a*S*)-*E*- $\epsilon$ -viniferin compound which  
35 presents the best anti-inflammatory and anti-oxidant activities.

36 **Keywords:** stilbene, viniferins, stereoisomers, chirality, vine, anti-inflammatory

37

## 38 **1. Introduction**

39 Chirality is omnipresent in chemistry and biology. It is not surprising that this  
40 phenomenon also plays a major role in food chemistry and natural products. Chirality is a  
41 geometric property of some molecules that are non-superposable with their mirror images. A  
42 chiral compound and its mirror image are called enantiomers, and could interact in different  
43 ways with receptors, transport systems and enzymes, leading to diverse effects such as  
44 dissimilar taste or aroma, or different biological activities. Therefore, the determination of  
45 enantiomeric excess in chiral natural molecules is a research of great interest in food chemistry.

46 The hydroxylated derivatives of stilbene, especially resveratrol and its congeners have  
47 attracted much attention owing to their various benefits in human health. It is now accepted that  
48 resveratrol possesses a large number of pharmacological properties including cardioprotective  
49 (Saiko et al., 2008), neuroprotective (Richard et al., 2011), and chemopreventive effects (Ko et  
50 al., 2017). More than one thousand stilbenoids have been identified until now, and several  
51 articles tried to make a catalog (Shen et al., 2009; Rivière et al., 2012; Keylor et al., 2015).  
52 These specialized metabolites occur naturally with a limited but heterogeneous distribution in  
53 the plant kingdom (Rivière et al., 2012). Stilbenoids can be divided in monomers and oligomers.  
54 There are two main hypotheses dealing with the biosynthesis of oligomers. The first approach  
55 is chemical, while the second involves chiral intermediates and possibly enzymes. Given the  
56 different structures of existing dimers, it seems that both possibilities are present. In any case,  
57 it is the ability of this type of compounds, like most polyphenols, to form and trap radicals,  
58 which makes it possible to obtain such diversity by radical coupling. Indeed, they are  
59 mechanisms of the Sequential Proton Loss Electron Transfer (SPLET) and Hydrogen Atom  
60 Transfer (HAT) type which, by radical and proton transfer, would lead to such reactivity (Shang  
61 et al., 2009; Stojanović & Brede, 2002). It was shown that some peroxidases from grapevine  
62 are capable to form the  $\delta$ -viniferin and other dimers (Calderón et al., 1992; Morales & Barceló,

63 1997; Barceló et al., 2003). Despite numerous attempts using Horseradish peroxidase (HRP) or  
64 other peroxidases, even from the grapevine, no data have been published, showing that these  
65 enzymes are involved in the formation of the *E-ε*-viniferin (Barceló et al., 2003). The presence  
66 of a chiral intermediate, however, is strongly assumed, as the plants seem able to produce  
67 specifically the (+)-*E-ε*-viniferin, as in Vitaceae and Dipterocarpaceae or (-)-*E-ε*-viniferin as  
68 in some Cyperaceae (Yoshiaki & Masatake, 2001). Laccase from *Botrytis cinerea* was  
69 considered capable to catalyze the reaction of resveratrol toward the (+)-*E-ε*-viniferin (Pezet,  
70 1998), but subsequent studies have refuted this hypothesis (Breuil et al., 1998; Cichewicz et al.,  
71 2000).

72 Structurally, *E-ε*- and *E-ω*-viniferins are resveratrol dimers belonging to the group A  
73 according to the natural stilbenes classification with two resveratrol units linked by two C-C  
74 and C-O-C connection (Shen and Lou, 2009). This structure has two stereogenic carbons on the  
75 benzofuran unit with four possible stereoisomers (**Figure 1**). As observed for drugs, it is  
76 possible that enantiomers of viniferins can have different activities. Recently, research carried  
77 out on the characterization of the molecular determinants responsible for the taste of wines  
78 showed how stereochemistry could influence taste properties. Thus, taste properties of  
79 lyoniresinol stereoisomers were evaluated and only one lyoniresinol enantiomer were strongly  
80 bitter whereas the other one was tasteless and the diastereoisomer is slightly sweet (Cretin et  
81 al., 2015). In order to better understand the different properties of each stereoisomer of *E-ε*- and  
82 *E-ω*-viniferins, it is crucial to isolate and characterize them.

83 To perform structural and biological measurements, it is necessary to acquire a large  
84 amount of pure stereoisomers of viniferin. However, this amount is very dependent on the  
85 investigated plant material. Thus, for grapevine, *E-ε*- and *E-ω*-viniferins can be extracted from  
86 grape berries, leaves, stalks and roots with different efficiencies. Indeed, their extraction

87 represents around 0.1 – 0.5 % of dried weight (DW) from stalks of grapevine whereas the  
88 amount is one hundred lower from grape berries (Gabaston et al, 2020).

89 This paper reports the chiroptical properties (vibrational and electronic circular  
90 dichroisms) of two stilbene dimers, *E-ε*-viniferin and *E-ω*-viniferin from stalks of grapevine in  
91 order to determine their absolute configurations. We have shown that the two dimers are present  
92 as a mixture of enantiomers, depending on the grape variety. All the stereoisomers were also  
93 evaluated for their anti-inflammatory and anti-oxidant activities in Lipopolysaccharide (LPS)-  
94 stimulated macrophages.

95

## 96 **2. Material and Methods**

### 97 **2.1. General Experimental Procedures.**

98 All <sup>1</sup>H and <sup>13</sup>C NMR spectra were recorded on a Bruker Avance III 600 MHz NMR  
99 spectrometer (Wissembourg, France) equipped with a 5-mm TXI probe. Compounds were  
100 measured in 3 mm NMR tubes, using acetone-*d*<sub>6</sub> (Euriso-Top, Gif-sur-Yvette, France) as the  
101 solvent at 27°C. <sup>1</sup>H and <sup>13</sup>C chemical shifts were referenced to solvent signals. Data were  
102 processed using Bruker software Topspin 3.2. The specific optical rotations were determined  
103 in methanol at 20 °C on a JASCO P-2000 polarimeter (Tokyo, Japan) using the sodium emission  
104 wavelength ( $\lambda = 589$  nm). The centrifugal partition chromatography (CPC) used in this study  
105 (FCPC200®) was provided by Kromaton Technologies (Sainte-Gemmes-sur-Loire, France).  
106 The solvents were pumped by a Gilson 321-H1 2-way binary high-pressure gradient pump. The  
107 samples were introduced into the CPC column via a high pressure injection valve (3725i-038  
108 Rheodyne) equipped with a 20 mL sample loop. The CPC fractions were monitored with a  
109 Varian Prostar 325 DAD detector (Victoria, Australia), at wavelengths of 306 and 280 nm.  
110 HPLC preparative separations were carried out using a Gilson PLC 2050 Purification System  
111 (Villiers-le-bel, France) equipped with a binary pump, a UV-VIS Detector, a fraction Collector,

112 and a Phenomenex Kinetex XB-C18 AXIA column (5  $\mu\text{m}$ , 150 x 21.2 mm). The mobile phase  
113 was composed of two solvents: (A) 0.025% TFA in  $\text{H}_2\text{O}$  and (B) MeCN. The preparative  
114 enantioseparations were performed using the same HPLC system as above equipped with a  
115 Phenomenex Lux Amylose-1 (5  $\mu\text{m}$ , 250 x 10 mm) chiral column. The mobile phase consisted  
116 of n-Hexane/2-Propanol (85/15, v/v) acidified with 0.01% TFA.

## 117 **2.2. Plant Material.**

118 Grapevine stalks (Merlot) were collected in the “Château Rochemorin” vineyard in the  
119 region of Bordeaux (44°43’17’’N, - 0°33’45’’W, Martillac, France) in January 2017. They were  
120 obtained from Riparia Gloire de Montpellier rootstocks which were planted in 1985. Stalks  
121 specimens were deposited in the Molécules d’Intérêt Biologique (MIB) laboratory at ISVV  
122 (Villenave d’Ornon, France). Grapevine stalks of three other grape varieties (Cabernet  
123 Sauvignon, Sauvignon Blanc, and Merlot) were collected in the “Domaine Haut Dambert”  
124 vineyard in the region of Bordeaux (44°38’58’’N, - 0°10’48’’W, Gornac, France) in January  
125 2015. The accession numbers are listed in **Table 1**.

126 **Table 1.** Cultivar/rootstock combinations, deposit number, and origins

Cultivar	rootstock	Deposit number	Origin (city, region, country)
Merlot	101-14	MIB_M-2017	Martillac (region of Bordeaux, France)
Carbernet Sauvignon	101-14	MIB_CS-TB	Gornac (region of Bordeaux, France)
Merlot	420A	MIB_M-TB	Gornac (region of Bordeaux, France)
Sauvignon Blanc	101-14	MIB_SB-TB	Gornac (region of Bordeaux, France)

127

## 128 **2.3. Extraction and Isolation.**

129 Dried and finely powdered stalks of *Vitis vinifera* (100 g DW) were defatted with  
130 petroleum (1 L) using soxhlet extractor, extracted with 60% aqueous acetone (1 L, 2 times) at  
131 room temperature and filtered. This aqueous acetone extract was evaporated under reduced

132 pressure. The filtrate was concentrated at 35°C under reduced pressure. Aqueous residue (200  
133 mL) was partitioned with EtOAc (4 x 200 mL). The organic extract was concentrated and  
134 freeze-dried to yield 0.7 – 1.5 g depending on the grape variety. The highest concentration in  
135 stilbenes was found with the Merlot (14.3 g.kg<sup>-1</sup> DW), followed by Sauvignon Blanc (9.5 g.kg<sup>-1</sup>  
136 DW) and Cabernet Sauvignon (7.4 g.kg<sup>-1</sup> DW).

137 One g of the organic extract was subjected to the centrifugal partition chromatography  
138 (CPC) using the quaternary biphasic Arizona-K system n-Heptane/EtOAc/MeOH/Water  
139 (1:2:1:2, v/v). The CPC rotor was entirely filled with the aqueous stationary phase in the  
140 descending mode at 500 rpm. After injection of the organic extract, dissolved in 8 mL of the  
141 organic/aqueous phase mixture (1:1, v/v), the aqueous mobile phase was pumped into the  
142 column in descending mode at a flow-rate of 3 mL/min. Then the rotation speed was increased  
143 from 500 to 1200 rpm. The back pressure was 2.5 MPa. The content of the outgoing organic  
144 phase was monitored by online UV absorbance measurement at 280 and 306 nm. Six fractions  
145 were collected (**Supplementary material** Figure S1). *E-ε*-viniferin and *E-ω*-viniferin, obtained  
146 as a white solid were purified from the fraction 6 (around 200 mg) by preparative HPLC with  
147 elution program: 17% B (0-1.12 min), 17-30% B (1.12 -13.12 min), 30-38% B (13.12-22.12  
148 min), 38-100% B (22.12-27 min), 100% (27-30 min). The concentrations of *E-ε*-viniferin were  
149 found in the 0.23 – 0.35 % range (3.5 g.kg<sup>-1</sup> DW for Merlot, 2.6 g.kg<sup>-1</sup> DW for Sauvignon Blanc  
150 and 2.3 g.kg<sup>-1</sup> DW for Cabernet Sauvignon).

151 The enantiomeric excess of the two enantiomers of *E-ε*-viniferin, **1**, extracted from  
152 Cabernet Sauvignon, Merlot and Sauvignon Blanc grape varieties was measured by analytical  
153 chiral HPLC. The mixture of enantiomers of each compound was solubilized in mobile phase  
154 and filtered on PTFE 0.45 μm. The two enantiomers of **1** were separated using a chiral HPLC  
155 column (Chiralpak IF, 250 × 4.6 mm). The mobile phase consisted of n-Hexane/2-Propanol  
156 (90/10, v/v) acidified with 0.001 % TFA. Isocratic elution was performed at a flow-rate of 2

157 mL/min. It was observed that the (–)-enantiomer of **1** was first eluted at 17.2 min, followed by  
158 the (+)-enantiomer at 30.8 min (**Supplementary material** Figure S2).

159 To obtain the two enantiomers of **1** and **2** in fair quantities, a preparative Phenomenex  
160 Lux Amylose-1 (250 × 10 mm, eluent: n-Hexane/2-Propanol 85/15 acidified with 0.01 % TFA,  
161 5 mL/min) was used. For **1**, the first enantiomer (**1a**) was collected at 21 min and the second  
162 one (**1b**) at 30 min, whereas for **2**, the first enantiomer (**2a**) was eluted at 17 min and the second  
163 one (**2b**) at 30 min (**Supplementary material** Figure S3).

#### 164 **2.4. Electronic Circular Dichroism (ECD) measurements.**

165 ECD spectra of compounds **1** and **2** were recorded in EtOH at 20 °C with a 0.2 cm path  
166 length quartz cell. The concentration of the two compounds was taken in the range  $1 \cdot 10^{-4} - 1.5$   
167  $10^{-4}$  M. Spectra were recorded in the 210 – 400 nm wavelength range with a 0.5 nm increment  
168 and a 1s integration time. Spectra were processed with standard spectrometer software, baseline  
169 corrected and slightly smoothed by using a third order least square polynomial fit. Spectral units  
170 were expressed in difference of molar extinction coefficients ( $\Delta\epsilon$  in L/mol/cm).

#### 171 **2.5. Vibrational Circular Dichroism (VCD) measurements.**

172 IR and VCD spectra were recorded with a ThermoNicolet Nexus 670 FTIR spectrometer  
173 equipped with a VCD optical bench (Buffeteau et al., 2005). In this optical bench, the light  
174 beam was focused by a BaF<sub>2</sub> lens (191 mm focal length) to the sample, passing an optical filter,  
175 a BaF<sub>2</sub> wire grid polarizer (Specac), and a ZnSe photoelastic modulator (Hinds Instruments,  
176 Type II/ZS50). The light was then focused by a ZnSe lens (38.1 mm focal length) onto a 1x1  
177 mm<sup>2</sup> HgCdTe (ThermoNicolet, MCTA\* E6032) detector. IR and VCD spectra were recorded  
178 at a resolution of 4 cm<sup>-1</sup>, by coadding 50 scans and 36000 scans (12h acquisition time),  
179 respectively. The sample was held in a fixed path length (100 μm) cell with BaF<sub>2</sub> windows. IR  
180 and VCD spectra of the two enantiomers *E*- $\epsilon$ -viniferin **1** and *E*- $\omega$ -viniferin **2** were measured in  
181 DMSO-*d*<sub>6</sub> at a concentration of 40 mM. Baseline correction of the VCD spectrum was

182 performed by subtracting the two enantiomer VCD spectra of **1** and **2** (recorded under the same  
183 experimental concentration), with division by two. In all experiments, the photoelastic  
184 modulator was adjusted for a maximum efficiency at 1400 cm<sup>-1</sup>. Calculations were done with  
185 the standard ThermoNicolet software, using Happ and Genzel apodization, de-Haseth phase-  
186 correction and a zero-filling factor of one. Calibration spectra were recorded using a  
187 birefringent plate (CdSe) and a second BaF<sub>2</sub> wire grid polarizer, following the experimental  
188 procedure previously published (Nafie & Vidrine, 1982). Finally, in the presented IR spectra,  
189 the solvent absorption was subtracted out.

## 190 **2.6. DFT calculations.**

191 All DFT calculations were carried out with Gaussian 09 (Frisch et al., 2009). The  
192 calculation of the IR and VCD spectra began by a conformational analysis of (7a*S*,8a*S*)- and  
193 (7a*R*,8a*S*)-viniferin (**1a** and **2b**), considering a *trans* conformation of the C=C bond.  
194 Preliminary conformer distribution search of **1a** and **2b** was performed at the molecular  
195 mechanics level of theory, employing MMFF94 force fields incorporated in ComputeVOA  
196 software package. 290 conformers of **1a** (305 conformers for **2b**) were found within roughly 4  
197 kcal/mol of the lowest energy conformer. Their geometries were optimized at the DFT level  
198 using B3LYP functional and 6-31G\*\* basis set, leading to 74 (**1a**) and 61 (**2b**) different  
199 conformers within an energetic window of 3.25 (**1a**) and 2.87 (**2b**) kcal/mol. Finally, only the  
200 twenty four (**1a**) and twenty five (**1b**) lowest energetic geometries were kept, corresponding to  
201 Boltzmann population higher than 1%. Vibrational frequencies, IR and VCD intensities were  
202 calculated at the same level of theory. The spectra were calculated for the isolated molecule *in*  
203 *vacuo*. For comparison to experiment, the calculated frequencies were scaled by 0.968 and the  
204 calculated intensities were converted to Lorentzian bands with a full-width at half-maximum  
205 (FWHM) of 7 cm<sup>-1</sup>.

## 206 **2.7. Macrophages cell culture.**

207 RAW 264.7 cells were obtained from the American Type Culture Collection (ATCC).  
208 They were cultured in 75 cm<sup>2</sup> flasks containing 20 mL of DMEM supplemented with 10% of  
209 FBS. Cells were maintained in a humidified incubator at 37°C and 5% of CO<sub>2</sub>. In order to  
210 perform the experiments, every 3 days cells were detached by scrapping and sub-cultured in 96  
211 transparent (for cytotoxicity and NO measurements) or black (ROS measurement) well plates  
212 with the same culture medium (200 µL) supplemented with 4 mM of glutamine at a density of  
213 40,000 cells per well.

#### 214 **2.8. MTT assay.**

215 The cytotoxicity of stereoisomers of viniferin (**1a**, **1b**, **2a** and **2b**) was carried out by using  
216 MTT that allows to measure the cellular metabolic activity of cells. After 24 hours of incubation  
217 in 96 well plates, cells were incubated with different concentrations of the four stereoisomers  
218 (0.5 to 100 µM) of viniferin (**1a**, **1b**, **2a** and **2b**). After 24 hours of treatment, cells were  
219 incubated with 0.5 mg/mL of MTT during 3 hours at 37°C and 5% of CO<sub>2</sub>. Finally, the blue  
220 formazan crystals formed at the well bottom were dissolved with 100 µL of DMSO and, 30  
221 minutes after, the absorbance was measured with a microplate reader (FLUOstar Optima, BMG  
222 Labtech) set at 595 nm. Results are expressed as mean of four replicates (*n*=4).

#### 223 **2.9. Measurement of NO production.**

224 In order to evaluate the anti-inflammatory potential of the stereoisomers of viniferin (**1a**,  
225 **1b**, **2a** and **2b**), RAW 264.7 cells were incubated during 24 hours with all compounds at  
226 different non-cytotoxic concentrations (0.5, 1, 2.5, 5 and 10 µM) in the presence or absence of  
227 LPS (inflammatory triggering agent, 0.1 µg/mL) in RPMI medium. Then, 70 µL of supernatant  
228 were mixed with 70 µL of Griess reagent and after an incubation of 15 minutes at room  
229 temperature, the absorbance was measured at 540 nm by using a microplate reader (FLUOstar  
230 Optima, BMG Labtech). NO concentration by using a calibration standard curve of sodium  
231 nitrite (0-100 µM). Results are expressed as mean of four replicates (*n*=4).

## 232 **2.10. Intracellular ROS measurement.**

233 The intracellular generation of ROS in cells was analyzed using the fluorometric probe  
234 DCFH<sub>2</sub>-DA. After treatment with the stereoisomers of viniferin (**1a**, **1b**, **2a** and **2b**) at different  
235 concentrations (0.5, 1, 2.5, 5 and 10 μM) during 24 hours in 96 black well plates, cells were  
236 washed and 5 mM of DCFH<sub>2</sub>-DA diluted in PBS was added. After 30 minutes of incubation in  
237 the darkness at 37°C and 5% of CO<sub>2</sub>, the fluorescence intensity was measured using a  
238 microplate reader (FLUOstar Optima, BMG Labtech) set at 485 nm (excitation wavelength)  
239 and 520 nm (emission wavelength). Results are expressed as mean of four replicates (*n*=4).

## 240 **2.11. Statistical Analysis.**

241 Data were subjected to one-way ANOVA followed by a Tukey's test (*p* < 0.05) with  
242 Microsoft Excel® XLSTAT (Version 1.1.463) to explore significant differences for cell  
243 viability, NO and ROS measurements.

244

## 245 **3. Results and Discussion**

### 246 **3.1. Isolation of viniferin dimers and chiroptical properties in grape varieties**

247 One hundred g of dry fine powder of *Vitis vinifera* cv. Merlot stalks, previously defatted  
248 with petroleum ether, was extracted two times with 60% aqueous acetone at room temperature.  
249 The extract was then filtered and the filtrate was concentrated *in vacuo*. The aqueous phase was  
250 further partitioned between EtOAc and water. The organic extract was separated by  
251 combination of centrifugal partition chromatography (**Supplementary material** Figure S1) and  
252 preparative RP-18 HPLC to obtain *E-ε*-viniferin with  $[\alpha]_{589}^{20} = +10.4^{\circ}$  (c 0.2, MeOH) and *E-ω*-  
253 viniferin with  $[\alpha]_{589}^{20} = -103^{\circ}$  (c 0.15, MeOH). In addition, the *E-ε*-viniferin was purified from  
254 three different grape varieties (Cabernet Sauvignon, Merlot, and Sauvignon Blanc). The  
255 specific optical rotation values of *E-ε*-viniferin varied between -12 and +46° (**Supplementary**  
256 **material** Table S1), indicating that *E-ε*-viniferin is not enantiopure. This could be related to the

257 fact that the enantiomeric ratio of *E-ε*-viniferin could be different due to the grape varieties. For  
 258 example, Cabernet Sauvignon variety gives the dextrorotatory form of *E-ε*-viniferin whereas  
 259 the Merlot variety gives preferentially the levorotatory form. On the other hand, Sauvignon  
 260 Blanc exhibits a lower value of specific rotation that probably means the presence of rather  
 261 racemic mixture (**Supplementary material** Table S1). These values are in agreement with  
 262 those reported in the literature from *V. vinifera* (Vitaceae) and others plant families, as shown  
 263 in **Table 2**. The proportion of the two enantiomers of *E-ε*-viniferin and the enantiomeric excess  
 264 (ee) for the three grape varieties are given in **Supplementary material** Table S2. The  
 265 enantiomeric excess (ee) extracted from Cabernet Sauvignon, Merlot and Sauvignon Blanc  
 266 grape varieties was measured by analytical chiral HPLC (**Supplementary material** Figure S2).  
 267 **Table 2.** Optical rotation values of *E-ε*-viniferin measured in this study and found in the  
 268 literature.

Species	Family	$[\alpha]_{589}^{20}$	Conditions	Reference
<i>Vitis vinifera</i> cv. Merlot	Vitaceae	+10.4°	0.13, MeOH	This study
<i>Vitis vinifera</i> cv. Cabernet Sauvignon	Vitaceae	+46.4°	0.064, MeOH	This study
<i>Vitis vinifera</i> cv. Merlot	Vitaceae	-12.1°	0.07, MeOH	This study
<i>Vitis vinifera</i> cv. Sauvignon Blanc	Vitaceae	+5.9°	0.083, MeOH	This study
<i>Vitis amurensis</i>	Vitaceae	+41°	0.13, MeOH	(Pawlus et al., 2013)
<i>Vitis vinifera</i>	Vitaceae	+34°	0.32, MeOH	(Mattivi et al., 2011)
<i>Vitis heyneana</i>	Vitaceae	+39°	0.40, MeOH	(Li et al., 1996)
<i>Vitis chunganensis</i>	Vitaceae	+32°	0.27, MeOH	(He et al., 2009)
<i>Carex pumila</i>	Cyperaceae	-27,9°	0.843, MeOH	(Kurihara et al., 1990)
<i>Carex kobomugi</i>	Cyperaceae	-46°	0.5, MeOH	(Kurihara et al., 1991)
Rhubarb	Polygonaceae	-47°	0.5, MeOH	(Ngoc et al., 2008)

269

## 270 3.2. Absolute configuration of viniferin stereoisomers using NMR, VCD and ECD

271 According to the above observations, *E-ε*-viniferin (mixture of enantiomers) was then  
272 purified by chiral HPLC to separate the two enantiomers (**Supplementary material** Figure S3).  
273 The first eluted compound showed a specific optical rotation value  $[\alpha]_{589}^{20} = -43.4^\circ$  (c 0.06,  
274 MeOH) whereas a value  $[\alpha]_{589}^{20} = +46^\circ$  (c 0.06, MeOH) was measured for the second eluted  
275 compound. Accordingly, we have shown that *E-ω*-viniferin was also a mixture of enantiomers  
276 and it was purified by chiral HPLC as mentioned above to yield  $[\alpha]_{589}^{20} = +107^\circ$  (c 0.07, MeOH)  
277 for the first eluted compound and  $[\alpha]_{589}^{20} = -155^\circ$  (c 0.14, MeOH) for the second eluted  
278 compound. The NMR data ( $^1\text{H}$  and  $^{13}\text{C}$ ) of *E-ε*- and *E-ω*-viniferin were found to be similar to  
279 those previously obtained in our laboratory and in literature (**Supplementary material** Table  
280 S3, Figures S4 and S6) (Pawlus et al., 2013; Mattivi et al., 2011). The relative configuration  
281 was established by ROESY. For *E-ε*-viniferin, the absence of NOE correlation between protons  
282 H7a/H8a (**Supplementary material** Figure S5) indicated that these protons were *trans*-  
283 orientated whereas for *E-ω*-viniferin, the cross peak between H7a/H8a (**Supplementary**  
284 **material** Figure S7), indicated these protons were cofacial (*cis*-orientation). In addition, the IR  
285 spectra of *E-ε*- and *E-ω*-viniferin allow the discrimination of the two diastereoisomers, using  
286 the intensity of the band at  $1148\text{ cm}^{-1}$ . Indeed, the *E-ω*-viniferin compound exhibits a high  
287 intensity for this band, whereas the  $1148\text{ cm}^{-1}$  band is weak for the *E-ε*-viniferin compound  
288 (**Supplementary material** Figure S8).

289 The absolute configurations of the chiral centers (C7a and C8a) of *E-ε*-viniferin and *E*-  
290 *ω*-viniferin were deduced in the same manner as for the two enantiomers of (–)-*E*-gnetin C  
291 (Buffeteau et al., 2014), using vibrational circular dichroism (VCD) associated with theoretical  
292 calculations. VCD spectra of the two enantiomers of compounds **1** and **2** were recorded in

293 DMSO-*d*<sub>6</sub> at a concentration of 40 mM and the raw and baseline corrected VCD spectra are  
294 reported in **Supplementary material** Figures S9 and S10. For each compound, opposite VCD  
295 spectra were measured for the two enantiomers, as expected for enantiopure compounds.

296 The theoretical calculations began by a conformational analysis of (7*aS*,8*aS*)-*E-ε*-  
297 viniferin (**1a**) and (7*aR*,8*aS*)-*E-ω*-viniferin (**2b**). Preliminary conformer distribution search of  
298 **1a** and **2b** was performed at the molecular mechanics level of theory, employing MMFF94  
299 force fields incorporated in ComputeVOA software package. 290 conformers of **1a** (305  
300 conformers for **2b**) were found within roughly 4 kcal/mol of the lowest energy conformer. Their  
301 geometries were optimized at the DFT level using B3LYP functional and 6-31G\*\* basis set,  
302 leading to 74 (**1a**) and 61 (**2b**) different conformers within an energetic window of 3.25 (**1a**)  
303 and 2.87 (**2b**) kcal/mol. Finally, only the twenty four (**1a**) and twenty five (**1b**) lowest energetic  
304 geometries were kept, corresponding to Boltzmann population higher than 1%. Calculations  
305 were performed for the isolated molecule *in vacuo*. Harmonic vibrational frequencies were  
306 calculated at the same level to confirm that all structures were stable conformations and to  
307 enable free energies to be calculated. The predicted VCD spectra, taking into account the  
308 relative populations of (7*aS*,8*aS*)-*E-ε*-viniferin and (7*aR*,8*aS*)-*E-ω*-viniferin, were compared to  
309 the experimental VCD spectra of the second eluted compound of **1** and **2** in **Figure 2**. The  
310 predicted VCD spectra of (7*aS*,8*aS*)-*E-ε*-viniferin and (7*aR*,8*aS*)-*E-ω*-viniferin reproduced  
311 fairly well the intensity and the sign of most bands observed in the experimental VCD spectra,  
312 allowing the definitive determination of the 8*aS* configuration of the beta stereogenic carbon of  
313 the benzofuran group. The determination of the configuration of the alpha stereogenic carbon  
314 was less obvious from VCD data, even though a better agreement between theoretical and  
315 experimental spectra in the 1550-1400 cm<sup>-1</sup> spectral range was obtained with the 7*aS*  
316 configuration for the second eluted compound of **1** and with the 7*aR* configuration for the  
317 second eluted compound of **2**. The 7*aS* configuration of the alpha stereogenic carbon of

318 benzofuran group for the second eluted compound of **1** was confirmed by the absence of a cross-  
319 peak between the protons H7a ( $\delta=5.41$  ppm) and H8a ( $\delta=4.47$  ppm) in the ROESY spectrum  
320 (**Supplementary material** Figure S5), indicating the opposite orientation of these two protons.  
321 Similarly, the 7a*R* configuration of the alpha stereogenic carbon of benzofuran group for the  
322 second eluted compound of **2** was confirmed by the presence of a cross-peak between the  
323 protons H7a ( $\delta=5.86$  ppm) and H8a ( $\delta=4.70$  ppm) in the ROESY spectrum (**Supplementary**  
324 **material** Figure S7), indicating the cofacial orientation of these two protons. Thus, this VCD  
325 analysis, associated with NMR results, unambiguously established the (+)-(7a*S*,8a*S*)  
326 configuration for *E*- $\epsilon$ -viniferin and the (+)-(7a*R*,8a*S*) configuration for *E*- $\omega$ -viniferin. This  
327 result confirm the first proposition of the absolute configuration, (-)-(7a*R*,8a*R*), for *E*- $\epsilon$ -  
328 viniferin isolated from *Carex pumila* (Cyperaceae) by Kurihara et al. (1990).

329 The experimental VCD spectra measured for *E*- $\epsilon$ -viniferin extracted from different  
330 grape varieties are compared in **Figure 3** with the VCD spectrum of the enantiopure second  
331 eluted compound purified by chiral HPLC. The VCD spectrum of *E*- $\epsilon$ -viniferin extracted from  
332 Cabernet Sauvignon stalks is quasi identical to the VCD spectrum of the enantiopure  
333 compound, revealing that this grape variety allows the extraction of *E*- $\epsilon$ -viniferin with an  
334 enantiomeric excess close to 1. Chiral HPLC measurements on this compound revealed an  
335 enantiomeric excess of 98.34% (**Supplementary material** Table S2). This feature is very  
336 interesting since the enantiopure (+)-(7a*S*,8a*S*)-*E*- $\epsilon$ -viniferin compound can be obtained  
337 directly by extraction from Cabernet Sauvignon. The VCD spectrum of *E*- $\epsilon$ -viniferin extracted  
338 from Merlot is opposite with an intensity divided by almost 4, as expected by the enantiomeric  
339 excess measured by chiral HPLC (ca. 23.32%). Finally, the VCD spectrum of *E*- $\epsilon$ -viniferin  
340 extracted from Sauvignon Blanc exhibits a very weak intensity, with the same sign than the one  
341 of Cabernet Sauvignon, as expected by chiral HPLC measurements.

342 As electronic circular dichroism (ECD) experiments are currently used in the structural  
343 studies of stilbenes, ECD spectra of the second eluted compound of **1** and **2** are reported in  
344 **Supplementary material** Figures S11 and S12, respectively. The ECD spectrum of (+)-*E-ε*-  
345 viniferin exhibits a positive band at 236 nm (+22.7) and a broad negative band around 300 nm  
346 (-3.8), in agreement with the ECD spectrum reported in the literature (Ito et al., 2009). The ECD  
347 spectrum of (+)-*E-ω*-viniferin is slightly different, with a positive band at 227.5 nm (+17), a  
348 negative band at 250 nm (-3.3) and a broad negative band around 310 nm (-7).

### 349 *3.3. Antioxidant and anti-inflammatory activities of viniferin stereoisomers in LPS-stimulated* 350 *macrophages*

351 The four stereoisomers of viniferin (**1a**, **1b**, **2a** and **2b**) were evaluated for their anti-  
352 inflammatory and anti-oxidant activities in LPS-stimulated macrophages. Firstly, the MTT  
353 assay was performed in order to evaluate the cytotoxicity of all stereoisomers. Thus, cells were  
354 treated with different concentrations of viniferin **1a**, **1b**, **2a** and **2b** (0.5-100 μM) during 24  
355 hours. **Figure 4a** displays the cell viability expressed as percentage relative to the non-treated  
356 cells. As expected, the LPS did not affect the cell viability. Concerning viniferin stereoisomers,  
357 it can be observed that at low concentrations, between 0.5 to 10 μM, the metabolic activity of  
358 cells was not affected. However, from 25 μM, all compounds presented a significant cytotoxic  
359 effect, by killing between 40-70% of cells (**Figure 4a**). It can be also observed that compound  
360 **2a** presents a more slight toxic effect at 25 μM comparing with the others compounds at the  
361 same concentrations. No significant differences were observed between all stereoisomers at the  
362 highest concentrations (50-100 μM). Based on these results, the concentrations ranging between  
363 0.5 to 10 μM were selected to further evaluate the potential effect of viniferin stereoisomers to  
364 diminish the nitric oxide (NO) and reactive oxygen species (ROS) production.

365 RAW 264.7 cells were activated with LPS (0.1 μg/mL) in the presence of the four  
366 stereoisomers of viniferin at 0.5, 1, 2.5, 5 and 10 μM during 24 hours. Afterwards, the NO<sub>2</sub> in

367 culture media were measured by the Griess reaction. The NO content ( $\mu\text{M}$ ) of cells treated with  
368 only LPS (positive control) increased more than tenfold ( $26.9 \mu\text{M}$ ) in comparison with the  
369 negative control ( $2.4 \mu\text{M}$ ) (cells without LPS treatment) (**Figure 4b**). A significant diminution  
370 of NO was observed at all concentrations of **1a** and **1b**. However, this effect is significant for  
371 **2a** and **2b** only from  $2.5 \mu\text{M}$ . Regarding differences between compounds, at the highest  
372 concentration tested ( $10 \mu\text{M}$ ) it can be seen a more potent effect of **1a** with a diminution of 60%  
373 of NO production while for **1b** this decrease is 41%. By contrast, at this concentration the **2a**  
374 and **2b** exhibited the same effect (52 and 55%, respectively) (**Figure 4b**).

375 In addition, the intracellular ROS production induced by LPS was investigated by using  
376 the fluorometric probe DCFH<sub>2</sub>-DA, which permits the detection and quantification of ROS. The  
377 results show that **1a** is significantly the most active stereoisomer diminishing the intracellular  
378 ROS from the lowest concentration and reaching a reduction of 63% comparing with LPS alone.  
379 We can also observe differences between **2a** and **2b**, being this last significantly more anti-  
380 oxidant, and diminishing the ROS production on 48% while only a 21% was observed for **2a**  
381 in comparison with control (**Figure 4c**).

382 Based on these results it can be concluded that viniferin stereoisomers possess *in vitro*  
383 anti-inflammatory and anti-oxidant properties in macrophages cells and that their activity varies  
384 according to their spatial configuration. Apart from resveratrol, other oligomeric stilbenes, as  
385 different viniferins, are showing promising results as anti-inflammatory, anti-oxidant,  
386 neuroprotective, anti-obesity, anticancer agents (Nassra et al., 2013; Ohara et al., 2015; Ficarra  
387 et al., 2016; Caillaud et al., 2019; Nivelles et al., 2018; Vion et al., 2018; Sergi et al., 2021).

388 Our results demonstrate that the four stereoisomers are toxic from  $10 \mu\text{M}$  concentration  
389 in RAW 264.7 cells. The same observation has been described for viniferin compounds in the  
390 same cellular model (Ha et al., 2018), but also in other cellular models as BV2 or Caco-2 cells  
391 (Nassra et al., 2013; Medrano-Padial et al., 2020).

392 Concerning anti-inflammatory properties, Nassra and co-workers showed that viniferins  
393 (*E*- $\delta$ -viniferin, *E*- $\epsilon$ -viniferin and *E*- $\omega$ -viniferin present very similar inhibitory capacity to reduce  
394 LPS-induced NO production in BV2 microglial cells. They showed that *E*- $\epsilon$ -viniferin is the  
395 most active compound (IC<sub>50</sub>: 8.6) presenting even better results than *E*-resveratrol (IC<sub>50</sub>: 13.1)  
396 (Nassra et al., 2013). Additionally, other more recent published article has demonstrated that  
397 *E*- $\epsilon$ -viniferin, also at low concentrations, is able to counteract the inflammation induced by  
398 LPS-activated microglia in N9 cells (Sergi et al., 2021). Only one recent article has  
399 demonstrated in our same cellular model (RAW 264.7 macrophage cells) that *E*- $\epsilon$ -viniferin  
400 decreased NO, PGE<sub>2</sub>, iNOS, and COX-2 productions after LPS stimulation and that this activity  
401 is may be mediated by the NF- $\kappa$ B activation (Ha et al., 2018). The present findings demonstrate  
402 for the first time that viniferin stereoisomers possess anti-inflammatory and anti-oxidant  
403 activities. Moreover and even though their structures are quite similar, this paper proved that  
404 these bioactivities are different according to their configuration.

#### 405 **4. Conclusion**

406 In summary, this work demonstrated for the first time the presence of four stereoisomers  
407 of viniferin stilbene (*7aS,8aS*)-*E*- $\epsilon$ -viniferin, (*7aR,8aR*)-*E*- $\epsilon$ -viniferin, (*7aS,8aR*)-*E*- $\omega$ -viniferin,  
408 and (*7aR,8aS*)-*E*- $\omega$ -viniferin in grapevine branches. The absolute configurations were clearly  
409 established by vibrational circular dichroism (VCD) spectroscopy in combination with density  
410 functional theory (DFT) calculations. Moreover, the anti-inflammatory and anti-oxidant  
411 activities of the four identified viniferin stereoisomers revealed that viniferin stereoisomers  
412 possess different bioactivities according to their configuration. In addition, for the first time,  
413 the two enantiomers of *E*- $\epsilon$ -viniferin in grapevine are present and the enantiomeric excess are  
414 grape variety-dependent. Overall, the present study extends our knowledge of absolute  
415 stereochemistry of viniferin dimers present in grapevine and paves the way for further  
416 investigation related to their structure-activity relationship.

417

## 418 **ASSOCIATED CONTENT**

### 419 **Supporting Information**

420 The following data are available as supplementary material: Specific optical rotation values of  
421 *E-ε*-viniferin (Table S1), enantiomeric excess for the three grape varieties (Table S2), NMR  
422 data of *E-ε*-viniferin and *E-ω*-viniferin (Table S3), CPC chromatogram (Figure S1), analytical  
423 (Figure S2) and preparative (Figure S3) chiral HPLC chromatograms, <sup>1</sup>H NMR and <sup>1</sup>H-<sup>1</sup>H-  
424 ROESY NMR spectra of *E-ε*-viniferin (Figure S4 and S5), <sup>1</sup>H NMR and <sup>1</sup>H-<sup>1</sup>H-ROESY NMR  
425 spectra of *E-ω*-viniferin (Figure S6 and S7), IR spectra of *E-ε*-viniferin and *E-ω*-viniferin  
426 (Figure S8), VCD spectra of *E-ε*-viniferin and *E-ω*-viniferin (Figures S9 and S10), ECD spectra  
427 of *E-ε*-viniferin and *E-ω*-viniferin (Figures S11 and S12).

### 428 **ACKNOWLEDGMENTS**

429 The authors thank R. Cooke for proofreading the manuscript.

### 430 **FUNDING**

431 Research support was provided by the French Ministry of Higher Education and Research.  
432 NMR experiments were performed at the Bordeaux Metabolome Facility and MetaboHUB  
433 (ANR-11-INBS-0010 project).

### 434 **REFERENCES**

- 435 Barceló, A. R., Pomar, F., López-Serrano, M., & Pedreño, M. A. (2003). Peroxidase: a  
436 multifunctional enzyme in grapevines. *Functional Plant Biology*, *30*(6), 577–591.  
437 <https://doi.org/10.1071/fp02096>
- 438 Breuil, A. C., Adrian, M., Pirio, N., Meunier, P., Bessis, R., & Jeandet, P. (1998). Metabolism  
439 of stilbene phytoalexins by *Botrytis cinerea*: 1. Characterization of a resveratrol  
440 dehydrodimer. *Tetrahedron Letters*, *39*(7), 537–540. [https://doi.org/10.1016/S0040-](https://doi.org/10.1016/S0040-4039(97)10622-0)  
441 [4039\(97\)10622-0](https://doi.org/10.1016/S0040-4039(97)10622-0)

442 Buffeteau, T., Cavagnat, D., Bisson, J., Marchal, A., Kapche, G. D., Battistini, I., Da Costa, G.,  
443 Badoc, A., Monti, J.-P., Mérillon, J.-M., & Waffo-Téguo, P. (2014). Unambiguous  
444 determination of the absolute configuration of dimeric stilbene glucosides from the  
445 rhizomes of *Gnetum africanum*. *Journal of Natural Products*, 77(8), 1981–1985.  
446 <https://doi.org/10.1021/np500427v>

447 Buffeteau, T., Lagugn -Labarthe, F., & Sourisseau, C. (2005). Vibrational circular dichroism  
448 in general anisotropic thin solid films: measurement and theoretical approach. *Applied*  
449 *Spectroscopy*, 59(6), 732–745. <https://doi.org/10.1366/0003702054280568>

450 Caillaud, M., Guillard, J., Richard, D., Milin, S., Chassaing, D., Paccalin, M., Page, G., & Bilan,  
451 A. R. (2019). *Trans*  $\epsilon$  viniferin decreases amyloid deposits and inflammation in a mouse  
452 transgenic Alzheimer model. *PLoS ONE*, 14(2) : e0212663.  
453 <https://doi.org/10.1371/journal.pone.0212663>

454 Calder n, A. A., Zapata, J. M., Pedre o, M. A., Mu oz, R., & Barcel , A. R. (1992). Levels of  
455 4-hydroxystilbene-oxidizing isoperoxidases related to constitutive disease resistance in  
456 *in vitro*-cultured grapevine. *Plant Cell, Tissue and Organ Culture*, 29(2), 63–70.

457 Cichewicz, R. H., Kouzi, S. A., & Hamann, M. T. (2000). Dimerization of resveratrol by the  
458 grapevine pathogen *Botrytis cinerea*. *Journal of Natural Products*, 63(1), 29–33.  
459 <https://doi.org/10.1021/np990266n>

460 Cretin, B. N., Sallembien, Q., Sindt, L., Daugey, N., Buffeteau, T., Waffo-Teguo, P.,  
461 Dubourdi u, D., & Marchal, A. (2015). How stereochemistry influences the taste of  
462 wine: isolation, characterization and sensory evaluation of lyoniresinol stereoisomers.  
463 *Analytica Chimica Acta*, 888, 191-198. <https://doi.org/10.1016/j.aca.2015.06.061>

464 Ficarra, S., Tellone, E., Pirolli, D., Russo, A., Barreca, D., Galtieri, A., Giardina, B., Gavezzotti,  
465 P., Riva, S., & Rosa, M. C. D. (2016). Insights into the properties of the two enantiomers  
466 of *trans*- $\delta$ -viniferin, a resveratrol derivative: antioxidant activity, biochemical and  
467 molecular modeling studies of its interactions with hemoglobin. *Molecular BioSystems*,  
468 12, 1276-1286. <https://doi.org/10.1039/c5mb00897b>

469 Frisch, M. J., Trucks, G. W., Schlegel, H. B., Scuseria, G. E., Robb, M. A., Cheeseman, J. R.,  
470 Scalmani, G., Barone, V., Mennucci, B., Petersson, G. A., Nakatsuji, H., Caricato, M.,  
471 Li, X., Hratchian, H. P., Izmaylov, A. F., Bloino, J., Zheng, G., Sonnenberg, J. L., Hada,  
472 M.; Ehara, M., Toyota, K., Fukuda, R., Hasegawa, J., Ishida, M., Nakajima, T., Honda,  
473 Y., Kitao, O., Nakai, H., Vreven, T., Montgomery, J. A. Jr., Peralta, J. E., Ogliaro, F.,  
474 Bearpark, M., Heyd, J. J., Brothers, E., Kudin, K. N., Staroverov, V. N., Kobayashi, R.,  
475 Normand, J., Raghavachari, K., Rendell, A., Burant, J. C., Iyengar, S. S., Tomasi, J.,  
476 Cossi, M., Rega, N., Millam, J. M., Klene, M., Knox, J. E., Cross, J. B., Bakken, V.,  
477 Adamo, C., Jaramillo, J., Gomperts, R., Stratmann, R. E., Yazyev, O., Austin, A. J.,  
478 Cammi, R., Pomelli, C., Ochterski, J. W., Martin, R. L., Morokuma, K., Zakrzewski, V.  
479 G., Voth, G. A., Salvador, P., Dannenberg, J. J., Dapprich, S., Daniels, A. D., Farkas, Ö  
480 ., Foresman, J. B., Ortiz, J. V., Cioslowski, J., Fox, D. J. Gaussian 09, Revision A.01;  
481 Gaussian Inc.: Wallingford, CT, 2009. Retrieved September 25, 2021, from  
482 <https://gaussian.com/glossary/g09/>

483 Gabaston, J., Valls Fonayet, J., Franc, C., Waffo-Teguo, P., de Revel, G., Hilbert, G., Gomès,  
484 E., Richard, T., Mérillon, J.-M. (2020). Characterization of stilbene composition in  
485 grape berries from wild *Vitis* species in year-to-year harvest. *Journal of Agricultural*  
486 *and Food Chemistry*, 68(47), 13408-13417. <https://doi.org/10.1021/acs.jafc.0c04907>

487 Ha, D. T., Long, P. T., Hien, T. T., Tuan, D. T., An, N. T. T., Khoi, N. M., Van Oanh, H., &  
488 Hung, T. M. (2018). Anti-inflammatory effect of oligostilbenoids from *Vitis heyneana*  
489 in LPS-stimulated RAW 264.7 macrophages via suppressing the NF- $\kappa$ B activation.  
490 *Chemistry Central Journal*, 12(1), 14. <https://doi.org/10.1186/s13065-018-0386-5>

491 He, S., Jiang, L., Wu, B., Li, C., & Pan, Y. (2009). Chunganenol: an unusual antioxidative  
492 resveratrol hexamer from *Vitis chunganensis*. *The Journal of Organic Chemistry*,  
493 74(20), 7966–7969. <https://doi.org/10.1021/jo901354p>

494 Ito, T., Abe, N., Oyama, M., & Iinuma, M. (2009). Absolute structures of C-glucosides of  
495 resveratrol oligomers from *Shorea uliginosa*. *Tetrahedron Letters*, 50, 2516–2520.  
496 <https://doi.org/10.1016/j.tetlet.2009.03.043>

497 Keylor, M. H., Matsuura, B. S., & Stephenson, C. R. J. (2015). Chemistry and biology of  
498 resveratrol-derived natural products. *Chemical Reviews*, 115(17), 8976–9027.  
499 <https://doi.org/10.1021/cr500689b>

500 Ko, J.-H., Sethi, G., Um, J.-Y., Shanmugam, M. K., Arfuso, F., Kumar, A. P., Bishayee, A., &  
501 Ahn, K. S. (2017). The role of resveratrol in cancer therapy. *International Journal of*  
502 *Molecular Sciences*, 18(12). <https://doi.org/10.3390/ijms18122589>

503 Kurihara, H., Kawabata, J., Ichikawa, S., Mishima, M., & Mizutani, J. (1991). Oligostilbenes  
504 from *Carex kobomugi*. *Phytochemistry*, 30(2), 649–653. [https://doi.org/10.1016/0031-](https://doi.org/10.1016/0031-9422(91)83745-7)  
505 [9422\(91\)83745-7](https://doi.org/10.1016/0031-9422(91)83745-7)

506 Kurihara, H., Kawabata, J., Ichikawa, S., & Mizutani, J. (1990). (-)-e-Viniferin and related  
507 oligostilbenes from *Carex pumila* Thunb. (Cyperaceae). *Agricultural and Biological*  
508 *Chemistry*, 54(4), 1097–1099.

509 Li, W. W., Ding, L. S. eng, Li, B. G. ng, & Chen, Y. Z. (1996). Oligostilbenes from *Vitis*  
510 *heyneana*. *Phytochemistry*, 42(4), 1163–1165. <https://doi.org/10.1016/0031->  
511 9422(96)00069-6

512 Mattivi, F., Vrhovsek, U., Malacarne, G., Masuero, D., Zulini, L., Stefanini, M., Moser, C.,  
513 Velasco, R., & Guella, G. (2011). Profiling of resveratrol oligomers, important stress  
514 metabolites, accumulating in the leaves of hybrid *Vitis vinifera* (Merzling × Teroldego)  
515 genotypes infected with *Plasmopara viticola*. *Journal of Agricultural and Food*  
516 *Chemistry*, 59(10), 5364–5375. <https://doi.org/10.1021/jf200771y>

517 Medrano-Padial, C., Puerto, M., Merchán-Gragero, M. D. M., Moreno, F. J., Richard, T.,  
518 Cantos-Villar, E., & Pichardo, S. (2020). Cytotoxicity studies of a stilbene extract and  
519 its main components intended to be used as preservative in the wine industry. *Food*  
520 *Research International*, 137, 109738. <https://doi.org/10.1016/j.foodres.2020.109738>

521 Morales, M., & Barceló, A. R. (1997). A basic peroxidase isoenzyme from vacuoles and cell  
522 walls of *Vitis vinifera*. *Phytochemistry*, 45(2), 229–232. <https://doi.org/10.1016/S0031->  
523 9422(96)00825-4

524 Nafie, L. A., Vidrine, D. W. In *Fourier Transform Infrared Spectroscopy*; Ferraro, J. R.; Basile,  
525 L. J., Eds.; Academic Press: New York, 1982; Vol. 3, pp 83–123.

526 Nassra, M., Krisa, S., Papastamoulis, Y., Kapche, G. D., Bisson, J., André, C., Konsman, J.-P.,  
527 Schmitter, J.-M., Mérillon, J.-M., & Waffo-Téguo, P. (2013). Inhibitory activity of plant  
528 stilbenoids against nitric oxide production by lipopolysaccharide-activated microglia.  
529 *Planta Medica*, 79(11), 966–970. <https://doi.org/10.1055/s-0032-1328651>

530 Ngoc, T. M., Hung, T. M., Thuong, P. T., Na, M., Kim, H., Ha, D. T., Min, B.-S., Minh, P. T.  
531 H., & Bae, K. (2008). Inhibition of human low density lipoprotein and high density

532 lipoprotein oxidation by oligostilbenes from rhubarb. *Biological & Pharmaceutical*  
533 *Bulletin*, 31(9), 1809–1812. <https://doi.org/10.1248/bpb.31.1809>.

534 Nivelles, L., Aires, V., Rioult, D., Martiny, L., Tarpin, M., & Delmas, D. (2018). Molecular  
535 analysis of differential antiproliferative activity of resveratrol, epsilon viniferin and  
536 labruscol on melanoma cells and normal dermal cells. *Food and Chemical Toxicology*,  
537 116(Pt B), 323–334. <https://doi.org/10.1016/j.fct.2018.04.043>

538 Ohara, K., Kusano, K., Kitao, S., Yanai, T., Takata, R., & Kanauchi, O. (2015). ε-Viniferin, a  
539 resveratrol dimer, prevents diet-induced obesity in mice. *Biochemical and Biophysical*  
540 *Research Communications*, 468(4), 877–882.  
541 <https://doi.org/10.1016/j.bbrc.2015.11.047>

542 Pawlus, A. D., Sahli, R., Bisson, J., Rivière, C., Delaunay, J.-C., Richard, T., Gomès, E.,  
543 Bordenave, L., Waffo-Téguo, P., & Mérillon, J.-M. (2013). Stilbenoid profiles of canes  
544 from *Vitis* and *Muscadinia* species. *Journal of Agricultural and Food Chemistry*, 61(3),  
545 501–511. <https://doi.org/10.1021/jf303843z>

546 Pezet, R. (1998). Purification and characterization of a 32-kDa laccase-like stilbene oxidase  
547 produced by *Botrytis cinerea* Pers.:Fr. *FEMS Microbiology Letters*, 167(2), 203–208.

548 Richard, T., Pawlus, A. D., Iglesias, M.-L., Pedrot, E., Waffo-Teguo, P., Merillon, J.-M., &  
549 Monti, J.-P. (2011). Neuroprotective properties of resveratrol and derivatives. *Annals of*  
550 *the New York Academy of Sciences*, 1215(1), 103–108. <https://doi.org/10.1111/j.1749->  
551 [6632.2010.05865.x](https://doi.org/10.1111/j.1749-6632.2010.05865.x)

552 Rivière, C., Pawlus, A. D., & Mérillon, J.-M. (2012). Natural stilbenoids: distribution in the  
553 plant kingdom and chemotaxonomic interest in Vitaceae. *Natural Product Reports*,  
554 29(11), 1317–1333. Scopus. <https://doi.org/10.1039/c2np20049j>

555 Saiko, P., Szakmary, A., Jaeger, W., & Szekeres, T. (2008). Resveratrol and its analogs: defense  
556 against cancer, coronary disease and neurodegenerative maladies or just a fad? *Mutation*  
557 *Research*, 658(1–2), 68–94. <https://doi.org/10.1016/j.mrrev.2007.08.004>

558 Sergi, D., Gélinas, A., Beaulieu, J., Renaud, J., Tardif-Pellerin, E., Guillard, J., & Martinoli,  
559 M.-G. (2021). Anti-apoptotic and anti-inflammatory role of *trans*  $\epsilon$ -viniferin in a  
560 neuron-glia co-culture cellular model of Parkinson's disease. *Foods*, 10(3), 586.  
561 <https://doi.org/10.3390/foods10030586>

562 Shang, Y.-J., Qian, Y.-P., Liu, X.-D., Dai, F., Shang, X.-L., Jia, W.-Q., Liu, Q., Fang, J.-G., &  
563 Zhou, B. (2009). Radical-scavenging activity and mechanism of resveratrol-oriented  
564 analogues: influence of the solvent, radical, and substitution. *The Journal of Organic*  
565 *Chemistry*, 74(14), 5025–5031. <https://doi.org/10.1021/jo9007095>

566 Shen, T., Wang, X.-N., & Lou, H.-X. (2009). Natural stilbenes: an overview. *Natural Product*  
567 *Reports*, 26(7), 916–935. <https://doi.org/10.1039/B905960A>

568 Stojanović, S., & Brede, O. (2002). Elementary reactions of the antioxidant action of *trans*-  
569 stilbene derivatives: resveratrol, pinosylvin and 4-hydroxystilbene. *Physical Chemistry*  
570 *Chemical Physics*, 4(5), 757–764. <https://doi.org/10.1039/b109063c>

571 Vion, E., Page, G., Bourdeaud, E., Paccalin, M., Guillard, J., & Rioux Bilan, A. (2018). *Trans*  
572  $\epsilon$ -viniferin is an amyloid- $\beta$  disaggregating and anti-inflammatory drug in a mouse  
573 primary cellular model of Alzheimer's disease. *Molecular and Cellular Neuroscience*,  
574 88, 1–6. <https://doi.org/10.1016/j.mcn.2017.12.003>

575 Yoshiaki, T., & Masatake, N. (2001). Oligostilbenes from Vitaceaeous plants. *Trends in*  
576 *Heterocyclic Chemistry*, 7, 41–54.

577 Yuk, H. J., Ryu, H. W., Jeong, S. H., Curtis-Long, M. J., Kim, H. J., Wang, Y., Song, Y. H., &  
578 Park, K. H. (2013). Profiling of neuraminidase inhibitory polyphenols from the seeds of  
579 *Paeonia lactiflora*. *Food and Chemical Toxicology*, 55, 144–149.  
580 <https://doi.org/10.1016/j.fct.2012.12.053>

581

582

583

584

## FIGURES CAPTIONS

**Figure 1.** Chemical structures of viniferins (only the **1a** and **2a** compounds are reported).

**Figure 2.** Comparison of experimental VCD spectra for the second eluted compound of **1** and **2** recorded in DMSO-*d*<sub>6</sub> solution (40 mM, 100 μm path length) with the predicted spectra of (7*aS*,8*aS*)-*E*-ε-viniferin and (7*aR*,8*aS*)-*E*-ω-viniferin.

**Figure 3.** Comparison of experimental VCD spectra for the second eluted compound of **1** recorded in DMSO-*d*<sub>6</sub> solution (40 mM, 100 μm path length) with the VCD spectra of *E*-ε-viniferin extracted from different grape varieties.

**Figure 4.** (A) Cell viability (%) (B) NO (μM) (C) ROS (fluorescence intensity) in LPS-stimulated RAW 264.7 cells. Cells were treated for 24 hours with LPS (0.1 μg/mL; + control) or LPS with **1a**, **1b**, **2a** and **2b** at different concentrations (from 0.5-100 μM for cell viability and between 0.5-10 μM for NO and ROS measurements). Results are expressed as mean SEM of eight replicates (*n*=8). Different letters mean significant differences (*p*<0.5).

**Figure 1.**

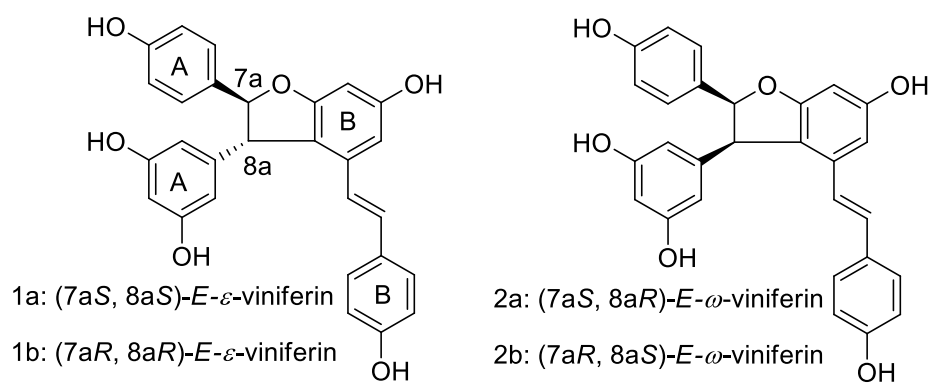


Figure 2.

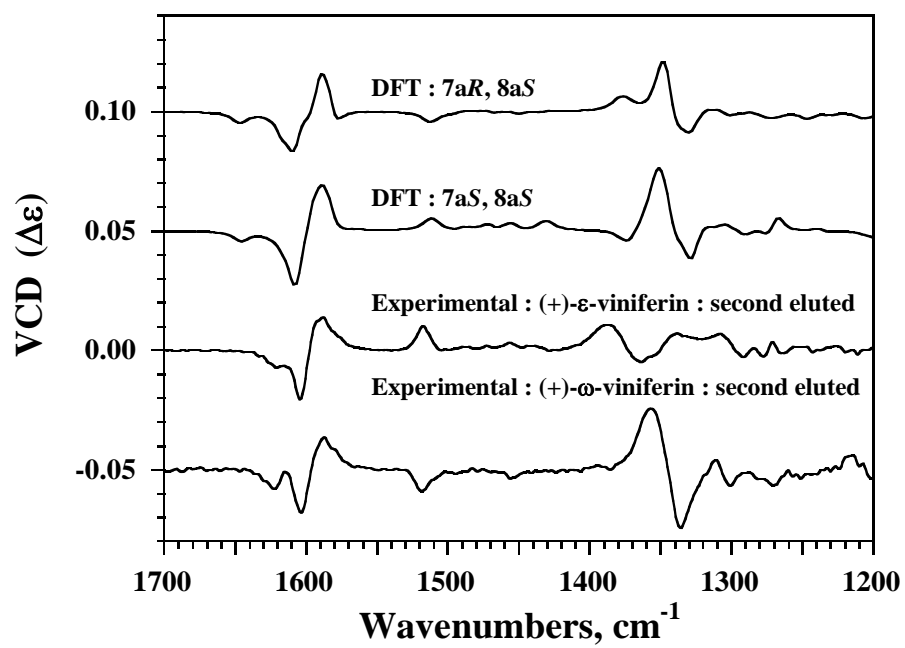
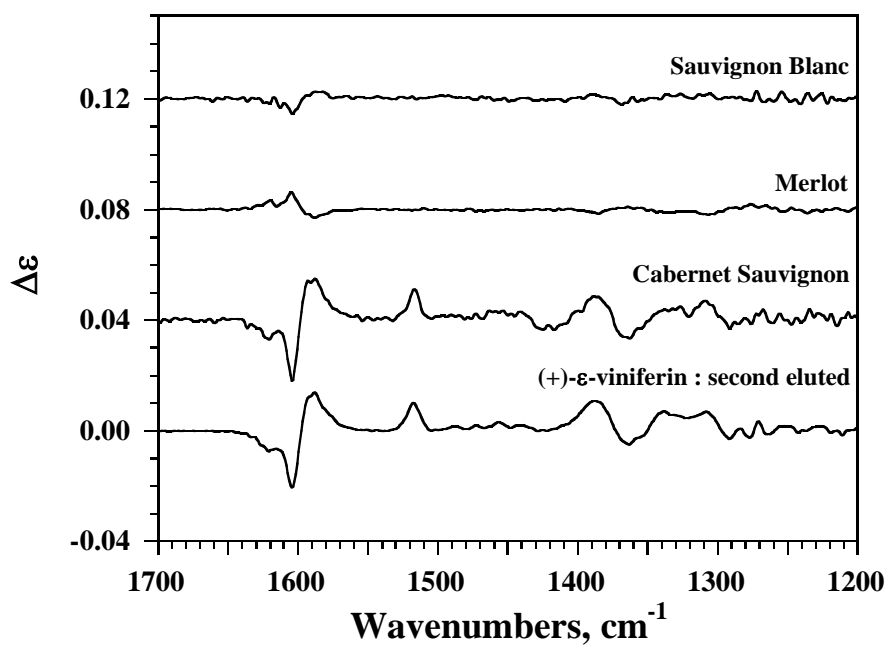
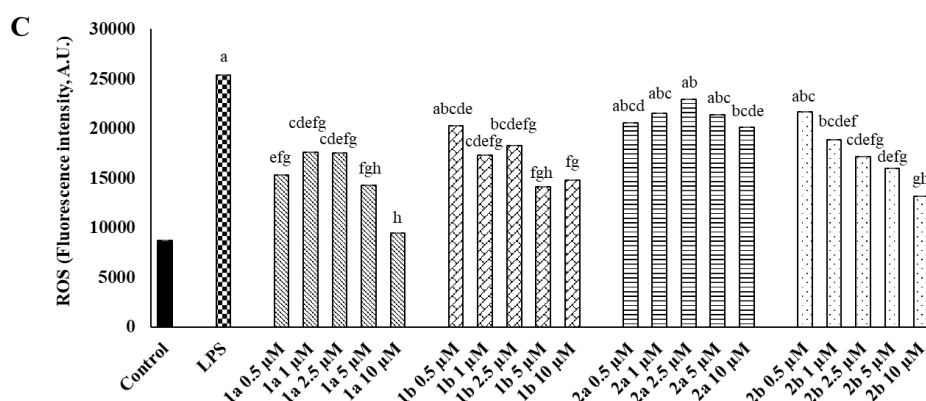
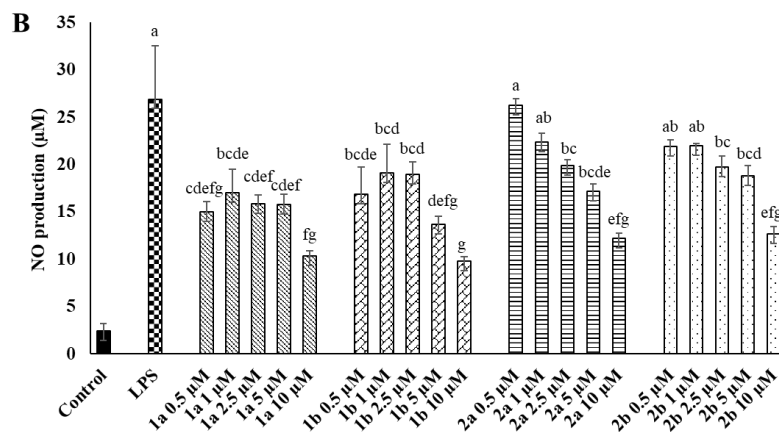
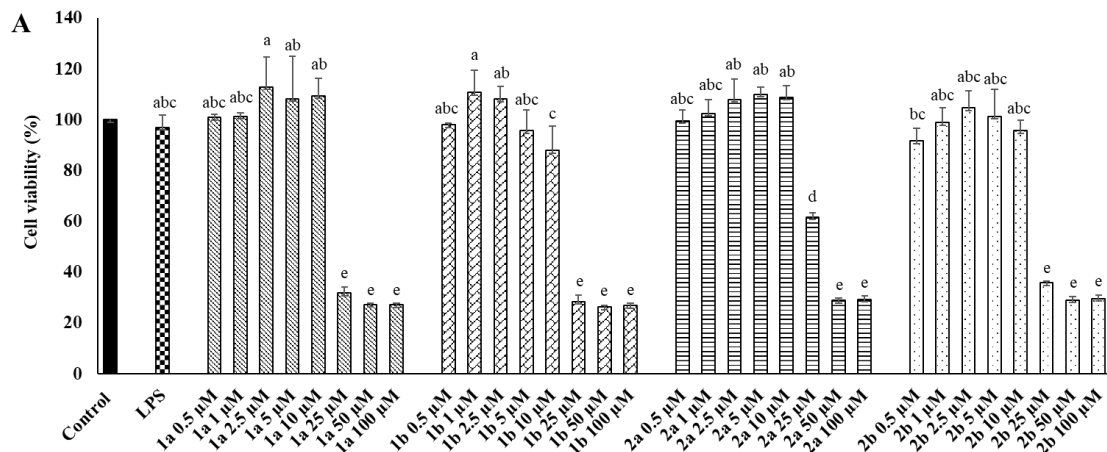


Figure 3.



**Figure 4.**

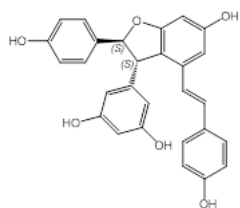


## For TOC Graphic only



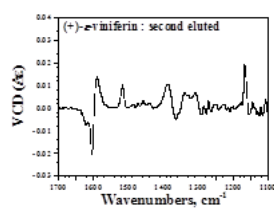
Cabernet Sauvignon stalks

Extraction  
CPC, HPLC



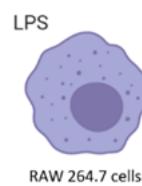
(7aS,8aS)-E-ε-viniferin

Absolute configuration  
determination



ee = 98.3%

Bioactivity



RAW 264.7 cells

anti-inflammatory and  
anti-oxidant activities

**Declaration of interests**

The authors declare that they have no known competing financial interests or personal relationships that could have appeared to influence the work reported in this paper.

The authors declare the following financial interests/personal relationships which may be considered as potential competing interests: